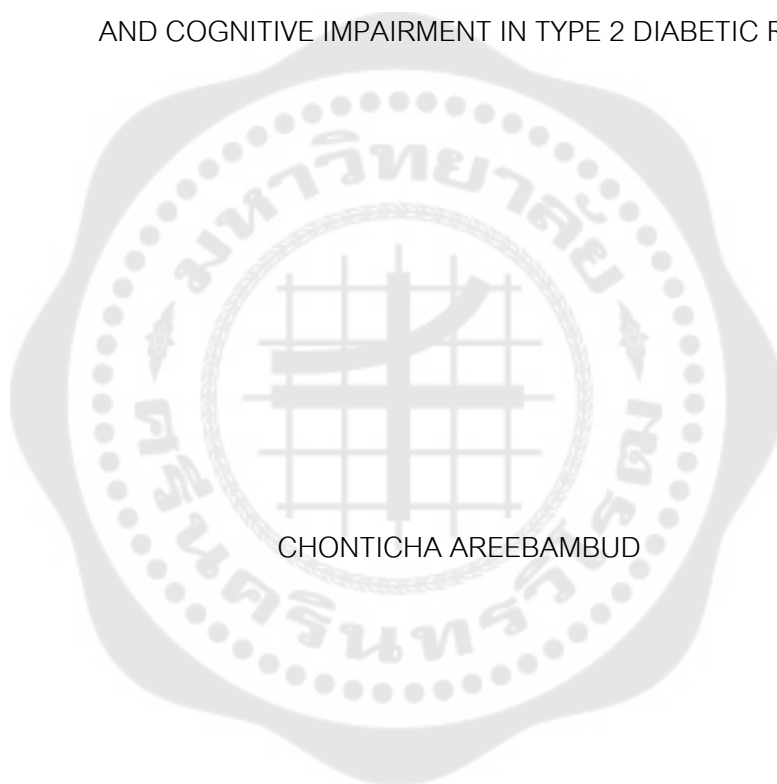




THE EFFECTS OF PUMPKIN SEED OIL ON NEURONAL CELL DEATH  
AND COGNITIVE IMPAIRMENT IN TYPE 2 DIABETIC RAT



CHONTICHA AREEBAMBUD

Graduate School Srinakharinwirot University

2021

ฤทธิ์ของน้ำมันเมล็ดฟักทองต่อการตายของเซลล์ประสาท  
และความบกพร่องด้านการเรียนรู้และความจำในหนูเบาหวานชนิด 2



ปริญญานิพนธ์นี้เป็นส่วนหนึ่งของการศึกษาตามหลักสูตร  
ปรัชญาดุษฎีบัณฑิต สาขาวิชาชีวภาพการแพทย์  
คณะแพทยศาสตร์ มหาวิทยาลัยศรีนครินทรวิโรฒ  
ปีการศึกษา 2564  
ลิขสิทธิ์ของมหาวิทยาลัยศรีนครินทรวิโรฒ

THE EFFECTS OF PUMPKIN SEED OIL ON NEURONAL CELL DEATH  
AND COGNITIVE IMPAIRMENT IN TYPE 2 DIABETIC RAT



CHONTICHA AREEBAMBUD

A Dissertation Submitted in Partial Fulfillment of the Requirements  
for the Degree of DOCTOR OF PHILOSOPHY  
(Biomedical Sciences)

Faculty of Medicine, Srinakharinwirot University

2021

Copyright of Srinakharinwirot University

THE DISSERTATION TITLED  
THE EFFECTS OF PUMPKIN SEED OIL ON NEURONAL CELL DEATH  
AND COGNITIVE IMPAIRMENT IN TYPE 2 DIABETIC RAT

BY  
CHONTICHA AREEBAMBUD

HAS BEEN APPROVED BY THE GRADUATE SCHOOL IN PARTIAL FULFILLMENT  
OF THE REQUIREMENTS FOR THE DOCTOR OF PHILOSOPHY  
IN BIOMEDICAL SCIENCES AT SRINAKHARINWIROT UNIVERSITY

-----  
(Assoc. Prof. Dr. Chatchai Ekpanyaskul, MD.)  
Dean of Graduate School  
-----

ORAL DEFENSE COMMITTEE

..... Major-advisor	..... Chair
(Assoc. Prof. Dr.Amporn Jariyapongskul)	(Assoc. Prof. Dr.Bhronprom Yoysungnoen)
..... Co-advisor	..... Committee
(Assoc. Prof. Dr.Sarin Tadtong)	(Prof. Dr.Chatsri Deachapunya)
	..... Committee
	(Dr.Ratchadaporn Pramong)

Title	THE EFFECTS OF PUMPKIN SEED OIL ON NEURONAL CELL DEATH AND COGNITIVE IMPAIRMENT IN TYPE 2 DIABETIC RAT
Author	CHONTICHA AREEBAMBUD
Degree	DOCTOR OF PHILOSOPHY
Academic Year	2021
Thesis Advisor	Associate Professor Dr. Amporn Jariyapongskul
Co Advisor	Associate Professor Dr. Sarin Tadtong

Type 2 diabetes induced cognitive impairment through several mechanisms, including beta-amyloid ( $A\beta$ ) accumulation, oxidative stress, and neuronal apoptosis. Pumpkin seed oil (PSO) is rich in unsaturated and saturated fatty acids, with the potential for anti-diabetic, anti-hyperlipidemic, antioxidant, and anti-apoptotic properties. The present study demonstrated the effects of PSO by *in vitro* and *in vivo* studies. The *in vitro* study aimed to determine the neuroprotective effect of PSO on  $A\beta_{42}$ -induced neuronal cell death using human neuroblastoma or the SH-SY5Y cell. The *in vivo* study investigated the effects of PSO on neuronal cell death and cognitive impairment in a type 2 diabetic rat model. In addition, the possible mechanisms of type 2 diabetic-induced cognitive impairment were examined. For the *in vitro* study, after SH-SY5Y cells were pretreated with PSO (0.001 and 10  $\mu$ g/mL). The cells were exposed to  $A\beta_{42}$  (1.25  $\mu$ M). The cell viability, intracellular reactive oxygen species (ROS), apoptotic proteins (Bax and caspase3) and anti-apoptotic protein (Bcl2) were determined. For the *in vivo* study, six-week-old male Sprague-Dawley rats were divided into four groups, including normal control rats (CON rats), type 2 diabetic rats (T2DM rats), type 2 diabetic rats administration with 10 mg/kg B.W. of pioglitazone (T2DM-PG rats) and 200 mg/kg B.W. of PSO (T2DM-PSO rats). The rats received 10% fructose drinking water for two weeks following streptozotocin injection (30 mg/kg B.W.) to induce type 2 diabetes. Cognitive function was assessed using novel object recognition (NOR) and Morris's water maze (MWM) test. The fasting blood glucose (FBG), blood cholesterol (CHOL), blood triglyceride (TG), plasma HbA1c, serum insulin, serum free fatty acid (FFA), and HOMA-IR were determined. Oxidative stress parameters in the hippocampal tissue and the expression of the nrf2 transcription factor (nrf2), superoxide dismutase (SOD), and malondialdehyde (MDA) were determined. In addition, the hippocampal  $A\beta_{42}$ , BACE1, and apoptotic proteins (Bax and caspase3) and anti-apoptotic protein (Bcl2) expression were evaluated. The results of *in vitro* study showed that PSO could protect  $A\beta_{42}$ -induced SH-SY5Y cell death through reduced intracellular ROS and apoptotic Bax, caspase3 proteins expression. In addition, the PSO pretreatment enhanced anti-apoptotic protein (Bcl2) expression. The *in vivo* study showed that PSO administration enhanced cognitive performance in non-spatial and spatial learning and memory. The metabolic parameters, including FBG, CHOL, TG, plasma HbA1c, serum insulin, serum free fatty acid, and HOMA-IR index were reduced in T2DM-PSO rats. In addition, the hippocampal MDA,  $A\beta_{42}$ , BACE1, Bax, and caspase 3 significantly decreased in T2DM rats. Moreover, PSO administration enhanced the level of nrf2, SOD, and Bcl2 in the hippocampus. Interestingly, PSO administration protected neuronal cell death by reducing apoptotic proteins and increasing anti-apoptotic protein in the T2DM hippocampal. From our *in vitro* and *in vivo* results indicated that PSO has a powerful neuroprotective effect which improved T2DM induced cognitive impairment through anti-diabetic, increased insulin sensitivity, anti-apoptotic, and antioxidant properties.

Keyword : Pumpkin seed, Type 2 diabetic rat, Beta-amyloid 42, Oxidative stress, Neuronal cell death

## ACKNOWLEDGEMENTS

It is a pleasure to thank those who made this thesis possible. First, I would like to thank my advisor, Associate Professor Amporn Jariyapongskul, for her valuable advice, helpful guidance, and encouragement, for sharing the time in the lab, kindness, and understanding in this study. All of this has enabled me to carry out my study successfully. Second, I am profoundly grateful and appreciative to my co-advisor, Associate professor Sarin Tadtong for their valuable suggestions, helpful criticism, kindness, and intensive supervision throughout this work. Furthermore, I would like to thank Dr. Vipaporn Sareedencha from the Faculty of Pharmacy, Srinakarinwirot University, for guiding, suggesting, and helping me about pumpkin seed oil extraction. Finally, I also sincerely thank all lecturers and staff of my department for their valuable advice during my study and special thanks to the committee, Associate Professor Bhronprom Yoysungnoen, Faculty of Medicine, Thammasat University for their constructive criticisms of and corrections of my thesis.

I would like to thank the Department of Physiology, Faculty of Medicine, and Faculty of Pharmacy, Srinakarinwirot University, for providing me with all instruments and facilities for my research. In addition, I would like to thank the Central Laboratory and Laboratory Animal Care and Use Unit, Faculty of Medicine, Srinakarinwirot University, for providing me with all instruments and facilities for my research.

I would like to give my family and all my friends for their love, care, understanding, and encouragement throughout my study. Without their support, my success would never become true.

Furthermore, I would like to thank the Research and Researchers for Industries (RRI) and LILY TOBEKA COMPANY (Thailand) for supporting the research funding.

CHONTICHA AREEBAMBUD

## TABLE OF CONTENTS

	Page
ABSTRACT .....	D
ACKNOWLEDGEMENTS.....	E
TABLE OF CONTENTS.....	F
LIST OF TABLES.....	I
LIST OF FIGURES .....	J
CHAPTER I INTRODUCTION .....	1
CHAPTER II REVIEW LITERATURE.....	5
1. Diabetes mellitus.....	5
1.1 Diagnostic of diabetes mellitus .....	5
1.2 Types of diabetes mellitus.....	5
2. Type 2 diabetes mellitus .....	6
3. Insulin function .....	7
3.1 Peripheral insulin function .....	7
3.2 Brain insulin function .....	8
4. Insulin resistance (IR) .....	11
4.1 Peripheral insulin resistance .....	11
4.2 Brain insulin resistance .....	13
5. Type 2 diabetes mellitus and cognitive impairment.....	15
5.1 Obesity .....	16
5.2 Inflammation .....	16
5.3 Oxidative stress .....	17

5.4 Mitochondria dysfunction .....	19
5.5 Beta-amyloid accumulation.....	19
5.6 Hyperphosphorylation of Tau protein .....	21
6. Apoptosis .....	21
6.1 Apoptotic pathways.....	21
6.2 Apoptosis in type 2 diabetes and cognitive impairment .....	23
7. Pumpkin seed oil.....	24
8. Type 2 diabetes animal models.....	26
9. Human neuroblastoma cell SH-SY5Y .....	29
10. Pioglitazone.....	30
RESEARCH OBJECTIVES .....	32
CONCEPTUAL FRAMEWORK.....	33
<i>In vitro</i> conceptual framework .....	33
<i>In vivo</i> (animal) conceptual framework.....	34
CHAPTER III MATERIALS AND METHODS .....	35
Preparation of pumpkin seed oil.....	36
Experimental protocol I: <i>In vitro</i> (cell culture) study.....	38
Experimental protocol II: <i>In vivo</i> (animal) study .....	43
Animal experimental design .....	44
CHAPTER IV RESULTS .....	58
Part I chemical composition of pumpkin seed oil.....	59
Part II reports the neuroprotective effect of pumpkin seed oil on human neuroblastoma cell line SH-SY5Y apoptosis induced by beta-amyloid 42 .....	60

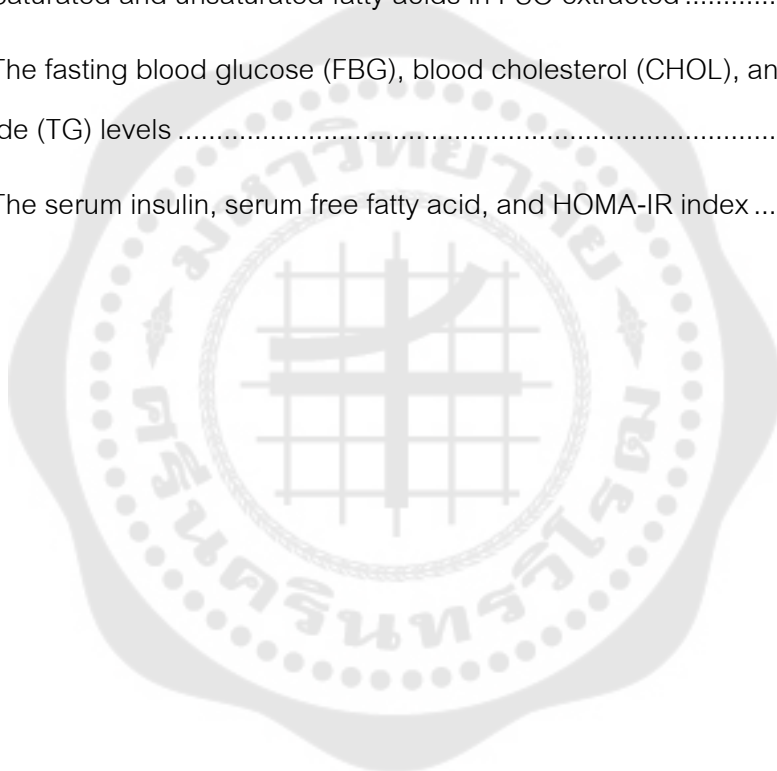


Part III: The effect of PSO on neuronal cell death and cognitive impairment in high fructose drinking-induced type 2 diabetic rat.....	68
CHAPTER V DISCUSSION .....	88
CONCLUSION .....	96
APPENDIX .....	98
REFERENCES.....	103
VITA .....	126



## LIST OF TABLES

	Page
Table 1 .....	1
Table 2 The criteria for diabetes mellitus .....	5
Table 3 Materials and reagents .....	35
Table 4 Saturated and unsaturated fatty acids in PSO extracted .....	59
Table 5 The fasting blood glucose (FBG), blood cholesterol (CHOL), and blood triglyceride (TG) levels .....	72
Table 6 The serum insulin, serum free fatty acid, and HOMA-IR index .....	77



## LIST OF FIGURES

	Page
Figure 1 Peripheral insulin signaling .....	7
Figure 2 Peripheral insulin may pass the blood-brain barrier through a receptor-mediated transport system.....	9
Figure 3 Central nervous insulin effects .....	10
Figure 4 Brain insulin signaling .....	11
Figure 5 The obesity promoting insulin resistance .....	13
Figure 6 Insulin signaling pathway under normal and insulin resistance .....	14
Figure 7 The association between T2DM or insulin resistance and neurodegeneration. 15	
Figure 8 The Nrf2/Keap1/ARE signaling in type 2 diabetes mellitus.....	18
Figure 9 APP processing under normal and insulin resistance conditions .....	20
Figure 10 Extrinsic and intrinsic pathways of apoptosis .....	22
Figure 11 The extraction procedure of pumpkin seed oil.....	37
Figure 12 Experimental timeline .....	45
Figure 13 Fatty acid assay reaction .....	48
Figure 14 Novel object recognition (NOR) test timeline .....	50
Figure 15 The box in each phase of the Novel Object Recognition (NOR) test .....	51
Figure 16 Morris's water maze setting experiment for learning test (escape latency time) .....	53
Figure 17 Morris's water maze setting experiment for memory test (probe trial time).....	53
Figure 18 MDA-TBAs complex formation .....	54
Figure 19 Scheme of the superoxide dismutase assay.....	55

Figure 20 Effect of beta-amyloid 42 on the viability of human neuroblastoma cell SH-SY5Y .....	61
Figure 21 Effect of pumpkin seed oil on the viability of human neuroblastoma cell SH-SY5Y .....	62
Figure 22 Effect of pumpkin seed oil on beta-amyloid 42-induced cytotoxicity on human neuroblastoma cell SH-SY5Y .....	63
Figure 23 Effect of pumpkin seed oil on beta-amyloid 42 -induced intracellular reactive oxygen species on human neuroblastoma cell SH-SY5Y .....	65
Figure 24 Effect of pumpkin seed oil on beta-amyloid 42 regulated anti-apoptotic and apoptotic proteins expression in human neuroblastoma cell SH-SY5Y. (A) The ratio of Bax expression/ $\beta$ -actin, (B) The ratio of caspase3 expression/ $\beta$ -actin, and (C) The ratio of Bcl2 expression/ $\beta$ -actin.....	67
Figure 25 The body weight changes during the experiment.....	70
Figure 26 The change in fasting blood glucose level during the experiment.....	71
Figure 27 The effect of pumpkin seed oil on glucose tolerance .....	73
Figure 28 The area under curve (AUC) of OGTT.....	74
Figure 29 The serum insulin level after two weeks of 10% w/v fructose drinking water ..	75
Figure 30 The fasting serum insulin level.....	75
Figure 31 The homeostatic model assessment for insulin resistance (HOMA-IR) index. 76	
Figure 32 The serum free fatty acid level.....	76
Figure 33 The exploring time between identical objects in the familiarization phase .....	78
Figure 34 The exploring time in the test phase.....	79
Figure 35 The percentage of Recognition index (% RI) in the test phase .....	80
Figure 36 The escape latency time and time spent in the target quadrant .....	82
Figure 37 The hippocampal beta-amyloid 42 levels of normal control rats .....	83

Figure 38 The hippocampal BACE1 expression.....	84
Figure 39 The hippocampal malondialdehyde (MDA) level .....	85
Figure 40 The hippocampal superoxide dismutase (SOD) activity.....	85
Figure 41 The hippocampal nrf2 expression .....	86
Figure 42 The hippocampal apoptotic and anti-apoptotic proteins expression .....	87



## CHAPTER I

### INTRODUCTION

Type 2 diabetes mellitus (T2DM) is a chronic metabolic disorder. Its characteristics are hyperglycemia, hyperinsulinemia, and insulin resistance<sup>(1)</sup>. Chronic hyperglycemia and insulin resistance are considered major causes of diabetic complications. This complication mainly affects the vascular system and organs such as the brain leading to brain structural and functional alteration<sup>(2, 3)</sup>. It is well established that long-term deleterious effects of T2DM in the brain lead to cognitive impairment<sup>(4, 5)</sup>. Several epidemiological, cognitive, and neuropathological evidence demonstrated a link between T2DM and neurodegenerative diseases such as Alzheimer's disease (AD)<sup>(6, 7)</sup>. The cellular and molecular mechanisms that underline diabetes-induced cognitive impairment are still not completely understood but can involve impaired insulin signaling, inflammation, beta-amyloid (A $\beta$ ) accumulation, and oxidative stress that promote neuronal dysfunction and neuronal apoptosis<sup>(4, 8, 9)</sup>. A $\beta$  proteins that accumulate to form the neurological hallmark of T2DM and AD have crucial roles in the pathogenesis of these diseases<sup>(10)</sup>. The production of A $\beta$  peptides is generated by beta-site amyloid precursor protein cleaving enzyme 1 (BACE1) or  $\beta$ -secretase, which cleaves an extracellular domain of amyloid precursor protein (APP)<sup>(11)</sup>. The accumulation of A $\beta$  and activation of BACE1 enzyme may be activated by oxidative stress. Previous studies demonstrated that the brain A $\beta$  and BACE1 were increased in type 2 diabetic mice, resulting from impaired insulin signaling and oxidative stress<sup>(12, 13)</sup>. A $\beta$  accumulation can lead to a release of pro-inflammatory cytokines and ultimately block downstream signaling pathways, including PI3K/Akt/MAPK pathway. The disruption of the PI3K pathway leads to synaptic and neuronal dysfunction, which promotes neurodegeneration<sup>(14, 15)</sup>. There are some evidences suggested that increased reactive oxygen species (ROS) production initiates APP processing and then triggers the generation of A $\beta$ . Therefore, oxidative stress might increase the production and accumulation of A $\beta$ <sup>(15, 16)</sup>.

It is widely known that oxidative stress plays a role in neurotoxicity<sup>(17-19)</sup>. Oxidative stress occurs when the oxidizing substances exceed the antioxidant system capacity. The cellular defense system nuclear factor erythroid 2-related factor 2 (nrf2) is the transcription factor that regulates the gene transcription of an antioxidant enzyme to attenuate oxidative stress-induced cellular damage<sup>(20)</sup>. The upregulation of nrf2 target genes, including superoxide dismutase (SOD), glutathione s-transferase, and catalase, promotes neuronal resistance to oxidative stress conditions<sup>(21, 22)</sup>. Manczak *et al.* (2006) reported that the level of nrf2 was reduced in the hippocampus of AD patients<sup>(23)</sup>. According to Uruno *et al.* (2020), the nrf2 pathway in the transgenic AD mice was impaired and concomitant with increased A $\beta$  accumulation in the brain<sup>(24)</sup>. Additionally, Gao *et al.* (2020) demonstrated the impairment of learning and memory in diabetic rats associated with a significant reduction in the hippocampal nrf2<sup>(25)</sup>.

In addition, previous research demonstrated that A $\beta$  induces NADPH oxidase (NOX) activation, generates more superoxide anions ( $O_2^{\cdot-}$ ), glutathione (GSH) reduction, lipid and protein damage, glucose homeostasis impairment, and mitochondria dysfunction. Furthermore, the enhanced NOX activity promotes ROS overproduction resulting in oxidative stress<sup>(26)</sup>. In the insulin resistance brain, the high ROS activates neuronal apoptosis through enhancing pro-apoptotic proteins (Bax, Bad, and Bak), decrease anti-apoptotic Bcl2, and activated caspases signaling activation. Several studies suggested that A $\beta$  accumulation in the brain induces neuronal cell death through apoptosis associated with oxidative stress<sup>(27, 28)</sup>. Muthaiyah *et al.* (2011) reported that exposure of A $\beta$  to PC12 cells activated ROS generation and induced neuronal cell death<sup>(29)</sup>.

Moreover, an *in vitro* study by Wang *et al.* (2009) and Zhang *et al.* (2010) showed A $\beta$ -induced neuronal cell death through the increased expression of Bax and caspase3 in human neuroblastoma, SH-SY5Y cells. They suggested that oxidative stress plays a role in A $\beta$ -induced neuronal cell death through the apoptosis pathway<sup>(30, 31)</sup>. Additionally, Soleymaninejad *et al.* (2017) reported that diabetic rats exhibited hippocampus neuron cell death, resulting from the high expression of Bax/Bcl2 and

Bax/Bcl-xL ratio. They also found that insulin treatment could prevent cell death by reversing apoptotic protein and anti-apoptotic protein alterations in the hippocampus<sup>(32)</sup>. It is well recognized that apoptosis is a crucial mechanism for hyperglycemia and insulin resistance-induced neuronal cell death<sup>(33)</sup>. Enzyme cysteine protease (caspase) and proteins of the Bcl2 family are related to the apoptosis mechanism<sup>(33, 34)</sup>. Caspase3 is the most important key regulator in promoting apoptosis. Bcl2 family is composed of Bcl2 and Bax proteins which are functionally opposed. Bcl2 is the apoptosis inhibitory protein, whereas Bax acts to promote apoptosis<sup>(35)</sup>.

Recently, herbal medicine has increasingly gained attention as a protector of diabetic complications, including cognitive impairment and AD. One of the Thailand crops, the pumpkin, is interesting because they are widely cultivated. Pumpkin seed oil is a supplement for natural essential fatty acids, polyunsaturated fatty acids, and vitamin E (tocopherol)<sup>(36)</sup>. Abou *et al.* (2014) demonstrated that the PSO administration increased the hepatic SOD and glutathione peroxidase activities in alcohol-induced hepatotoxicity rats<sup>(37)</sup>. The study by Eraslan *et al.* (2013) reported that PSO reduced the concentration of serum lipid peroxidation and malonaldehyde (MDA) content in subacute aflatoxin-induced poisoning mice<sup>(38)</sup>. Moreover, MAJID *et al.* (2020) demonstrated that PSO consumption had shown hypolipidemic activity by increasing the level of high-density lipoprotein cholesterol (HDL) in metabolic disorder patients<sup>(39)</sup>.

Interestingly, PSO contains unsaturated and saturated fatty acids, including linoleic acid, oleic acid, alpha-linoleic acid, and palmitic acid<sup>(40)</sup>. Eyjolfson *et al.* (2004) studied the effect of linoleic acid, which is a major unsaturated fatty acid component from PSO, on obese diabetic rats. They suggested that linoleic acid have anti-diabetic property by reducing fasting blood glucose and improving insulin sensitivity<sup>(41)</sup>. In addition, Feng *et al.* (2006) reported that linoleic acid activates pancreatic  $\beta$ -cell function<sup>(42)</sup>.

Based on the above reviews, no studies examined the protective effect of PSO in type 2 diabetes-induced cognitive impairment. Therefore, in the present study, the effects of pumpkin seed oil administration on the improvement of cognitive impairment,



A $\beta$ -induced neurotoxicity, oxidative stress, and neuronal apoptosis were studied both *in vitro*; human neuroblastoma cell (SH-SY5Y cell) and *in vivo*; high fructose drinking water combined with low dose streptozotocin induced type 2 diabetic rat model.



## CHAPTER II

### REVIEW LITERATURE

#### 1. Diabetes mellitus

Diabetes mellitus (DM) is a chronic metabolic disorder. It is characterized by elevated blood glucose concentration or hyperglycemia which resulting from insulin deficiency or insulin resistance (IR). A diabetic patient may decrease the body's ability to respond to insulin or reduce insulin production. This process leads to abnormalities in the metabolism of lipids, proteins, and carbohydrates. Long-term DM causes many complications, including diabetic retinopathy, nephropathy, sexual dysfunction, and neurodegenerative diseases<sup>(43)</sup>.

##### 1.1 Diagnostic of diabetes mellitus

The clinical diagnostic of DM is an assessment of symptoms such as thirst and weight loss. Besides, DM may diagnose based on the plasma glucose, fasting plasma glucose (FBG), and plasma glycosylated hemoglobin (HbA1c) levels are presented in table 1<sup>(44)</sup>.

Table 2 The criteria for diabetes mellitus

1. Fasting plasma glucose	$\geq 126$ mg/dL or $\geq 7.0$ mmol/L
2. Two hours plasma glucose	$\geq 200$ mg/dL or $\geq 11.1$ mmol/L
(During an oral glucose tolerance test)	
3. Plasma HbA1c	$\geq 6.5\%$

Fasting is no caloric intake for at least 8 hours.

##### 1.2 Types of diabetes mellitus

The classification of DM was published by WHO in 1980 (WHO Expert Committee on Diabetes mellitus, 1980)<sup>(44)</sup>. There are many types of DM, such as insulin-dependent diabetes mellitus (IDDM) or type 1 diabetes mellitus (T1DM), non-insulin

dependent diabetes mellitus (NIDDM) or type 2 diabetes mellitus (T2DM), gestational diabetes mellitus (GDM), and other types following general categories:

**Type 1 diabetes mellitus (T1DM)** or insulin-dependent diabetes mellitus (IDDM)

**Type 2 diabetes mellitus (T2DM)** or non-insulin dependent diabetes mellitus (NIDDM)

**Impaired glucose homeostasis:** a metabolic stage between normal glucose homeostasis and diabetes mellitus

**Impaired fasting glucose (IFG):** fasting blood glucose is higher more than normal condition, and less than the diagnostic state

**Impaired glucose tolerance (IGT):** after intake of a glucose at 75 grams, the fasting blood glucose higher than the normal condition

**Gestational diabetes mellitus (GDM):** impairment of glucose tolerance in pregnancy

## 2. Type 2 diabetes mellitus

Type 2 diabetes mellitus (T2DM) has become the most frequently encountered metabolic disorder in the world, the most common form of DM. T2DM is first described as a group of metabolic diseases in 1988<sup>(44)</sup>. In 2020, there were approximately 250 million people affected by T2DM worldwide. Insulin resistance (IR) plays a role in its development. IR results from the interaction between genetic and environmental factors. Environmental factors include the lack of exercise, overeating, smoking, alcohol drinking, and aging. In approximately 55% of T2DM cases, obesity is the major risk factor for IR and T2DM development<sup>(45)</sup>. People who have T2DM are leading to various short- and long-term complications. The complication from T2DM is included cardiovascular disease, diabetic retinopathy, nephropathy, and neurodegeneration<sup>(46)</sup>.

The pathogenesis of T2DM involves two fundamental abnormalities: 1) resistance to the biological activities of insulin in glucose and lipid metabolisms and 2) inadequate insulin secretion from the pancreatic  $\beta$ -cells. Prospective studies in diabetic

patients have shown that reduced insulin sensitivity is the first detectable abnormality, occurring many years before the onset of hyperglycemia<sup>(47, 48)</sup>.

### 3. Insulin function

#### 3.1 Peripheral insulin function

The peripheral insulin signaling is a biochemical pathway by increases the glucose uptake into adipose tissues and skeletal muscle, reduces liver glucose synthesis, and regulates glucose homeostasis. Figure 1 shows the peripheral insulin signaling, the insulin binds to its receptor, triggers the phosphorylation of insulin receptor substrate (IRS), and forms phosphatidylinositol 3-kinase (PI3K). After that, PI3K changes phosphatidylinositol 4,5-bisphosphate (PIP<sub>2</sub>) to phosphatidylinositol 3,4,5-trisphosphate (PIP<sub>3</sub>) and stimulates the signaling of phosphoinositide-dependent protein kinase 1 (PDK1)/Akt (PKB). PI3K/Akt signaling regulates the metabolic while Ras-mitogen-activated protein kinase pathway activates cell growth<sup>(49)</sup>.

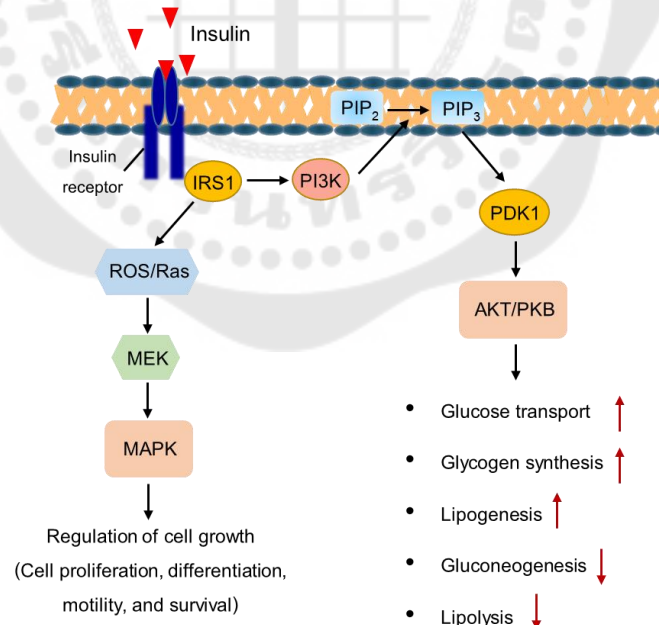
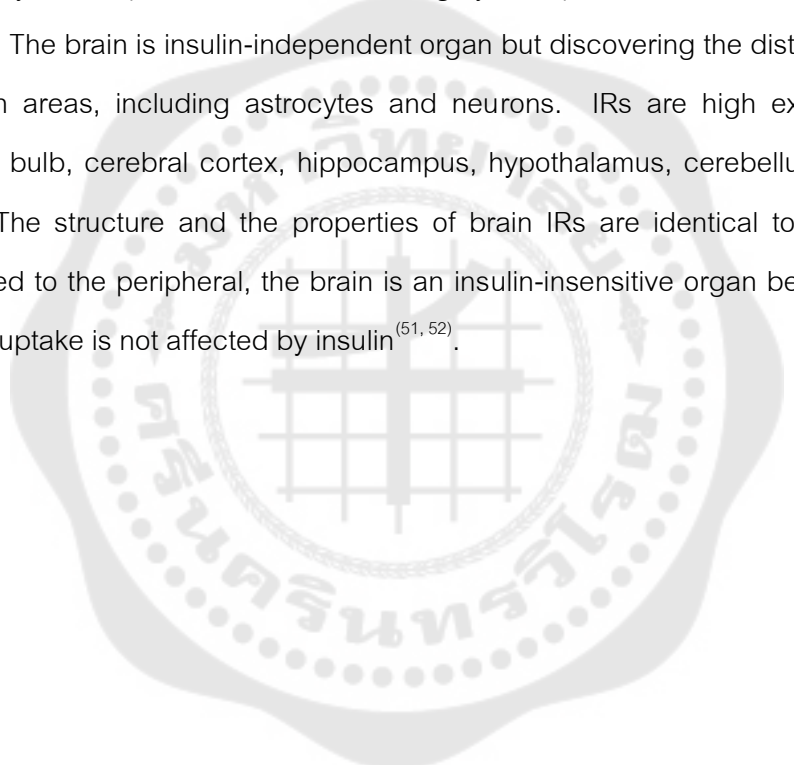


Figure 1 Peripheral insulin signaling

The picture of peripheral insulin signaling modified from Jung *et al.* (2004)<sup>(49)</sup>.

### 3.2 Brain insulin function

In the brain, most insulin comes from the peripheral. Moreover, insulin can be synthesized by the neurons in the brain. The peripheral insulin can pass the blood-brain barrier (BBB) into the brain through a receptor-mediated active transport (Figure 2). The BBB is formed by the endothelial cell composing insulin binding sites. There are two functions of the insulin binding sites are 1) as an insulin transporter across BBB to the brain and 2) as a classic insulin receptor. Insulin may induce glycoprotein expression, which plays an important role in BBB integrity and protect the brain from exogenous toxins<sup>(50)</sup>. The brain is insulin-independent organ but discovering the distribution of IRs in the brain areas, including astrocytes and neurons. IRs are high expression in the olfactory bulb, cerebral cortex, hippocampus, hypothalamus, cerebellum, and choroid plexus. The structure and the properties of brain IRs are identical to peripheral IRs. Compared to the peripheral, the brain is an insulin-insensitive organ because the brain glucose uptake is not affected by insulin<sup>(51, 52)</sup>.



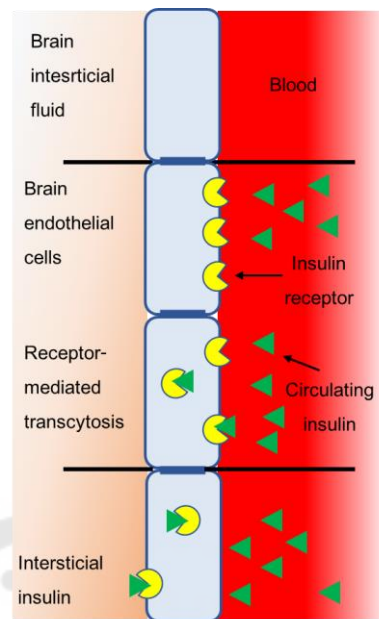


Figure 2 Peripheral insulin may pass the blood-brain barrier through a receptor-mediated transport system

The picture modified from Blázquez *et al.* (2014)<sup>(53)</sup>. In the central nervous system (CNS), insulin controls the food intake and weight by regulating the hypothalamus neuronal activity, reproductive regulation, regulates neuronal proliferation and differentiation, promotes neurite outgrowth, prevents neuron apoptosis, protects neurons against oxidative stress, and cognition.

Insulin-IRs binding activates two signaling pathways, including PI3K/ PDK1/ Akt pathway and the Ras/ extracellular signal-regulated kinase ( ERK) pathway (Figure 4). Insulin signaling in the CNS has regulated the peripheral tissues ( liver and adipose tissue) which are controlled through insulin action in the hypothalamus (Figure 3). The metabolic effects of the brain insulin signaling, including hepatic glucose production, lipolysis, amino acids, and hepatic triglyceride secretion<sup>(54)</sup>.

In the brain, IRs are expressed in neurons and glial cells. Insulin binds to IRs lead to the phosphorylation of intrinsic receptor tyrosine kinases to promoting downstream signaling that inhibits apoptosis and stimulates neuronal cell growth, neuronal survival, synaptic plasticity, and cognition<sup>(54, 55)</sup>.

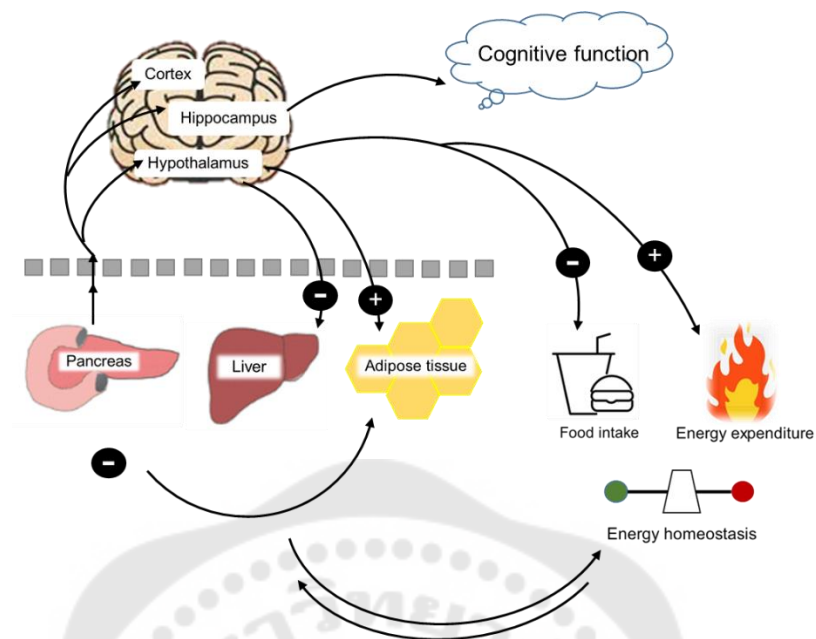


Figure 3 Central nervous insulin effects

The figure of the central nervous insulin effects modified from Hallschmid *et al.* (2009)<sup>(56)</sup>. In CNS, insulin regulates cognition, food intake, energy expenditure, and energy homeostasis.

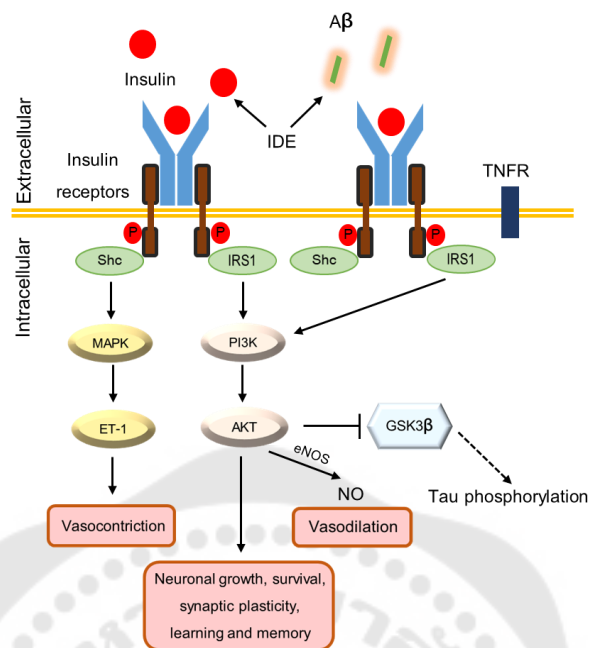


Figure 4 Brain insulin signaling

The figure of brain insulin signaling modified from Bedse *et al.* (2015)<sup>(57)</sup>. Under normal conditions, insulin binds with IRs leading to the insulin receptor substrate-1 (IRS1) phosphorylation, phosphoinositide 3-kinase (PI3K) activation, activating downstream signaling to modulate the neuronal cell growth, neuronal survival, synaptic plasticity, and cognition. In addition, the activation of IRS modulating the balance of vasodilatation and vasoconstriction.

#### 4. Insulin resistance (IR)

Insulin resistance (IR) is a core feature of T2DM, defined as a decreased the ability of insulin on the regulation of skeletal muscle and adipose glucose uptake and suppression of glucose output. IR is present for many years before the blood glucose level abnormality progression<sup>(58)</sup>. IR is a common characteristic of metabolic disorders such as obesity, dyslipidemia, metabolic syndrome, and T2DM<sup>(59)</sup>. IR is related with many factors, including obesity, aging, sedentary lifestyle, and genetic predisposition, which obesity is a significant risk factor. IR also contributes to many complications, including cardiovascular disease (CVS), diabetic retinopathy (DR), nephropathy, and neurodegenerative disease<sup>(60)</sup>.

##### 4.1 Peripheral insulin resistance

The effects of insulin, insulin deficiency, and IR vary according to the physiological tissues and organ's function concerned and their dependence on



metabolic processes, including adipose tissue and skeletal muscles. However, a recent report indicated that other factors may be important to induce IR are peptide hormones, inflammatory cytokines, and oxidative stress<sup>(61)</sup>.

The common insulin signaling pathways, including PI3K/Akt and MAPK pathways. IR results in 1) the impairment of the skeletal muscle, liver, and adipose tissue glucose uptake, 2) reduction of the liver and skeletal muscle glycogen synthesis, 3) increased hepatic gluconeogenesis, 4) increased lipolysis, and free fatty acid (FFA) release from adipose tissue. In IR condition, the pancreatic  $\beta$ -cell may increase insulin production and release to compensate, in this process leading to hyperinsulinemia. The compensation occurs when increasing insulin secretion from pancreatic  $\beta$ -cell to maintain the blood glucose level<sup>(62, 63)</sup>. It's well known that IR is a directly of obesity which associated with the exposure to high dietary food leading to the accumulation of toxic metabolic by-products<sup>(64, 65)</sup>. Adipocytes plays role in IR progression because they can produce adipokines, hormones and cytokines. The capacity of adipose tissue is lipid storage, resulting in abnormal accumulation and distribution of lipids to the other organs. Moreover, high plasma lipid level can activate the phosphorylation of IRs serine tyrosine kinase and impaired the insulin signaling pathway<sup>(65)</sup>.

In addition, adipocyte is an endocrine cell, which can produce and release inflammatory mediators, including leptin, tumor necrosis factor-alpha (TNF- $\alpha$ ), and adiponectin, all of these are related to IR progression. In skeletal muscle and adipose tissue, leptin and adiponectin have been recognized as anti-diabetogenic because their reduces triglyceride (TG) synthesis, stimulates  $\beta$ -oxidation, and enhances insulin action through the activating 5'-AMP-activated protein kinase (AMPK). Interestingly, the high level of leptin and low level of adiponectin are found in obese human and animal. Its suggesting that obesity induced leptin resistance and adiponectin deficiency<sup>(66, 67)</sup>. In addition, high free fatty acid (FFA) level has been found under obesity condition. Obesity affects to adipose tissue by inducing adipocyte hypertrophy, adipocyte apoptosis, FFA overproduction, and pro-inflammatory cytokines production (Figure 5)<sup>(68)</sup>. Previous studies shown the high FFA activated the inflammation through increased pro-

inflammatory cytokines and downstream signaling, including the serine kinases, IKKB, and JNK1, which inhibit IRS1 activation through promoting the IRS phosphorylation at serine sites and IRS degradation<sup>(69, 70)</sup>.

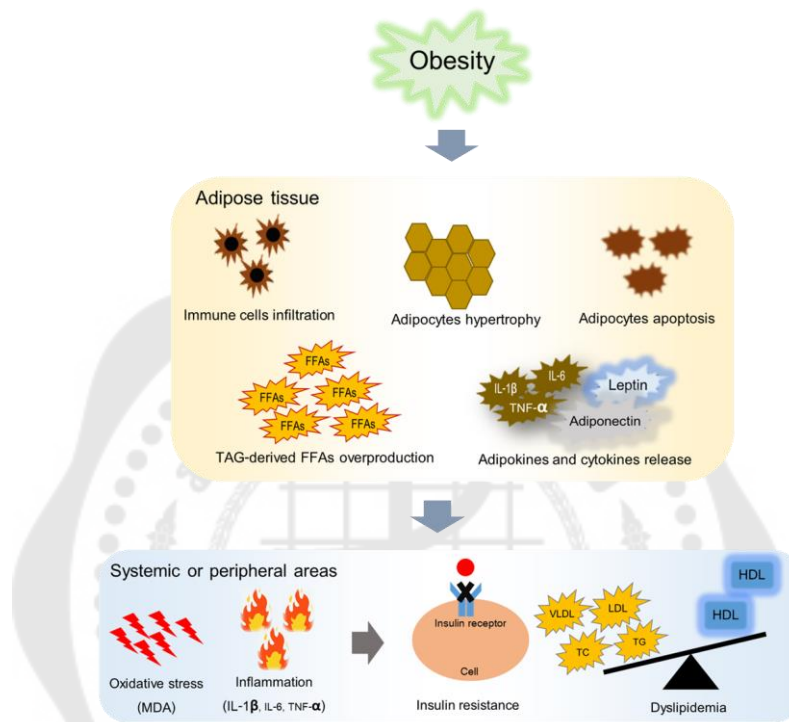


Figure 5 The obesity promoting insulin resistance

The figure shows the mechanisms of obesity-induced insulin resistance which modified from Srietchwande *et al.* (2018)<sup>(68)</sup>. Obesity is induced adipocyte hypertrophy, adipocyte apoptosis, free fatty acid overproduction, and pro-inflammatory cytokines release. These pathological conditions leading to the impairment of the cellular insulin signaling.

## 4.2 Brain insulin resistance

Peripheral IR or hyperinsulinemia alters the blood-brain barrier (BBB) function by reducing the IRs and BBB permeability, resulting in brain insulin functions impairment<sup>(71)</sup>. Brain IR defines as the brain cells cannot response to insulin action. At the cellular level, brain IR lead to the impairment of neuroplasticity, neurotransmitter release, and the processes that related with insulin metabolisms, including neuronal glucose uptake and inflammatory responses<sup>(72)</sup>.

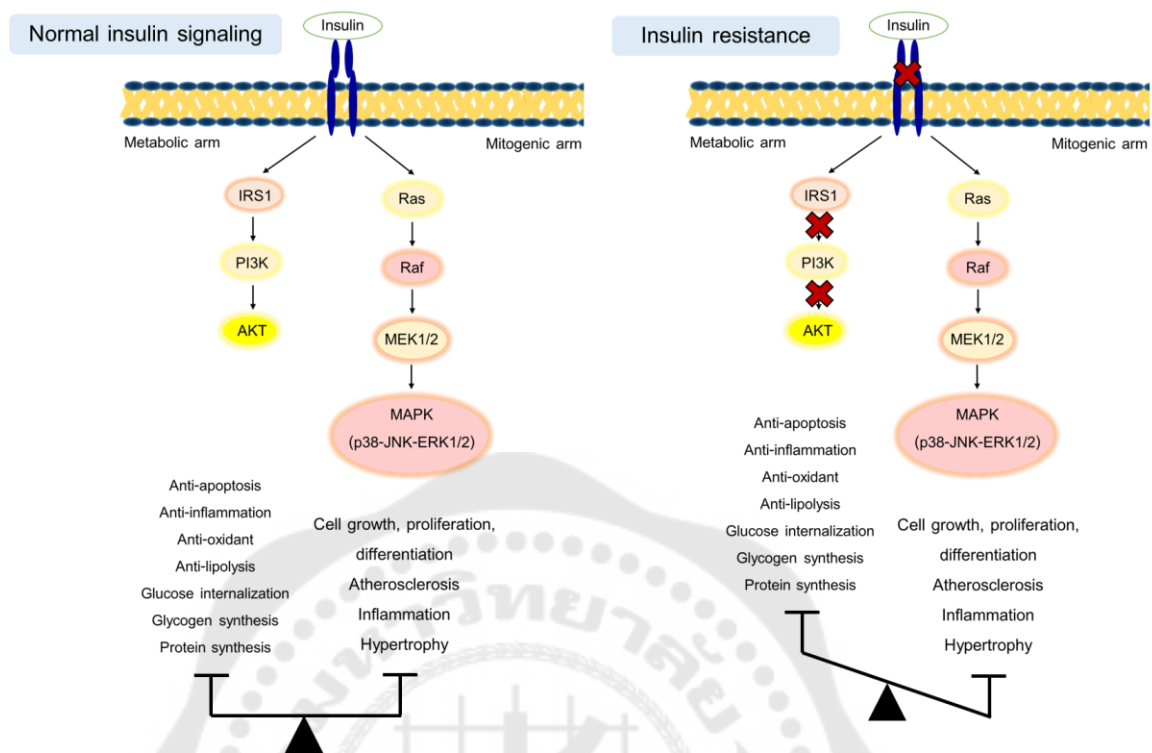


Figure 6 Insulin signaling pathway under normal and insulin resistance

The figure shows insulin signaling pathway and its impairment under insulin resistance condition which modified from D'Oria *et al.* (2017)<sup>(73)</sup>. Under insulin resistance condition, the impairment of PI3K signaling and downstream signaling leads to excessive the mitogenic arm stimulation, contributing to endothelial dysfunction and cardiovascular diseases<sup>(73)</sup>.

The binding of insulin and its receptor resulting the balanced of insulin signaling through PI3K/Akt pathway (metabolic regulation) and Ras/MAPK pathway (mitogenic regulation) (Figure 6). Metabolic effects of insulin regulating the glucose transport, glycogen synthase, protein synthesis, lipolysis, apoptosis, oxidative stress, and inflammation. Non-metabolic effects of insulin regulating the cell proliferative, cell survival, and inflammation. Under IR condition, the PI3K/Akt signaling is impaired caused by hyperglycemia, hyperlipidemia, and hyperinsulinemia, resulting in the more stimulation of the mitogenic arm and contributing to cardiovascular and endothelial dysfunction<sup>(73)</sup>.

## 5. Type 2 diabetes mellitus and cognitive impairment

The effects of T2DM on the brain are recognized. One of all dementia cases in the world may be effects from T2DM<sup>(2)</sup>. The most important mechanisms are insulin signaling impairment, accumulation of A $\beta$ , hyperphosphorylation of Tau protein, damage of the vascular, and inflammation (Figure 7).

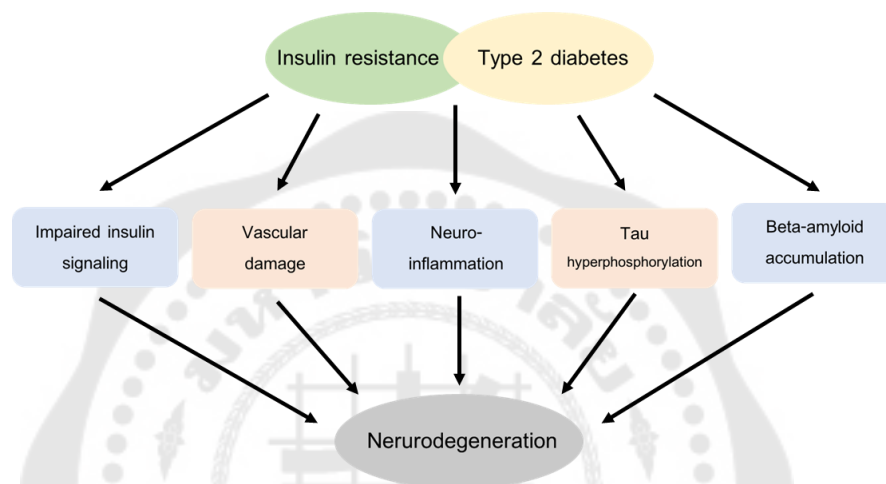


Figure 7 The association between T2DM or insulin resistance and neurodegeneration

The figure shows type 2 diabetes mellitus and insulin resistance causes of the neurodegenerative progression which modified from Tumminia *et al.* (2018)<sup>(74)</sup>. Type 2 diabetes mellitus and insulin resistance can impact on the brain leading to the synaptic plasticity impairment, impaired neuronal insulin signaling, vascular damage, neuroinflammation, tau phosphorylation, and A $\beta$  accumulation, resulting in the progression of neurodegeneration<sup>(75)</sup>.

In the brain, insulin plays a major role in the synaptic plasticity and cognitions. Therefore, insulin signaling impairment promoting cognition decline. There has been a reported on T2DM-induced neurodegenerative progression and refers to type 3 diabetes mellitus ( T3DM)<sup>(76)</sup>. It has been proposed that AD and diabetes have pathogenesis similarities, including insulin sensitivity and signaling impairment, A $\beta$  accumulation, Tau hyperphosphorylation, vasculopathy, mitochondrial dysfunction, oxidative stress, and inflammation. Numerous recent studies indicated that insulin signaling deficits arise due to IR occurs in AD patients. The impaired insulin signaling leads to cognitive impairment through induced various mechanisms, including inflammation, oxidative stress, A $\beta$  accumulation, and neuronal cell death<sup>(2, 4, 75)</sup>.

### 5.1 Obesity

The obesity is a metabolic disorder and association with various complications, including cardiovascular diseases, diabetes mellitus, and neurodegeneration<sup>(4, 77)</sup>. Numerous studies have demonstrated that obesity is correlated with cognitive impairment and AD. *In vivo* and clinical studies showed that obesity induced cognitive impairment through several mechanisms, including the leptin signaling impairment, A $\beta$  accumulation, and Tau protein hyperphosphorylation (pTau)<sup>(78)</sup>. Under IR condition, hyperinsulinemia disturbs the normal function of several vital organs, including brain. Previous studies demonstrated that obesity not only induces peripheral IR but can also lead to the brain IR development resulting in an impairment of long-term depression (LTD) through reducing brain insulin signaling<sup>(68, 79)</sup>. The possible for brain IR due to peripheral IR is high ceramide production from the liver. Ceramide is a compound of sphingosine and fatty acid. Ceramide can cross the BBB into the brain. Ceramide can stimulate oxidative stress, inflammation, and insulin resistance, which leading to the cognitive decline<sup>(80, 81)</sup>.

### 5.2 Inflammation

Previous research demonstrated that AD patients have decreased oxygen supplying to the brain, glucose, and nutrient and lead to decreased regional cerebral blood flow (rCBF). An impaired insulin signaling pathway partially mediates this phenomenon<sup>(82, 83)</sup>. Insulin signaling activates PI3K/Akt to regulation the vasodilation and vasoconstriction via endothelial nitric oxide synthase (eNOS) activation and nitric oxide (NO) production<sup>(84)</sup>. Under IR condition, PI3K signaling impairment leads to disrupt NO production and promotes vasoconstriction. Moreover, the decrease of blood supply to the brain lead to reduction in brain nutrient, which stimulated ROS production, oxidative stress, and inflammatory response<sup>(85, 86)</sup>.

Under peripheral IR condition, the production of pro-inflammatory cytokines can activate the IRS-1 serine phosphorylation (an inhibitor of IKK, JNK, and ERK2), which alters the insulin signaling by blocking the intracellular actions of insulin<sup>(87)</sup>. In the brain, the accumulation of A $\beta$  oligomer activates microglia cell resulting in pro-

inflammatory cytokines production and secretion<sup>(88)</sup>. T2DM and AD showed the elevated vascular pro-inflammatory cytokines, which interrupts brain insulin signaling<sup>(89, 90)</sup>.

### 5.3 Oxidative stress

Oxidative stress is an imbalance between the reactive oxygen species (ROS) production and antioxidant systems<sup>(91)</sup>. Oxidative stress has been shown to play a role in pathogenesis of AD<sup>(91-93)</sup>. IR progression relates with oxidative stress, DNA damage, reduced glucose utilization, a vicious mechanism resulting in cognitive impairment. The oxidative stress activates the damaging of proteins, lipids, and nucleic acids. Oxidative stress is disrupting cell metabolism and signaling, increases pro-inflammatory cytokine, and promoting cell death<sup>(92-95)</sup>.

Many studies indicated that people with T2DM have increased the ROS production and reduced antioxidant defense<sup>(96)</sup>. However, obesity is a strong risk factor of IR development through the activated adipocyte-derived factors release, such as tumor necrosis factor- $\alpha$  (TNF- $\alpha$ ), leptin, adiponectin, and FFA. Previous studies found that increased FFA levels can decreased insulin sensitivity and inhibited insulin signaling<sup>(97)</sup>. Moreover, high FFA concentration is a cause of mitochondrial dysfunction through increasing of superoxide production and impaired endogenous antioxidant defenses<sup>(98, 99)</sup>. The endogenous antioxidant prevents the cells from oxidative stress by increasing the cytoprotective enzymes through the regulation of the transcription factor nuclear factor erythroid 2-related factor 2 (Nrf2)<sup>(9, 100, 101)</sup>.

The oxidative stress protection of the cell is occurred at the transcriptional level. The Nrf2/Keap1/ARE is a mediator for these responses, which its regulating the expression of genes related to oxidative stress and cell survival, including antioxidant proteins, detoxification enzymes, toxic transportation, free radical metabolism, inhibition of inflammation, glutathione homeostasis, proteasome function, and DNA damage recognition (Figure 8)<sup>(9, 102)</sup>.



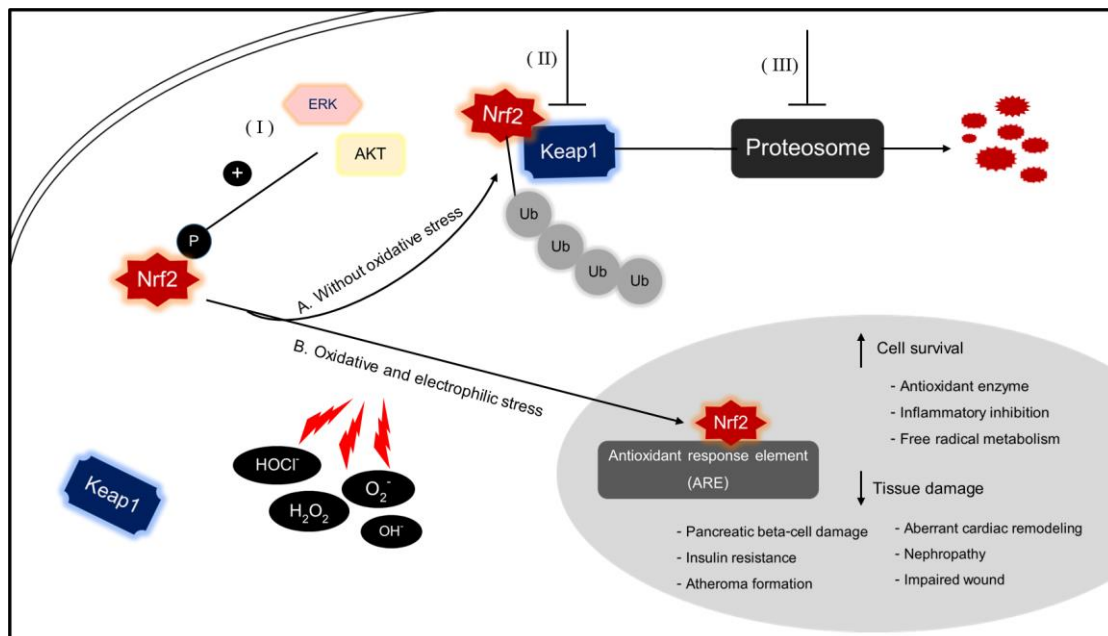


Figure 8 The Nrf2/Keap1/ARE signaling in type 2 diabetes mellitus

The figure of the Nrf2/Keap1/ARE pathway in type 2 diabetes mellitus modified from David *et al.* (2017)<sup>(103)</sup>. (A) under non-stressed and (B) under oxidative stress.

Under non-stress stimulation (A in Figure 8), the Nrf2 transcription factor binds to cysteine on Keap1 in the cytoplasm, resulting in an antioxidant response inhibition through ubiquitination and degradation by proteasome. Under oxidative stress condition (B in Figure 8), cysteine on Keap1 is modified and Nrf2 is translocate into the nucleus. In the nucleus, Nrf2 binds to the ARE and stimulates cytoprotective enzymes transcription to promoting cell survival through a several mechanisms, including the antioxidant defense, inflammatory inhibition, and the toxic metabolites transport. These cellular adaptations have been improved the tissue damage under the pathogenesis<sup>(9, 104, 105)</sup>.

Studies by Uruno *et al.* suggesting that Nrf2 activation improves insulin sensitivity in diabetes<sup>(106)</sup>. Moreover, more recent studies in the murine model indicate that Nrf2 signaling can improve IR via oxidative stress suppression<sup>(20, 106, 107)</sup>. Under brain IR, the overproduction of ROS is related with ATP production impairment, pro-inflammatory cytokines release, beta-amyloid accumulation, and neuronal apoptosis.

Thus, oxidative stress-induced cognitive impairment is associated with neuronal cell death through the apoptotic pathway by increased pro-apoptotic proteins (Bcl-2) and activation of caspase activities<sup>(108)</sup>.

#### 5.4 Mitochondria dysfunction

Mitochondria is recognized that subcellular organelle. It is essential for energy generation for the cellular function<sup>(109)</sup>. Mitochondria is an importance organelle of the cell not only for bioenergetic role but also involved in ion homeostasis, apoptosis, inflammation, and ROS production<sup>(110, 111)</sup>. DM and AD are correlated with impaired glucose homeostasis, mitochondrial dysfunction, and metabolic impairment. Inhibition of energy production has been reduced the secretion and action of insulin<sup>(3, 110)</sup>. Thus, insulin signaling impairment or IR can activate oxidative stress in both peripheral organs and brain. The oxidative stress occurs under brain IR resulting from the mitochondria dysfunction. Mitochondria dysfunction has demonstrated that is an early occur in the disease process. IR and insulin signaling alteration promoting the mitochondria dysfunction and oxidative stress. Moreover, oxidative stress also stimulating to the impaired cellular energy production, reduction of insulin secretion, and insulin sensitivity<sup>(111, 112)</sup>.

#### 5.5 Beta-amyloid accumulation

Brain IR stimulates the A $\beta$  accumulation and oxidative stress<sup>(112)</sup>. A $\beta$  peptides and formation of extracellular A $\beta$  plaques are pathogenesis AD hallmarks. Normally, insulin regulates brain A $\beta$  clearance, extracellular accumulation, and plaque formation. Several studies in the brain IR reported that ROS overproduction enhances the A $\beta$  accumulation and induces the proteins, lipids and nucleic acid damage<sup>(11)</sup>.



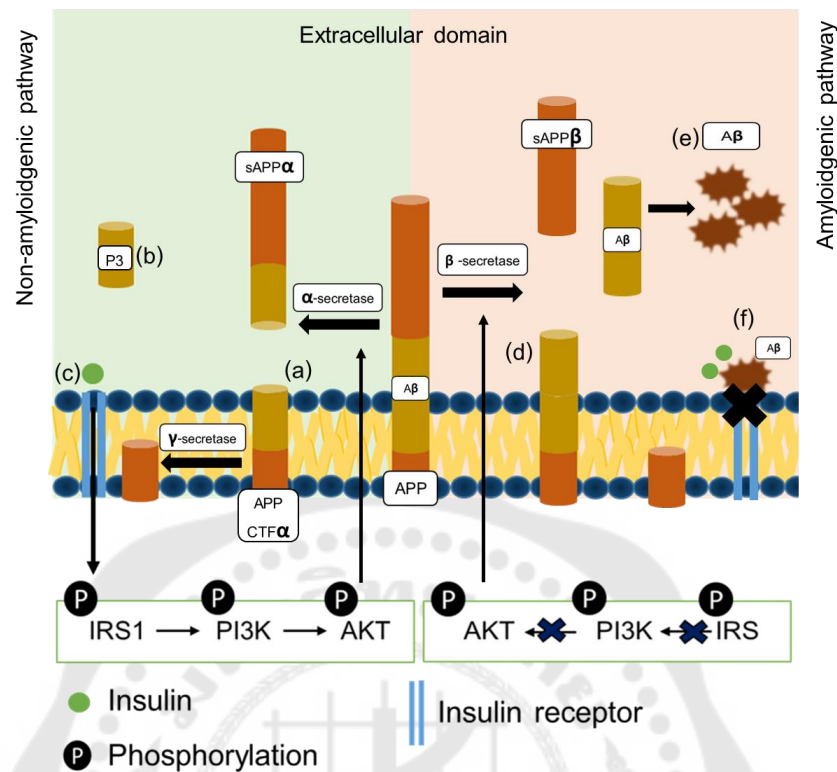


Figure 9 APP processing under normal and insulin resistance conditions

The figure of APP processing under normal and insulin resistance conditions modified from Shieh *et al.* (2020)<sup>(113)</sup>

Insulin signaling impairment directly contributes to A $\beta$  accumulation.

A $\beta$  peptide is generated through non-amyloidogenic and amyloidogenic pathways. In non-amyloidogenic pathway, APP is cleaved by  $\alpha$ -secretase, releasing an extracellular soluble APP $\alpha$  (sAPP $\alpha$ ) and an intracellular C-terminal of APP (APP-CTF $\alpha$ ) (Figure 9). Next, the peptide is cleaved by  $\gamma$ -secretase releasing p3 fraction. The sAPP $\alpha$  is the normal by-product, which play roles in neuronal and brain development<sup>(114)</sup>.

Under IR condition, APP is cleaved by  $\beta$ -secretase and releasing the sAPP $\beta$  and APP-CTF $\beta$  through amyloidogenic pathway. Next, the A $\beta$  is cleaved by  $\gamma$ -secretase and releasing insoluble A $\beta$  lead to A $\beta$  aggregates into A $\beta$  plaques. A $\beta$  plaques can degrades IRs and competitive binding with insulin to IRs causing the impairment of the insulin signaling and leading to activation of  $\alpha$ -secretase and  $\beta$ -secretase<sup>(114)</sup>. The activation of  $\alpha$ -secretase and  $\beta$ -secretase leading to the toxic A $\beta$  production.

The impairment of brain insulin signaling contributes to cognitive impairment through the activation of A $\beta$ PP-A $\beta$  by increasing APP expression, A $\beta$  accumulation, and oxidative stress. Under IR condition, chronic hyperinsulinemia induced cognitive impairment through increased A $\beta$ PP-A $\beta$  accumulation and reduced its clearance in the CNS. On the other hand, A $\beta$ PP-A $\beta$  can promote IR. This evidence suggests that a positive feedback loop of cognitive impairment progression can develop by IR drives A $\beta$  production and A $\beta$  peptide deposition. Normally, insulin regulates A $\beta$  clearance through promoting insulin-degrading enzyme (IDE) activity, is A $\beta$  scavenger protease. Insulin signaling regulates the expression IDE enzyme and can directly be competitive with A $\beta$  for binding to IDE. Therefore, the insulin signaling impairment results in decreased IDE expression leading to A $\beta$  accumulation and A $\beta$  plaques formation in the brain<sup>(10, 114)</sup>.

### 5.6 Hyperphosphorylation of Tau protein

The insulin signaling deficit exacerbates cognitive dysfunction by enhancing the phosphorylation of Tau protein, a neuronal microtubule-associated protein. Tau protein plays a role in the assembly and stability of microtubules and vesicle transport. The hyperphosphorylation Tau (pTau) lead to form neurofibrillary tangles (NFTs), the pathological hallmark in AD. Smaller aggregates of pTau contributing to neuronal dysfunction and degeneration<sup>(115)</sup>. Insulin regulates pTau by inhibiting GSK-3 $\beta$  activity, a critical kinase that phosphorylates Tau. The brain insulin signaling impairment leading to a reduction of Akt activity, increases GSK-3 $\beta$  activity, and phosphorylation of Tau protein<sup>(116, 117)</sup>. The enhancing of GSK-3 $\beta$  activity in T2DM might elevate production and increased Tau phosphorylation<sup>(118, 119)</sup>.

## 6. Apoptosis

### 6.1 Apoptotic pathways

Apoptosis is a physiological process of cell death. It is characterized by cell shrinkage, chromatin condensation, DNA fragmentation, and disassembly into apoptotic bodies. Apoptosis occurs when the pro-apoptotic mediators (Bad, Bid, Bik, and Bax) higher than the anti-apoptotic mediators (Bcl-2 and Bcl-xL). Apoptosis is divided into the extrinsic (death receptor) pathway and the intrinsic (mitochondrial pathway) (Figure

10)<sup>(33)</sup>. The characterized of apoptosis are activation of caspases, DNA and proteins breakdown, and phagocytes. Caspase is the cysteine protease family which widely expressed in most cells<sup>(33, 120)</sup>.

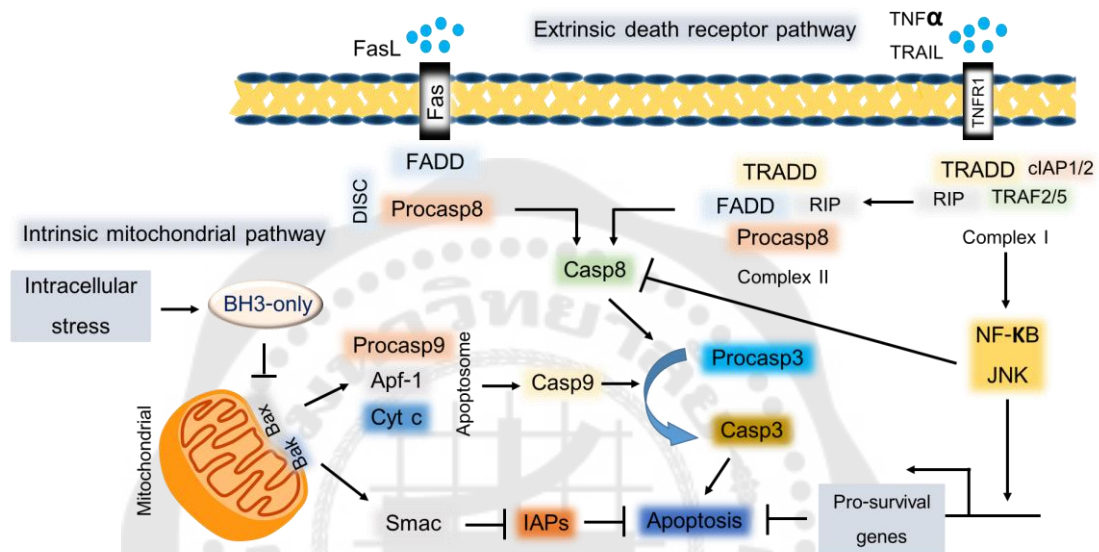


Figure 10 Extrinsic and intrinsic pathways of apoptosis

The extrinsic and intrinsic pathways of apoptosis modified from Elmore *et al.* (2007)<sup>(33)</sup>.

### 6.1.1 Extrinsic pathway

The extrinsic pathway is initiated by the binding of ligands (Fas ligand and Fas receptor (FasL/ FasR), tumor necrosis factor (TNF), TNFR1, Apo3L/ DR3, Apo2L/DR4 and Apo2L/DR5) to the death receptors at cell membrane<sup>(144)</sup>. This domain plays a role in extracellular death signaling-induced intracellular apoptotic through the adaptor proteins recruitment (Fas-associated death domain (FADD), and TNF receptor-associated death domain (TRADD)). The FasL-FasR binding results in FADD adaptor protein recruitment, which associates with procaspase-8 inducing signaling complex (DISC) and triggers apoptosis process by activation the caspase-3 downstream pathways<sup>(121, 122)</sup>.

### 6.1.2 Intrinsic pathway

The intrinsic pathway occurs within the cell, which regulated by the anti-apoptotic proteins (Bcl-2, Bcl-xL), pro-apoptotic proteins (Bax, Bak), and BH3 proteins (Bad, Bik, Bim). The pro-apoptotic proteins are inhibited by the anti-apoptotic proteins while BH3 proteins can counteract with anti-apoptotic proteins and release the pro-apoptotic proteins to stimulate the apoptosis. Under internal stimuli (hypoxia, DNA damage, and toxins), the BH-3 protein activates Bcl-2, Bax and Bak. The activation of Bax and Bak are induced the pores on the surface of mitochondria, resulting in cytochrome c (Cyt c) release. Cyt c is binding with with Apaf-1 and procaspase-9 to form apoptosome, leading to caspase-9 activation and apoptosis process. In addition, Bax and Bak proteins can induced a second mitochondrial-derived activator of caspase (Smac), which it disrupts the interaction of IAPs with caspase3 or caspase9, and then promotes caspase activation<sup>(33, 123)</sup>.

### 6.2 Apoptosis in type 2 diabetes and cognitive impairment

Numerous evidence shown that T2DM leads to cognitive impairment through oxidative stress-induced neuronal cell apoptosis<sup>(124)</sup>. Brain IR-induced oxidative stress through brain mitochondria dysfunction leads to ATP reduction and overproduction of ROS. In addition, hyperglycemia may contribute to oxidative stress through AGE-RAGEs, inflammation, and mitochondria dysfunction. This oxidative stress from both pathologies may trigger the accumulation of A $\beta$  through activated BACE-1 enzyme activity in the brain. The mitochondria dysfunction, ROS, A $\beta$  accumulation resulting in of mitochondria Cyt c release following the caspase activities and apoptosis. Evidence supports the activation of caspases may be responsible for the neurodegeneration associated with AD. Apoptosis can assessed by the pro-apoptotic and anti-apoptotic signaling through the stimulation from the environmental or extracellular factors, such as cytokines<sup>(33, 34)</sup>.

*In vitro* and *in vivo* studies discovered that the brain mitochondrial respiration reduction, mitochondrial DNA mutation, and abnormal of mitochondrial fusion and fission are occurred under IR condition<sup>(125)</sup>. The lowering ATP synthesis is a cause of O<sub>2</sub> consumption reduction, CO<sub>2</sub> generation, and ROS overproduction. Furthermore,

enhanced ROS levels stimulates the neuronal apoptosis through high the expression of pro-apoptotic proteins ( Bax, Bad, Bak) , lower levels of anti-apoptotic Bcl2, and caspases activity<sup>(108)</sup>. Moreover, mitochondrial dysfunction in IR and T2DM are related with apoptosis, cognitive decline, and cerebral degeneration<sup>(126)</sup>.

Hippocampus is one of most of the brain sensitive area in metabolic disorders, including DM<sup>(127, 128)</sup>. Numerous studies have found that DM has impacts on hippocampal neurons apoptosis through multiple mechanisms. *In vitro* and *in vivo* research indicated that the loss of hippocampal neuronal occurs in the DM. They suggested that neuronal apoptosis may be a major mechanism contributing to cognitive impairment<sup>(129, 130)</sup>. Eight months diabetic rats showed the high expression of Bax and caspase-3 activity, which related to the decreased neuronal density and impaired cognitive performance<sup>(131)</sup>. The activation of caspases is irreversible process of cell death. Numerous studies demonstrated that the hippocampal apoptosis in DM resulting from caspase mechanisms<sup>(131, 132)</sup>.

## 7. Pumpkin seed oil

Pumpkin seed oil ( PSO) is a product obtained from the pumpkin seed. The pumpkin is a pepo-type fruit which belongs to the Cucurbita genus and the Cucurbitaceae family, largest family in plant kingdom. The food industry has used the pumpkin for produce juices, purees, jams, and alcoholic beverages. In addition, pumpkin seed contains the bioactive compounds are used as traditional medicine and functional food<sup>(36)</sup>.

The pumpkin seed is known as pepita, which is a shell flat, dark green seed. It has a yellow-white shell, but some pumpkin seed without the shell. The pumpkin seed is a high energy source of proteins, carbohydrates, vitamins, and oil. Also, the oil from pumpkin seed has gained attention in the fat and oil industry. The oil of pumpkin seed can obtain from pumpkin seed with or without the shell. The PSO has a dark greenish color. It has been used as supplement for a natural source of proteins, fatty acids,

vitamins, carotenoids,  $\beta$ - and  $\gamma$ -tocopherols, phytosterols, chlorophyll, and trace elements (zinc and selenium)<sup>(133, 134)</sup>.

### 7.1 Antioxidant activity and free radical scavenger

Pumpkin seed has a high vitamin E content (tocopherol), an antioxidant<sup>(197)</sup>. Previous research reported that the tumor mice administration of pumpkin seed extract significantly increased the hepatic superoxide dismutase (SOD) activity and glutathione peroxidase (GPx), and reduced the malonaldehyde (MDA) content in the serum<sup>(36)</sup>.

In addition, previous research was determined the total phenolic contents in the PSO results show the ranges at 25-51 mg/kg of PSO. In the animal study, the PSO administration in the rat which small bowel from destruction for five days could decreased small intestine damage, serum myeloperoxidase (MPO), prostaglandin, MDA, xanthine oxidase, and increase GSH levels. They indicated that PSO has a potential on the anti-inflammation and antioxidant properties<sup>(135)</sup>.

### 7.2 Anti-diabetic activity

Numerous research indicated that the pumpkin seed contains the compounds that decreasing blood glucose level, called tocopherol or vitamin E. The raw pumpkin seed has found tocopherol isomers ( $\alpha$ ,  $\beta$ ,  $\gamma$ , and  $\delta$ ). It has been reported to be attenuated DM through its antioxidant activity. The previous study indicated that the tocopherol from PSO could reduce the lipid profiles and blood glucose levels in diabetic rats. They demonstrated that the tocopherol from PSO has hypoglycemic property<sup>(136)</sup>.

### 7.3 Hypolipidemic activity

A previous study determined the effect of PSO treatment on the total cholesterol, low-density lipoprotein cholesterol (LDL), and high-density lipoprotein cholesterol (HDL) in ovariectomized rats. The rats treatment with PSO had a high level of healthy lipid<sup>(18)</sup>.

### 7.4 Anti-microbial activity

The PSO contains the anti-microbial components. The 2% PSO concentration could inhibit *Aeromonas veronii*, *Candida albicans*, *Enterococcus faecalis*, *Escherichia coli*, *Salmonella enterica*, and *Staphylococcus aureus*<sup>(39)</sup>.



## 8. Type 2 diabetes animal models

Animal model has a long history used to diabetes mellitus research. The animal models for type 2 diabetes research are knockout mice, and tissue-specific knockout mice, diet models, and dietary combined with streptozotocin models.

### 8.1 Mouse models

The mouse model of T2DM are C57BL/6 mice, Nagoya-Shibata-Yasuda (NSY), B6.Cg-Lepob/J, B6.BKS (D)-Leprdb/J, and NONcNZO10/LtJ mice.

C57BL/6 mice is a genetically obese. It is characterized by central adiposity, metabolic abnormalities, and impaired glucose tolerance<sup>(137)</sup>.

Nagoya-Shibata-Yasuda (NSY) mouse is a mimics model of age-related T2DM people. it is characterized by an impaired insulin secretion and action and mild obesity (visceral fat accumulation)<sup>(138)</sup>.

B6.Cg-Lepob/J and B6.BKS (D)-Leprdb/J mice are a phenotype of spontaneous T2DM. It is characterized by hyperphagia, obesity, glucose intolerance, hyperglycemia, hyperinsulinemia, and pancreatic islet  $\beta$ -cell hypertrophy<sup>(139)</sup>.

### 8.2 Dietary models

#### 8.2.1 High-fat diet (HFD) model

Obesity is the risk factor for insulin resistance and T2DM development. Therefore, diet remains a critical factor to induced obesity. Previous studies shown that long-term the consumption of diet containing 40-60% of lipid could promote metabolic disorders, obesity, adipocyte hypertrophy, hypertension, and IR<sup>(140, 141)</sup>. Moreover, HFD consumption promotes pro-inflammatory cytokines production and hypertriglyceridemia. Thus, the lipid source in the diet is important for obesity and T2DM development.

#### 8.2.2 Sucrose diet model

A high sucrose diet is a typical food in developed countries. It is an environmental factor that leads to obesity and T2DM development<sup>(45, 142)</sup>. The capacity of high sucrose intake to induce obesity and IR in rodents is dependent on the species or animal strain. Wistar rats fed a standard diet combined with 30% sucrose drinking water showed a successful the induction of obesity, hypertension, hyperlipidemia, and hyperinsulinemia<sup>(143)</sup>. The previous study demonstrated that 32% sucrose diet does not

lead to obesity in C57BL/6 mice but the diet can cause adipocytes hypertrophy, glucose intolerance, hyperinsulinemia, hyperlipidemia, hepatic steatosis, and inflammation<sup>(144)</sup>.

The mechanism of a high sucrose diet-induced IR may be altering the post-receptor of insulin signaling. The sucrose cannot alter the number of IRs and IRs phosphorylation when exposure to insulin. However, IRS-1 and IRS-2 phosphorylation are decreased indicating that sucrose promotes post-receptor insulin signaling impairment<sup>(145, 146)</sup>.

### 8.2.3 Fructose diet model

Fructose is a monosaccharide consisting of six carbon atoms found in many fruits and honey. Fructose has a similar chemical formula to glucose, and it can pass the same pathway as glucose. Nowadays, fructose is the primary sugar consumption worldwide. Normally, fructose enters cells through diffusion via glucose transporter 5 (GLUT5), which is expressed in the intestine, and GLUT5 can be upregulated by fructose. After that, fructose diffuses into the blood circulation through GLUT2. The first metabolism of fructose occurs in the liver. Fructose will convert to pyruvate or glucose (under fasting conditions). Fructose will be phosphorylated to fructose 1-phosphate by fructokinase, cleaved by aldolase B to dihydroxyacetone phosphate (DHAP), glyceraldehyde formation, which ATP phosphorylates to form glyceraldehyde 3-phosphate, both are the intermediates of glycolysis. When converting to pyruvate, it enters the tricarboxylic acid (TCA) cycle and fatty acid (FA) synthesis. This metabolism is the reason why excess fructose can lead to obesity, thereby affecting T2DM. When large amounts ingest of fructose can toxic, it contributes to obesity and T2DM development. Numerous studies have shown that short- and long-term fructose intake lead to hyperinsulinemia, obesity, and T2DM development. Two weeks in the liver of rats fed with 66% fructose chow diet showed insulin-induced insulin receptor phosphorylation reduction. Moreover, six weeks of fructose supplementation-induced hyperglycemia is associated with glucose intolerance. Indeed, 6 and 12 weeks of fructose consumption showed a higher serum insulin level. However, short-term fructose consumption can decrease insulin sensitivity and is commonly used to induce IR. Acute



fructose ingestion is causing of insulin and leptin secretion failure and attenuated postprandial ghrelin suppression<sup>(147)</sup>. Thus, long term high fructose consumption could increase body weight and contributing to obesity. In addition, chronic fructose ingestion resulting in hyperleptinemia and leptin resistance<sup>(148, 149)</sup>.

### 8.3 High-fat diet combined with streptozotocin model

This model is induced by using HFD and streptozotocin (STZ) injection combination, which is designed to mimic T2DM pathogenesis for a short time than in T2DM people. IR, and the resulting compensatory insulin release. After HFD intake following STZ injection to induced partial  $\beta$ -cell death. HFD feeding lead to hyperinsulinemia, IR, and glucose intolerance, while STZ injection reduces  $\beta$ -cell mass and function<sup>(150, 151)</sup>.

In addition, the other studies used the rat feeding with HFD for two weeks following a single injection of 50 mg/kg B.W. or 35 mg/kg B.W. of STZ to develop a T2D model<sup>(152)</sup>. The characteristics of rat feeding with HFD combined with STZ are insulin resistance and hyperglycemia. It is suggested that the HFD is a good to initiate for insulin resistance induction. STZ is widely used to induce type 1 and type 2 diabetes mellitus, which STZ induced  $\beta$ -cell damage<sup>(153)</sup>. A low dose of STZ causes a mild impaired insulin secretion, which is like the last stage of T2DM. Therefore, a rat model feeding with HFD combined with a low dose STZ is closely mimic the natural history of T2DM progression in the human (from insulin resistance to  $\beta$ -cell dysfunction)<sup>(150, 154, 155)</sup>.

### 8.4 Fructose consumption combined with streptozotocin model

On the other hand, the alternative model for T2DM is fructose consumption combined with a low dose STZ injection. The combination of fructose consumption and low dose STZ injection effectively induces T2DM in experimental animals. Moreover, the onset of hepatic IR has been linked to consuming fructose-rich diets in humans and experimental animals. For IR or T2DM induction, fructose has been supplied *ad libitum* by dissolving in drinking water or diet at 10 -15% concentration for a short or long period. however, the IR and T2DM induction by fructose feeding is use more time and is a high cost. Thus, the researcher designed T2DM rat model through short-term fructose

feeding combined with a low dose STZ injection. This model may be induced all major pathogeneses in T2DM, including IR and hyperglycemia. Wilson *et al.* studied the T2DM rat model using a fructose solution combined with a low dose STZ. They used a six-week-old male Sprague-Dawley (SD) rat and induced by feeding 10%, 20%, and 30% fructose drinking water for two weeks following a low dose STZ (40 mg/kg B.W.) injection. The rats in 10% fructose-fed STZ group showed enhancing glucose tolerance, HOMA-IR, hyperglycemia, serum LDL, and cholesterol, which are the characteristics of the human T2DM<sup>(156)</sup>. This model has a stable of diabetic condition over an 11<sup>th</sup> week experimental. Therefore, fructose combined with a low dose STZ injection model is a new non-genetic alternative model of T2DM that quickly and successfully induce all pathogenesis of T2DM. It can be used for acute and chronic studies for pharmacological of anti-type 2 diabetic.

#### 9. Human neuroblastoma cell SH-SY5Y

The SH-SY5Y cell is a cloned of the SK-N-SH cell, a bone marrow biopsy of metastatic neuroblastoma of a 4<sup>th</sup> year female. There are three characteristics, including adherent, floating cells, and both types. Biedler *et al.*, suggested that SK-N-SH cells contained two phenotypes, including neuroblast-like cell and epithelial-like cell. Neuroblast-like cell has a characteristic of catecholaminergic, including a positive for tyrosine hydroxylase (TH) and dopamine- $\beta$ -hydroxylase. In contrast, the epithelial-like cell lacked these enzymatic activities. In addition, SH-SY5Y cell can differentiated into a mature neuron-like phenotype. Usually, SH-SY5Y cell is used as *in vitro* studies of neuron functions under neurodegenerative processes. These cells can convert to various functional neurons by adding specific compounds<sup>(157)</sup>.

Previous research used the human neuroblastoma SH-SY5Y cell as a relevant cellular model for biochemical investigations on AD. Many studies were designed to induce *in vitro* AD model by treating SH-SY5Y cell with hydrogen peroxide, zinc, and A $\beta$  peptides. Many experiments generated the SH-SY5Y cell to develop the *in vitro* AD model through exposure to A $\beta$  peptides. These models have shown oxidative stress,

neurotoxicity, and apoptosis correlated with Alzheimer's disease-like pathological changes. Wang *et al.* have been demonstrated that A $\beta_{42}$ -induced cytotoxicity and autophagic cell death in SH-SY5Y cell through triggered ROS accumulation<sup>(158)</sup>. Moreover, Liu *et al.* has shown A $\beta_{25-35}$  induced oxidative stress and activated injury, autophagy, and decreased total antioxidant capacity through inhibiting Nrf2 translocation into the nucleus in SH-SY5Y cell<sup>(159)</sup>.

## 10. Pioglitazone

Pioglitazone (PG) is a new type 2 diabetic drug in thiazolidinediones (TZDs) group<sup>(160, 161)</sup>. TZDs discovered by screening compounds for hypoglycemic action<sup>(162)</sup>. TZDs improves insulin action in obese, insulin resistance, and T2DM models<sup>(163)</sup>. There are three TZDs, including troglitazone, rosiglitazone, and pioglitazone. There have been treated in T2DM people since the late 1990s. The FDA has approved TZDs used to treat T2DM people combined with diet and exercise. In addition, the FDA recommends using monotherapy or combined with metformin or sulfonylureas to manage T2DM<sup>(164)</sup>. PG developing by Takeda Chemical Industries (Osaka, Japan), with 392.91 Da of a molecular weight. The metabolite of PG is occurred in the liver by cytochrome P (CYP) 450. It has been indicated that PG could improve insulin sensitivity and  $\beta$ -cell function in type 2 diabetes<sup>(161, 165)</sup>.

PG is a peroxisome proliferator-activated receptor-gamma (PPAR $\gamma$ ) agonist. PPAR $\gamma$  is expressed in many tissues, including the colon, skeletal muscle, liver, heart, macrophages, and adipocytes. The activity of pioglitazone includes 1) binding to PPAR $\gamma$  and 2) improving insulin sensitivity by a change in fat metabolism (reduction in circulating FFA)<sup>(162)</sup>.

### 10.1 Insulin sensitivity, beta-cell function, and blood glucose levels

The effects of PG on T2DM are reduced hyperglycemia and hyperinsulinemia. It reduces fasting and postprandial blood glucose. In addition, PG administration improves peripheral insulin sensitivity, enhances glucose uptake, reduces insulin resistance, and improves the  $\beta$ -cell function<sup>(161, 166)</sup>. The  $\beta$ -cell function

improvement could be mediated by PPAR $\gamma$  activation in pancreatic  $\beta$ -cells or reduces lipotoxicity associated with reduced IR<sup>(167)</sup>. Moreover, PG prevents  $\beta$ -cell apoptosis through inhibiting NF- $\kappa$ B signaling pathway<sup>(168)</sup>.

### 10.2 Lipid metabolism and fat redistribution

Dyslipidemia is a cause by high triglycerides (TGs), low high-density lipoprotein (HDL) cholesterol, and small-dense low-density lipoprotein (LDL) cholesterol<sup>(169)</sup>. PG has a potential to reducing TG levels and enhancing HDL cholesterol<sup>(170)</sup>. Nagashima *et al.* (2003) demonstrated that PG treatment could increase plasma TG clearance mediated by increased lipoprotein lipase<sup>(171)</sup>.

### 10.3 Adipose tissue

The visceral adipose tissue accumulation is a common feature of IR<sup>(161)</sup>. PG regulates the expression of adipocyte genes, such as adiponectin, TNF- $\alpha$ , and resistin. In type 2 diabetes shown the low adiponectin level and high leptin level. PG improves leptin resistance and increases adiponectin production, resulting in enhances insulin sensitivity<sup>(172)</sup>.

## RESEARCH OBJECTIVES

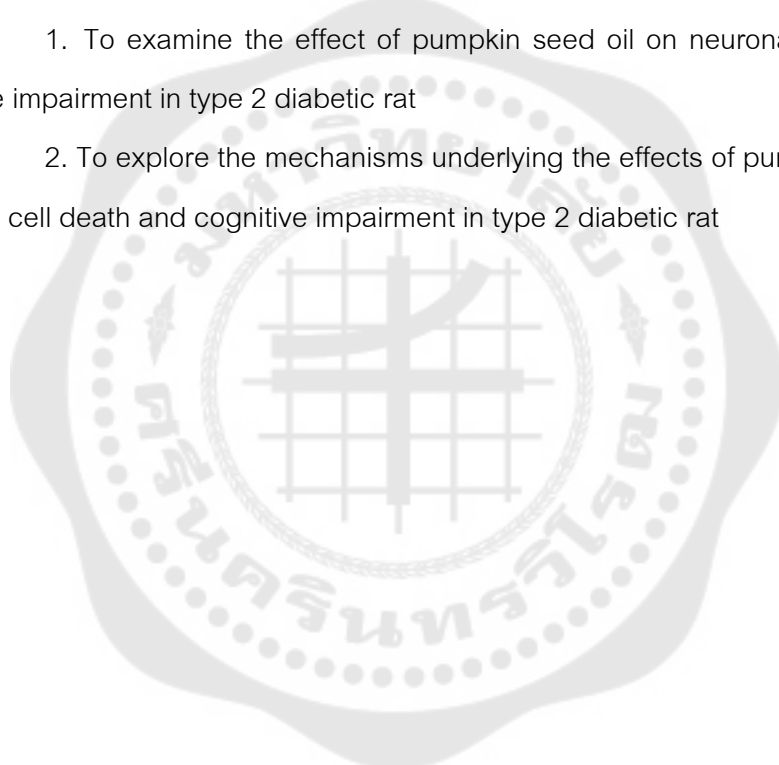
The present study is divided into two experimental protocols, including *in vitro* and *in vivo* (animal) studies that have the objectives below

### *In vitro* (cell culture) research objective

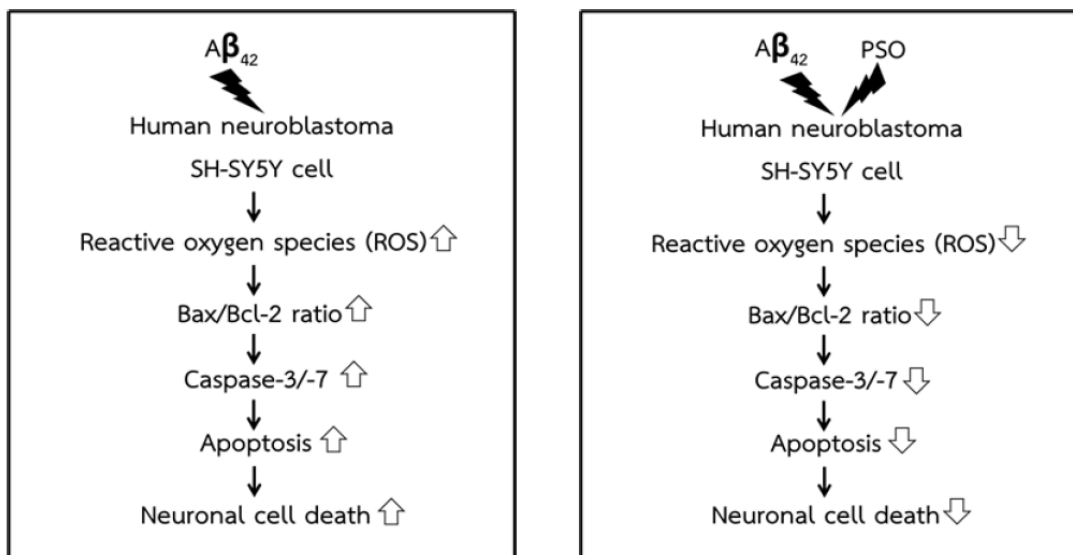
1. To examine the neuroprotective effect of pumpkin seed oil (PSO) on beta-amyloid 42 ( $A\beta_{42}$ )-induced neuronal cell death in human neuroblastoma cell line SH-SY5Y

### *In vivo* (animal) research objective

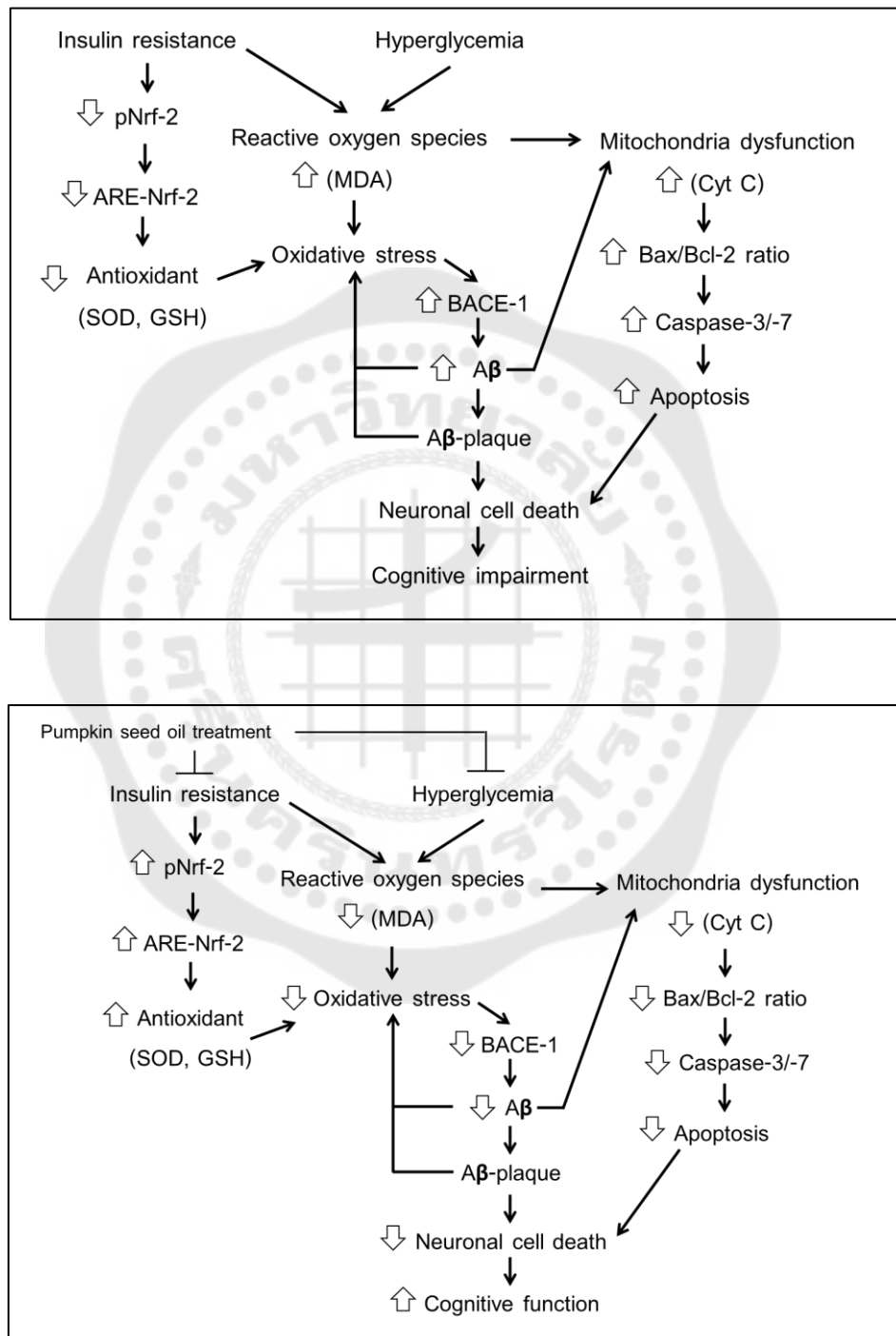
1. To examine the effect of pumpkin seed oil on neuronal cell death and cognitive impairment in type 2 diabetic rat
2. To explore the mechanisms underlying the effects of pumpkin seed oil on neuronal cell death and cognitive impairment in type 2 diabetic rat



## CONCEPTUAL FRAMEWORK

*In vitro* conceptual framework

*In vivo* (animal) conceptual framework



### CHAPTER III

### MATERIALS AND METHODS

Table 3 Materials and reagents

No.	Materials and reagents	Sources
1	Antibiotic-antimycotic	Invitrogen, USA
2	Anti- $\beta$ -actin antibody	Millipore, MO, USA
3	Anti-Bax antibody	Abcam, USA
4	Anti-Bcl-2 antibody	Abcam, USA
5	Anti-BACE1 antibody	Abcam, USA
6	Anti-caspase3 antibody	Abcam, USA
7	Anti-nrf2 antibody	Abcam, USA
8	Anti-rabbit IgG HRP-linked antibody	Bio-Rad, CA, USA
9	Beta-amyloid 42	Millipore, MO, USA
10	Cholesterol strip	Roche, Germany
11	Curcumin	Millipore, MO, USA
12	Dimethyl sulfoxide	Invitrogen, USA
13	Dulbecco's Modified Eagle's-Medium	Gibco, USA
14	Enhance chemiluminescence	Pierce, USA
15	F12 medium	Gibco, USA
16	Fetal bovine serum	Invitrogen, USA
17	Fluorescent CM-H <sub>2</sub> DCFDA dye	Invitrogen, USA
18	Fructose powder	Charoentavorn, Thailand
19	Human neuroblastoma cell line SH-SY5Y	ATTC, USA
20	Pioglitazone	Millipore, MO, USA
22	Polyvinylidene difluoride membrane	Millipore, MO, USA
22	Protease inhibitor cocktails	Millipore, MO, USA
23	Radioimmunoprecipitation assay buffer	Millipore, MO, USA
24	Rat A $\beta$ <sub>42</sub> ELISA assay kit	Invitrogen, USA



Table 3 (Continued)

No.	Materials and reagents	Sources
25	Rat free fatty acid ELISA assay kit	Cayman Chemical, USA
26	Rat insulin ELISA assay kit	Millipore, MO, USA
27	Sodium pyruvate	Invitrogen, USA
28	Streptozotocin	Millipore, MO, USA
29	Superoxide dismutase assay kit	Cayman Chemical, USA
30	Thiobarbituric acid reactive substances assay kit	Cayman Chemical, USA
31	Triglyceride strip	Roche, Germany
32	Trypan blue	Invitrogen, USA
33	X-ray film	Kodak, US
34	3-(4,5-dimethylthiazol-2-yl)-2,5-diphenyltetrazolium bromide (MTT) dye	Invitrogen, USA

### Preparation of pumpkin seed oil

#### Sample preparation and pumpkin seed oil extraction

The pumpkins were obtained from a community enterprise in Santisuk district, Nan province, Thailand. Removed the seeds and separated them all from the pumpkin pulp. Pumpkin seeds were washed and then dried in a hot air oven at 60 °C for 6 hours. The seeds were ground to powder with the grinder. The pumpkin seed oil (PSO) was extracted using the Soxhlet procedure (AOAC 1995, 920.85) according to the method by Srbinoska *et al.*<sup>(173)</sup>. Figure 11 shows the extraction procedure of PSO.

Briefly, 100 grams of pumpkin seed powder were weighed and extracted in the boiling glass regulators at 80 °C using ethanol as the solvent. After 2 hours of extraction, the solvent was released from the product into the rotary vacuum evaporator (35 °C, 100 mPa). The yield of oil was calculated as a percentage of yield following the formula:

$$\% \text{ Yield of pumpkin seed oil} = \frac{\text{Weight of oil (g)}}{\text{Weight of pumpkin seed (g)}} \times 100$$

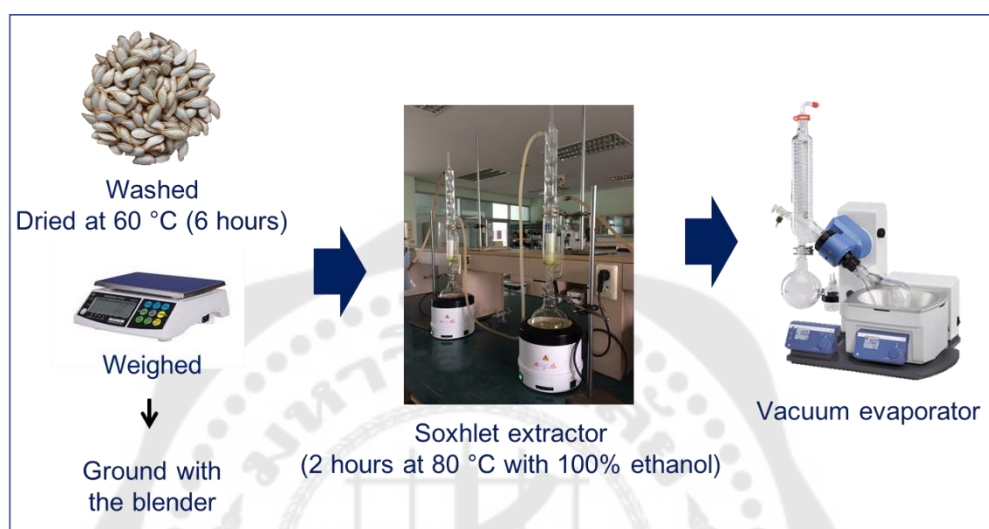


Figure 11 The extraction procedure of pumpkin seed oil

#### Determination of the fatty acid composition and tocopherol in the pumpkin seed oil

The rich of fatty acid compositions in the PSO, including palmitic (C16:0), stearic (C18:0), arachidic (C20:0), oleic (C18:1), and linoleic acids (C18:2), were identified by In-house method WI-TMC-05 based on AOAC (2019) 996.06, 969.33 using gas chromatography (GC) analysis. In addition, tocopherol was evaluated by the In-house method WI-TMC-13 based on BS EN 12823-1 (2000) using High-Performance Liquid Chromatography (HPLC). These analyses were performed by the Institute of Food Research and Product Development (IFRPD), Kasetsart University, Bangkok, Thailand.

### Experimental protocol I: *In vitro* (cell culture) study

The objective of *in vitro* study was to examine the neuroprotective effect of pumpkin seed oil (PSO) on beta-amyloid 42 ( $A\beta_{42}$ )-induced neuronal cell death in human neuroblastoma cell line SH-SY5Y. In the present study, the cell was divided into five groups, including 1) Control (CON): the SH-SY5Y cell cultured in a normal culture medium without 0.5% DMSO, 2) Solvent control (SOL): the SH-SY5Y cell cultured in the medium containing 0.5% DMSO, 3)  $A\beta_{42}$  group (AB): the SH-SY5Y cell was exposed with 1.25  $\mu$ M of beta-amyloid 42 in the culture medium containing 0.5% DMSO, 4) Positive control (CUR): the SH-SY5Y cell was treated with 0.001 ng/mL of curcumin in the culture medium containing 0.5% DMSO, 5) Pumpkin seed oil 1 (PSO1): the SH-SY5Y cell was treated with 10  $\mu$ g/mL of pumpkin seed oil in the culture medium containing 0.5% DMSO, and 6) Pumpkin seed oil 2 (PSO2): the SH-SY5Y cell was treated with 0.001  $\mu$ g/mL of pumpkin seed oil in the culture medium containing 0.5% DMSO.

#### 1. Cell culture preparation

The human neuroblastoma cell line SH-SY5Y was purchased from American Type Culture Collection (ATCC<sup>®</sup>; No.CRL-2266). The cells were cultured and maintained in a cultured medium containing 50% Eagle's Minimum Essential Medium (EMEM) and 50% F12 medium, supplemented with 10% fetal bovine serum (FBS), 1% sodium pyruvate, and 1% antibiotic-antimycotic at 37 °C (5% CO<sub>2</sub>) in an incubator. After 80% of confluence cells grow, the cells were sub-cultured every three days. The viable and dead cells were determined by staining with trypan blue and counted using a hemocytometer.

#### 2. Determination of pumpkin seed oil toxicity on SH-SY5Y cell

The toxicity of pumpkin seed oil (PSO) on a human neuroblastoma cell line (SH-SY5Y) was assessed by the cell viability percentage. The cell viability was performed by the 3-(4,5-dimethylthiazol-2-yl)-2,5-diphenyltetrazolium bromide (MTT) assay. The SH-SY5Y cells ( $1 \times 10^4$  cells/well) were seeded to a clear sterile 96-well plate and maintained in a cultured medium under 37 °C (5% CO<sub>2</sub>) for 24 hours. Next, the

medium was removed and replaced with the different concentrations of PSO (1-100 ng/mL and 1-10  $\mu$ g/mL) in a cultured medium containing 0.5% dimethyl sulfoxide (DMSO), incubated for 24 hours at 37 °C (5% CO<sub>2</sub>). After that, the medium was removed, washed with phosphate buffer saline solution (PBS), added 50  $\mu$ L of MTT solution (0.5 mg/mL in cultured medium without serum), and incubated at 37 °C for 4 hours. After incubation, the solution of each well was removed and washed with PBS. Finally, 100  $\mu$ L of 100% DMSO was added to dissolve the purple formazan. The optical density absorbance was measured at 570 nm using a microplate spectrophotometer. The cell viability percentage was calculated. The control and positive control groups were used a normal cultured medium and cultured medium containing 0.5% DMSO to control and positive control, respectively.

### 3. Determination of beta-amyloid 42 induced toxicity in SH-SY5Y cell

The toxicity of beta-amyloid 42 (A $\beta$ <sub>42</sub>) was assessed by the inhibitory concentration at 50% (IC<sub>50</sub>), calculated from the cell viability percentage. The MTT assay was used to measure cell viability. The SH-SY5Y cells were seeded in a clear sterile 96-well plate (1  $\times$  10<sup>4</sup> cells/well) and grown in the cultured medium under 37 °C (5% CO<sub>2</sub>) for 24 hours. After 24 hours, the medium was removed and replaced with the different concentrations of A $\beta$ <sub>42</sub> (0.15-2.5  $\mu$ M) in a cultured medium containing 0.5% DMSO and incubated for 24 hours (37 °C, 5% CO<sub>2</sub>). After that, the medium was removed, washed one time with PBS, and added 50  $\mu$ L of MTT solution (0.5 mg/mL in cultured without serum), incubated at 37 °C for 4 hours. After incubation, the solution of each well was removed, washed with PBS, and added 100  $\mu$ L of 100% DMSO to dissolve the purple formazan. The optical density absorbance was measured at 570 nm using a microplate spectrophotometer and calculated the IC<sub>50</sub>. IC<sub>50</sub> was calculated using the GraphPad Prism.

#### 4. Determination of the neuroprotective effect of pumpkin seed oil in A $\beta$ <sub>42</sub>-induced toxicity in SH-SY5Y cell

##### 4.1 A $\beta$ <sub>42</sub>, pumpkin seed oil, and curcumin preparation

The lyophilized A $\beta$ <sub>42</sub> peptide was dissolved in sterile water to prepare a stock 50  $\mu$ M A $\beta$ <sub>42</sub> solution and stored at -20 °C. The A $\beta$ <sub>42</sub> working solution was diluted from stock (50  $\mu$ M) to prepare 1.25  $\mu$ M in a cultured medium containing 0.5% DMSO.

The working concentrations of PSO (1 ng/mL and 10  $\mu$ g/mL) and curcumin (0.001 ng/mL) were prepared in a culture medium containing 0.5% DMSO.

##### 4.2 Cell viability determination

First, the cells were seeded in a 96-well plate ( $1 \times 10^4$  cells/well) and grown in a cultured medium for 24 hours under 37 °C (5% CO<sub>2</sub>). Next, the medium was removed. Next, the cells were pretreated with different concentrations of PSO (1 ng/mL and 10  $\mu$ g/mL) and curcumin (0.001 ng/mL) and incubated in an incubator for 24 hours. Then, the cells were exposed to 1.25  $\mu$ M of A $\beta$ <sub>42</sub> and incubated further for 24 hours. The A $\beta$ <sub>42</sub> was removed and washed one time with PBS. Next, the 50  $\mu$ L of MTT solution (0.5 mg/mL in cultured medium without serum) was added and incubated at 37 °C for 4 hours. After incubation, the MTT solution was removed and replaced with 100  $\mu$ L of 100% DMSO. Finally, the optical density absorbance was measured at 570 nm using a microplate spectrophotometer. The percentage of cell viability was calculated from the optical density absorbance at 570 nm.

##### 4.3 Determination of the intracellular reactive oxygen species

The intracellular reactive oxygen species (ROS) was detected by the probe with a fluorogenic dye 2', 7'-dichlorodihydrofluorescein diacetate (H<sub>2</sub>-DCFDA) following the research of Wang *et al.*<sup>(158)</sup>. Briefly, the SH-SY5Y cells were seeded in a 96-well plate ( $1 \times 10^4$  cells/well) and pretreated with PSO (1 ng/mL and 10  $\mu$ g/mL) and curcumin (0.001 ng/mL), incubated for 24 hours (37 °C, 5% CO<sub>2</sub>). After 24 hours, the PSO was removed. The cells were exposed to 1.25  $\mu$ M of A $\beta$ <sub>42</sub> and incubated for 24 hours (37 °C, 5% CO<sub>2</sub>). The cells were washed once time with PBS, added 50  $\mu$ L of 10  $\mu$ M H<sub>2</sub>DCFDA, and incubated at 37 °C for 30 min. The cells were washed twice with

PBS. The fluorescent density from ROS produced was using a fluorescence microplate spectrophotometer.

#### 4.4 Determination of apoptotic parameters by Western blot analysis

The SH-SY5Y cells were seeded and cultured in 35 mm plates ( $2 \times 10^6$  cells/well) and pre-treated with PSO (1 ng/mL and 10  $\mu$ g/mL) and curcumin (0.001 ng/mL), incubated in an incubator for 24 hours (37 °C, 5% CO<sub>2</sub>), following the cells were exposed with 1.25  $\mu$ M of A $\beta$ <sub>42</sub> for 24 hours (37 °C, 5% CO<sub>2</sub>). After incubation, the cells were harvested by centrifuging at 14,000 rpm for 5 min. Next, the cells were lysed using the ice-cold radioimmunoprecipitation assay (RIPA) buffer containing protease inhibitor cocktails. Next, the cell lysate was centrifuged at 13,000 rpm for 25 min at 4 °C to remove the insoluble debris. Finally, the supernatant was collected and used to determine the total protein concentration using Bio-Rad protein assay (Bio-Rad, CA, USA).

The apoptotic parameters were detected using western blot analysis, including Bax, Bcl2, and caspase3 expression. Thirty micrograms of protein were separated by 10% sodium dodecyl sulfate-polyacrylamide gel electrophoresis (SDS-PAGE) at 30 mA. Next, the proteins were transferred from SDS-PAGE to the polyvinylidene difluoride (PVDF) membrane at 100 volts for one hour. The non-specific binding proteins on the membrane were blocked with 5% skim milk in 0.1% Tween20-Tris buffer saline (TBST) pH 7.6 for one hour at room temperature. Next, the membrane was incubated with primary antibodies of Bax (1:1,000), Bcl2 (1:1,000), caspase3 (1:1,000), and  $\beta$ -actin (1:40,000) at 4 °C, overnight, followed by HRP-conjugated anti-rabbit IgG secondary antibody (1:5,000) incubation. The protein bands were visualized by the Enhanced Chemiluminescence (ECL) system and exposed X-ray film. The protein target band density was analyzed with Scion Image software.

In addition, the present study was designed to determine the effect of PSO on cognitive impairment through insulin resistance-induced oxidative stress, beta-amyloid expression correlation with beta-amyloid, and neuronal cell death in type 2 diabetes. This study was used a type 2 diabetic rat model induced by fructose feeding

combined with low dose streptozotocin (STZ) injection. The animal study is described follow below.





## Experimental protocol II: *In vivo* (animal) study

The objectives of the animal study were to determine the effects of pumpkin seed oil (PSO) on cognition impairment and neuronal cell death in a type 2 diabetic rat model.

### 1. Animal preparation

Six-week-old male Sprague Dawley rats (SD-rat) weighted 180-200 g obtained from Nomura Siam International Co., Ltd., (Bangkok, Thailand) were used in this research. Before the experiment, the rats were rested for a week after arrival at the Animal Center, Faculty of Medicine, Srinakharinwirot University. Then, they were kept under optimal conditions (constant room temperature at  $22 \pm 2$  °C, 12/12-hour light/dark cycle). This research was passed ethics committee of Srinakharinwirot University, Ethics Certificate number COA/AE-010-2562.

#### 1.1 Experimental design

The rats were divided into four groups (N=8 rats per group), including the normal control group (CON), type 2 diabetic group (T2DM), type 2 diabetic rat-pumpkin seed oil supplementation group (T2DM-PSO), and type 2 diabetic rat treated with pioglitazone group (T2DM-PG).

**Group I:** Normal control group (CON), a normal rats received normal drinking water

**Group II:** Type 2 diabetic group (T2DM), the rats fed with 10% w/v fructose in drinking water combined with a low dose of streptozotocin injection

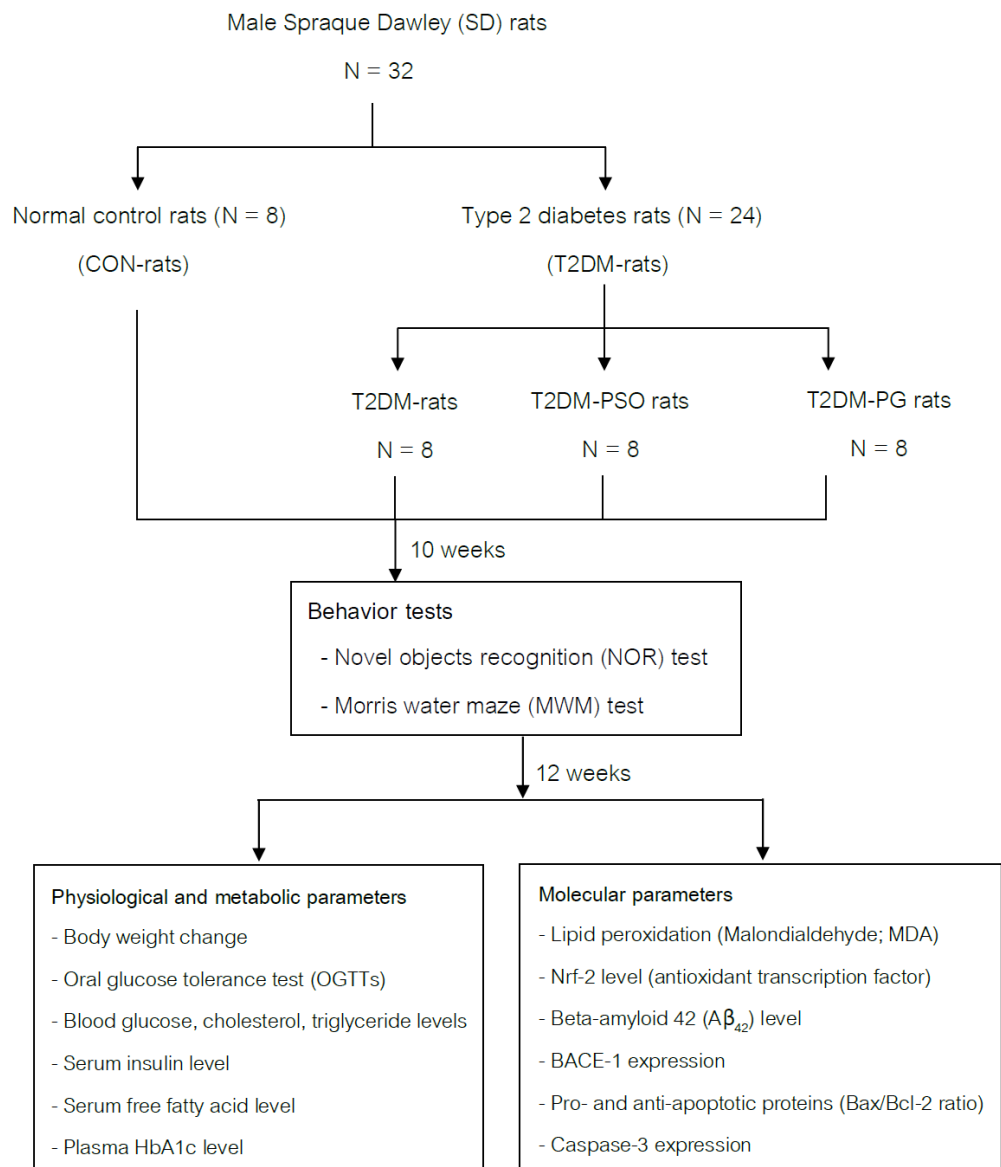
**Group III:** Type 2 diabetes rats administration with PSO group (T2DM-PSO)

**Group IV:** Type 2 diabetes rats administration with pioglitazone group (T2DM-PG) or positive control

Rats in groups II, III, and IV were continuously received 10% w/v fructose in drinking water for 12 weeks.



## Animal experimental design



## 1.2 Type 2 diabetic rat model induction

Type 2 diabetic rat model was performed following Wilson and Islam research<sup>(156)</sup>. The rats were received 10% fructose drinking water combined with a low dose of streptozotocin (STZ) injection. Two weeks after providing fructose drinking water, rats were intravenous (I.V.) injected with STZ (30 mg/kg B.W., dissolved in 0.9% NaCl), while normal control rats were I.V. injected with 0.5 mL of 0.9% NaCl. The fasting blood glucose (FBG) level was determined after 48 hours of STZ or 0.9% NaCl injection. Rats with fasting blood glucose (FBG)  $\geq 250$  mg/dL were considered diabetes. The rats were continuously received 10% w/v fructose drinking water every day until the end of the experiment (12 weeks).

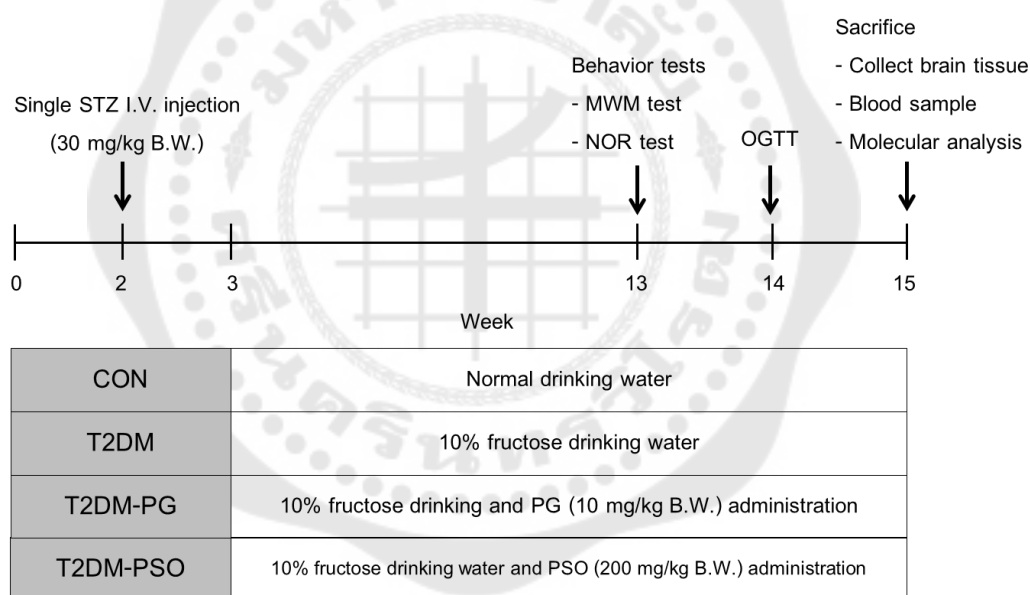


Figure 12 Experimental timeline

## 2. Pumpkin seed oil (PSO) and pioglitazone (PG) administration

The PSO and PG were prepared by dissolved in 1% w/v carboxymethyl cellulose (CMC) and drinking water. Daily gavage feeding of PSO 200 mg/kg B.W./day and PG 10 mg/mg B.W./day were performed a week after STZ injection and continued feeding for 12 weeks. Rats were received PSO and PG at 9:00 am for every day.

In the present study, T2DM-treated with pioglitazone (T2DM-PG) was used as a positive control group. Pioglitazone (PG) is an anti-diabetic drug that reduces blood glucose by improving the body's insulin response.

### **3. Determination of metabolic parameters**

After STZ or vehicle injection or supplementation with PG or PSO, the body weight (BW) was monitored every week, while FBG, blood cholesterol (CHOL), and blood triglyceride (TG) levels were determined every two weeks until the end of the experimental (12 weeks). At the end of the experiment, the blood sample was collected from a cardiac puncture to measure the plasma HbA1c, serum insulin, and free fatty acid (FFA) levels. BG, TG, and CHOL levels were measured using a glucostrip Accu-Check<sup>®</sup>, and cholesterol, triglyceride strip Accu-trend<sup>®</sup> GCT meter (Roche, Boehringer Mannheim, Germany), respectively. Plasma HbA1c was determined using the turbidimetric immune inhibition assay (Professional Laboratory Management Crop. Co., Ltd, Thailand). An enzyme-linked immunosorbent (ELISA) assay analyzed serum insulin and FFA levels.

### **4. Oral glucose tolerance test**

An oral glucose tolerance test (OGTT) is the method to evaluate the body's ability to metabolize glucose and clear it from the bloodstream. After fasting overnight (12 hours), rats were given a single dose gavage feeding of glucose solution (50 % w/v, 2 g/kg BW). The blood glucose level was measured before glucose administration and every 30 minutes up to two hours (0, 30, 60, 90, and 120 minutes) after glucose administration.

### **5. Determination of serum insulin level**

Fasting serum insulin level was measured by a sandwich Enzyme-linked immunosorbent assay (ELISA) technique, following the manufacturer's protocol. Briefly, 10  $\mu$ L of the serum samples were added to 96 well-plated coated with mouse monoclonal anti-rat insulin antibodies, followed by 80  $\mu$ L of detection antibody to each

well and incubated at room temperature for two hours. Next, decant the solution from each well and washed the wells three times with washing buffer solution. Added 100  $\mu\text{L}$  of enzyme solution to each well and incubated at room temperature for 30 minutes. Decanted the solution from each well and washed it six times with washing buffer solution. Added 100  $\mu\text{L}$  of the substrate solution and shaken for approximately 5 to 20 minutes. The blue color was formed in wells. Finally, 100  $\mu\text{L}$  of stop solution was added, and the blue color was changed into yellow color. Read the absorbance at 450 and 590 nm using a microplate spectrophotometer (BioTex<sup>®</sup> Instruments, USA). The serum insulin concentration was calculated from the insulin standard graph.

#### 6. Homeostasis model assessment of insulin resistance (HOMA-IR) calculation

The HOMA-IR index was calculated by using FBG (mmole/L) and fasting serum insulin (mU/L) according to the following formula<sup>(174)</sup>.

$$\text{HOMA-IR} = \frac{\text{Glucose (mmole/L)} \times \text{Insulin (mU/L)}}{22.5}$$

#### 7. Determination of serum free fatty acid level

Following the manufacturer's protocol, the serum free fatty acid (FFA) was measured using a fatty acid fluorometric assay (Cayman Chemical, USA). The fluorometric FFA assay utilizes a couples of enzyme reactions to determine the FFA concentration in the sample. First, acyl CoA synthetase (ACS) catalyzes fatty acid acylation of coenzyme A. Next, acyl CoA is oxidized by acyl CoA oxidase (ACOD) and generates hydrogen peroxide ( $\text{H}_2\text{O}_2$ ). Finally,  $\text{H}_2\text{O}_2$  reacts with 10-aceyl-3,7-dihydroxyphenoxazine (ADHP) in a 1:1 ratio to develop the highly fluorescent product, called resorufin. Resorufin fluorescence concentration is measured using a fluorescence spectrophotometer with an excitation wavelength of 530 nm and an emission wavelength of 590 nm. The reaction during assay performance is shown in Figure 13.

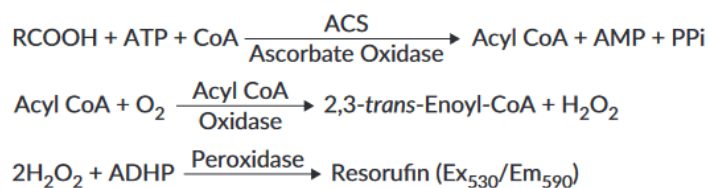


Figure 13 Fatty acid assay reaction

Briefly, the serial FFA standard concentrations between 0-250  $\mu\text{M}$  were prepared. First, 10  $\mu\text{L}$  of standards and samples were added to the black 96 well plate, following 200  $\mu\text{L}$  of FFA assay buffer. Next, 200  $\mu\text{L}$  of the combined FFA cofactor mixture was added to all standard wells and sample wells. Next, covered the plate with the plate cover and incubated at 37° C for 30 minutes. After that, 100  $\mu\text{L}$  of developer solution was added to each well, covered, and incubated at 37° C for 15 minutes. Finally, the fluorescent concentration was measured at 530 nm excitation wavelength and 590 nm emission wavelength using a fluorescent microplate spectrophotometer (BioTex<sup>®</sup> Instruments, USA). The serum FFA concentration was calculated using the following formula.

$$\text{Free Fatty Acid Concentration } (\mu\text{M}) = \left[ \frac{\text{CSF} - (\text{y-intercept})}{\text{Slope}} \right] \times \text{Sample dilution}$$

## 8. Assessment of cognitive function

The cognitive performance assessment was performed on week 10<sup>th</sup> after PG treatment or PSO supplementation. The novel object recognition (NOR) and Morris's water maze (MWM) tests were performed for non-spatial and spatial learning and memory assessment.

### 8.1 Non-spatial learning and memory assessment Novel objects recognition test

The novel object recognition (NOR) test assesses rodents' non-spatial learning and memory based on the spontaneous tendency of rodents to spend more time exploring a novel object than an old object<sup>(234)</sup>. The experiments were performed in a black open field box (100 cm × 100 cm × 50 cm) with two identical objects (A; ■) and one different object (B; ▲). The NOR test consists of three phases, including habituation, familiarization, and test phases.

In the habituation phase, place the rat into the box without an object to habituate to reduce stress. While the familiarization phase or learning phase, the rat was returned to the same box containing two identical objects, and the rat was freely exploring the objects. The last step is the test phase, the phase for memory assessment in which the rat was returned to the same box containing two objects (original and new objects). Naturally, the normal rat will spend more time exploring the new object than the rat can remember the object.

The habituation phase was performed on day 1 of the experiment. First, the rats were habituated to the empty box for 10 minutes. The next phase is familiarization, performed after 24 hours of the habituation phase. The rat was returned to the same box containing two identical objects (A1 + A2) and free exploring for 5 minutes. The objects in this phase are square and made from wood (3 cm × 8 cm × 8 cm). After that, the rat was returned to their home cages for 2 hours (inter-trial interval). After that, the rat was placed in the same box for the test phase. The test phase is divided into two tests. The first test is the task to assess short-term memory, performed after 2 hours of the familiarization phase. The second test evaluates long-term memory performed after 24 hours of the familiarization phase. In both the first and second tests, the rat was placed in the box with two objects, original (A) and a new object (B), for 5 minutes. Object B was made from wood and triangular shape (3 cm × 8 cm × 8 cm). During the inter-trial interval, the objects and the box were cleaned with 70% alcohol spray. The exploration time of each rat was recorded by a digital video camera located above the box. Each rat was measured the total time of rats spent exploring each object

on the first and second tests. The recognition index (RI) was calculated as the percentage of time spent at the new object divided by the total time spent at both objects.

$$\text{Recognition Index (\%)} = \frac{(\text{TN} - \text{TO})}{(\text{TN} + \text{TO})} \times 100$$

While TN is the exploration time of the new object and TO is the exploration time of the old object.

	Day 1	Day 2	Day 3	
CON	Habituation phase (10 min)	Familiarization phase (5 min)	Test phase	
T2DM			Short-term memory (5 min)	Long-term memory (5 min)
T2DM-PSO				
T2DM-PG			2 hrs after familiarization phase	24 hrs after familiarization phase

Figure 14 Novel object recognition (NOR) test timeline

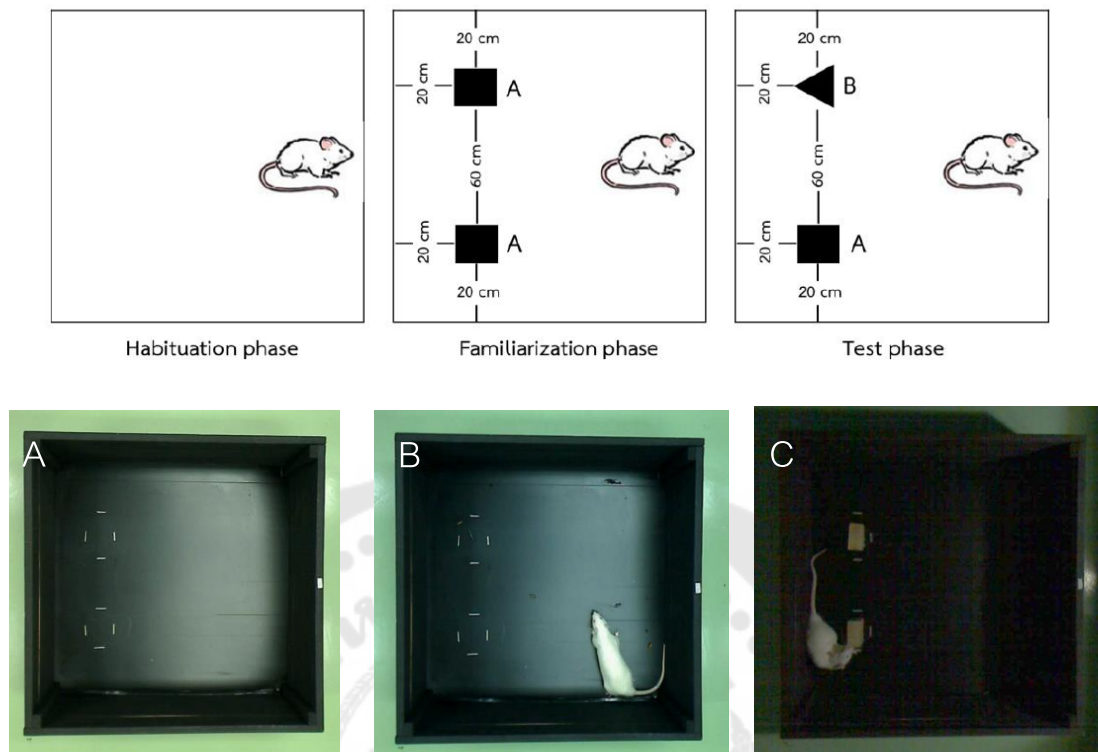


Figure 15 The box in each phase of the Novel Object Recognition (NOR) test

A) The black open field box (100 cm × 100 cm × 50 cm), B) The rat was freely explored in the habituation phase, C) The rat was freely explored in the familiarization or test phase

## 8.2 Spatial learning and memory assessment by using Morris's water maze test

At 10<sup>th</sup> weeks of STZ or PSO or PG administration the spatial learning and memory was performed by using Morris's water maze (MWM) test was performed<sup>(175)</sup>. The MWM consisted of a circle pool (214 cm diameter, 50 cm high) and a platform (15 cm diameter, 80 cm high). The pool was divided into four quadrants and filled the water until the platform submerged (1-1.5 inches). The platform was located at the middle of a certain quadrant and unchanged throughout the experiment. Non-toxic white dye was added to make the water opaque (rendering the platform invisible) and maintained water temperature at  $25 \pm 0.5$  °C. The experiment was performed in a quiet room and controlled light and temperature. The rats were acclimatized in the test room



for one day. Each rat's swimming was monitored and recorded by a digital video camera. The experiment consists of 2 phases, including learning test and memory test.

The experiment was carried out for six consecutive days, the five days in the learning test (escape latency time) and the one later day in the memory test (probe trial time).

### **8.2.1 Learning test**

In the learning test, the rat swimming and learned to escape from the water by finding and locating at a hidden platform (Figure 16). The time that rats were used to find the hidden platform is the escape latency time. In this phase, the rat received five consecutive daily training trials with four intervals of one trial. Each interval has a maximal time at 120 seconds. First, the rat was placed into water at the randomly started quadrant for each interval by turning the rat's head facing the wall of the pool. The rat swimming to find the platform until it climbed on the platform and the rat staying for 20 seconds. If the rat could not find the hidden platform within 120 seconds, it was conducted to the platform and allowed to stay there for 20 seconds. Each interval has the resting period for 120 seconds before starting the next interval. Therefore, the time to find the hidden platform was calculated as escape latency time (seconds).

### **8.2.2 Memory test (Probe-trial time)**

The memory test or probe trial was performed after the learning test. In this test, the hidden platform was removed from the pool (Figure 17). Then, the rat was placed into the pool from the start location opposite the former platform quadrant and allowed to swim in the pool for 60 sec. The rat's time spent in the former platform was recorded within 60 sec.

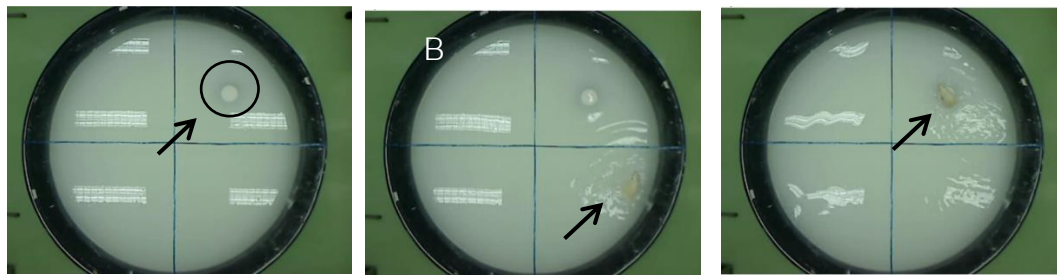


Figure 16 Morris's water maze setting experiment for learning test (escape latency time)

- A) The arrow pointed out at the hidden platform, submerged 1-1.5 inches in the water
- B) The rat was swimming to find the hidden platform
- C) After finding the hidden platform, the rat will climb onto the platform for 20 seconds

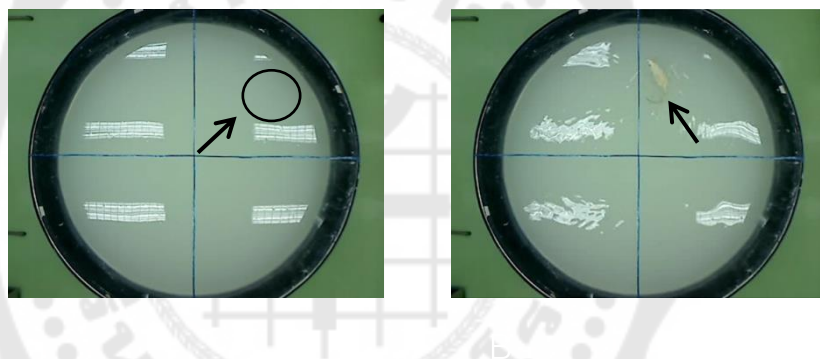


Figure 17 Morris's water maze setting experiment for memory test (probe trial time)

- A) The platform was removed from the pool
- B) The rat swimming in the former platform quadrant

## 9. Preparation of hippocampal tissue

At the end of the experiment, the rats have sacrificed with an overdose intraperitoneal (I.P.) injection of sodium pentobarbital. The brain was rapidly removed, and hippocampal tissue was separated from the whole brain. The hippocampal tissue was homogenized in RIPA buffer containing 1% protease inhibitor cocktails. The hippocampal homogenate was centrifuged at 12,000 rpm, 4 °C for 15 minutes. The supernatant was collected and stored at -80 °C until used to determine the expression of  $\beta$ -secretase (BACE1), nuclear factor E2-related factor 2 (nrf2), and apoptosis parameters using Western blot analysis. The hippocampal  $A\beta_{42}$  and lipid peroxidation

were determined using ELISA and thiobarbituric acid reactive substance (TBARs) assay, respectively.

#### 10. Determination of lipid peroxidation

The present study was measured the hippocampal oxidative stress by measuring the malondialdehyde (MDA) level. The MDA is the natural by-product of lipid peroxidation and is used as an oxidative stress biomarker in the cell or tissue. MDA level was measured using the thiobarbituric acid reactive substances (TBARs) assay kit. TBARs is a well-established assay for screening and monitoring lipid peroxidation<sup>(176)</sup>. The MDA in the sample forms with thiobarbituric acid (TBA) under high temperature (90-100 °C) and acidic conditions, called the MDA-TBA complex (Figure 18). This complex was measured colorimetrically at 540 nm using a microplate spectrophotometer. The MDA concentration was calculated from the MDA standard curve.

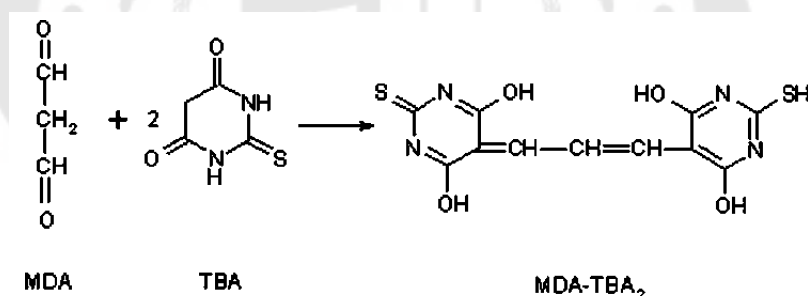


Figure 18 MDA-TBAs complex formation

The hippocampal MDA level was measured by following the manufacturer's protocol. First, the serial concentrations of MDA standards (0.625-50 µM) were prepared. Next, 100 µL of the hippocampal homogenate and MDA standards were added to the tube following 100 µL of sodium dodecyl sulfate (SDS) solution and 4 mL of a color reagent. Next, all tubes were boiled at 100 °C for one hour and placed for 10 minutes on ice to stop the reaction. Then, all samples and standards were centrifuged at 1,600×g for 10 minutes (4 °C) and placed 30 minutes at room temperature. Finally, 150 µL from each tube was loaded into a 96 well plate. The optical density was measured at

540 nm using a microplate spectrophotometer (BioTex<sup>®</sup> Instruments, USA). The MDA concentration was calculated from the following formula.

$$\text{MDA } (\mu\text{M}) = \frac{(\text{Corrected absorbance}) - (\text{y-intercept})}{\text{Slope}}$$

### 11. Determination of superoxide dismutase activity

The hippocampal superoxide dismutase (SOD) level was determined using SOD assay kit. This assay kit utilizes tetrazolium salt to detect the superoxide radicals generated by xanthine oxidase and hypoxanthine (Figure 19). This assay kit determined the activity of SOD by detecting superoxide radicals with tetrazolium salt.

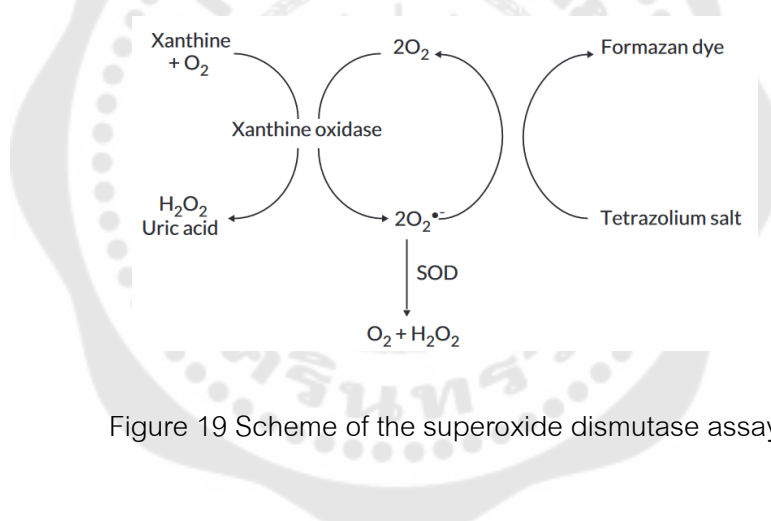


Figure 19 Scheme of the superoxide dismutase assay

The hippocampal SOD level was measured by following the manufacturer's protocol. First, the serial concentrations of SOD activity standards (0 – 0.05 U/mL) were prepared. This assay was performed using 96 well plate. Briefly, the hippocampal tissue homogenate, standards, and radical detector were added to each well. Next, xanthine oxidase was added to the sample and standard wells to initiate the reaction and generate superoxide radicals. Next, incubated the plate on a shaker at room temperature for 30 minutes. Read the absorbance at 440-460 nm by a microplate reader. The SOD activity was calculated by a standard curve equation following the assay's manufacturers.

## 12. Determination of A $\beta$ <sub>42</sub> level in the hippocampal tissue

The hippocampal A $\beta$ <sub>42</sub> level was determined using a solid-phase sandwich ELISA assay kit. Each well of the 96-well plate was pre-coat with a monoclonal antibody specific to A $\beta$ <sub>42</sub> protein. The standards (100  $\mu$ L) and samples (100  $\mu$ L) were added to each well, amount of A $\beta$ <sub>42</sub> in the samples was bound with immobilized (capture) antibody and incubated at room temperature for 2 hours. The solution from each well was removed and washed with a washing buffer solution. Next, the A $\beta$ <sub>42</sub> detection antibody was added to each well and incubated at room temperature for one hour. In this step, the solution was changed to blue color. After incubation, the solution was removed, and the well was washed with a washing buffer solution. After washing, 100  $\mu$ L of anti-IgG HRP was added to each well, and the solution was yellow and incubated at room temperature for one hour. Next, the solution was removed, washed with washing buffer, and added 100  $\mu$ L of stabilized chromogen to each well. Finally, the stop solution was added to each well. The optical density was measured at 450 nm using a microplate spectrophotometer (BioTex<sup>®</sup> Instruments, USA). The hippocampal A $\beta$ <sub>42</sub> level was calculated from the A $\beta$ <sub>42</sub> standard curve.

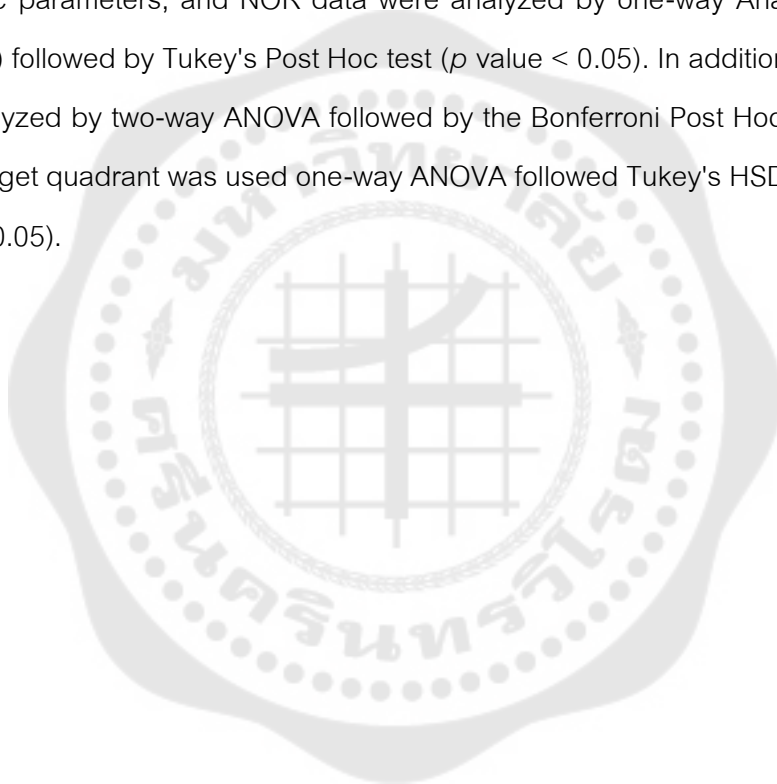
## 13. Determination of nrf2, BACE1, Bax, Bcl2, and caspase3 expression in the hippocampal tissue

The hippocampal nrf2, BACE-1, Bax, Bcl2, and caspase3 expressions were determined using Western blot analysis. First, the total hippocampal protein concentration was measured using the Bradford protein assay. Thirty micrograms of protein were separated by 10% SDS-PAGE at 30 mA. Then, the protein was transferred to the PVDF membrane at 100 volts for one hour. The membrane was blocked non-specific binding protein with 5% skim milk dissolving in 0.1% TBST pH 7.6 for one hour at room temperature and overnight incubated with primary antibody of nrf2 (1:1,000), BACE1 (1:1,000), Bax (1:1,000), Bcl2 (1:1,000), caspase3 (1:1,000) and  $\beta$ -actin (1:40,000) at 4 °C. After that, the membrane was incubated with horseradish peroxidase (HRP)-conjugated anti-rabbit IgG secondary antibody (1:5,000) for one hour at room temperature. Finally, the target protein band was visualized by the ECL system, and X-

ray film was exposed. The density of the protein target band was analyzed with Scion Image software.

#### 14. Statistical analysis

All data were analyzed using Graph Pad Prism version 7.0 software and presented as mean  $\pm$  standard error (mean $\pm$ SEM). The differences in the mean of cell culture study, body weight change, biochemical parameters, MDA, nrf2, BACE1, A $\beta_{42}$ , apoptotic parameters, and NOR data were analyzed by one-way Analysis of Variance (ANOVA) followed by Tukey's Post Hoc test ( $p$  value  $< 0.05$ ). In addition, escape latency was analyzed by two-way ANOVA followed by the Bonferroni Post Hoc test. Time spent in the target quadrant was used one-way ANOVA followed Tukey's HSD Post Hoc test ( $p$  value  $< 0.05$ ).



## CHAPTER IV

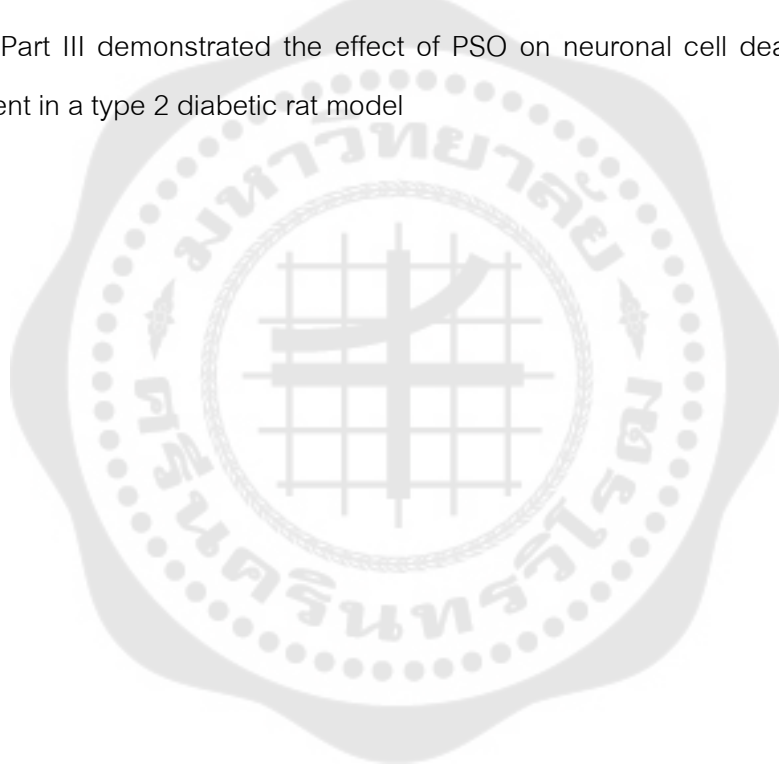
### RESULTS

The results are divided into three major parts according to the experimental design, including

Part I demonstrated the pumpkin seed oil (PSO) chemical composition

Part II demonstrated the effect of PSO on beta-amyloid-induced neuronal cell death in human neuroblastoma cell line SH-SY5Y

Part III demonstrated the effect of PSO on neuronal cell death and cognitive impairment in a type 2 diabetic rat model



### Part I chemical composition of pumpkin seed oil

Our study showed that the ethanolic extraction gave 30 grams of pumpkin seed oil (PSO) per 100 grams of pumpkin seed. The chemical composition of PSO includes unsaturated and saturated fatty acids, as shown in Table 3. In addition, PSO also contains phenolic compounds and tocopherol (vitamin E), which have antioxidant properties. Moreover, vitamin E (alpha-tocopherol) was not detected in PSO extracted. This study used the Sholex extractor for oil extraction. This extraction method was performed under 80-100 °C, which destroys vitamin E.

Table 4 Saturated and unsaturated fatty acids in PSO extracted

Saturated fatty acids (g/100 g)		Unsaturated fatty acid (g/100 g)	
Palmitic acid (C16:0)	19.30	Cis-9-oleic acid (C18:1n:9c)	28.10
Stearic acid (C18:0)	8.02	Linoleic acid (C18:2n6c)	39.11
Arachidic acid (C20:0)	0.37	Alpha-linoleic acid (C18:3n3c)	0.27



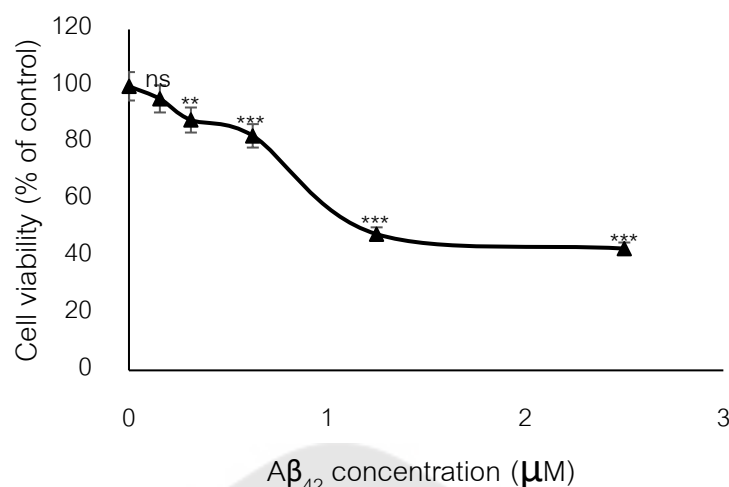
Part II reports the neuroprotective effect of pumpkin seed oil on human neuroblastoma cell line SH-SY5Y apoptosis induced by beta-amyloid 42

This part reports the effect of PSO on A $\beta_{42}$ -induced neuronal cell death through the apoptotic pathway using the human neuroblastoma SH-SY5Y cell line. First, the PSO and A $\beta_{42}$  cytotoxicity tests on normal SH-SY5Y cells were performed to find the optimal concentrations for a subsequent experiment.

### 1. Cytotoxicity of beta-amyloid 42 on human neuroblastoma SH-SY5Y cells

The A $\beta_{42}$  cytotoxicity was evaluated using the MTT assay. Figure 20 shows the SH-SY5Y cell viability after incubation with various concentrations of A $\beta_{42}$  (0.15625 – 2.5  $\mu$ M) for 24 hours. The A $\beta_{42}$  was toxic to SH-SY5Y cells beginning at 0.15  $\mu$ M and significantly decreased cell viability concentration-dependent. The cell viability of SH-SY5Y cells exposed with A $\beta_{42}$  at 0.15625, 0.3125, 0.625, 1.25 and 2.5  $\mu$ M were  $95.57 \pm 0.55$  %,  $88.13 \pm 0.98$  %,  $82.56 \pm 0.68$  %,  $47.96 \pm 0.26$  %, and  $42.87 \pm 0.59$  % of control, respectively.

The inhibitory concentration at 50% (IC<sub>50</sub>) value was  $1.258 \pm 0.21$   $\mu$ M. However, treated cells with the solvent control (cultured medium containing 0.5% DMSO) had no significant toxicity to SH-SY5Y cells compared to cells without A $\beta_{42}$  exposure.



The values are expressed as mean  $\pm$  SEM. (N = 4)

ns; not significantly different compared to cells without Aβ<sub>42</sub> exposure

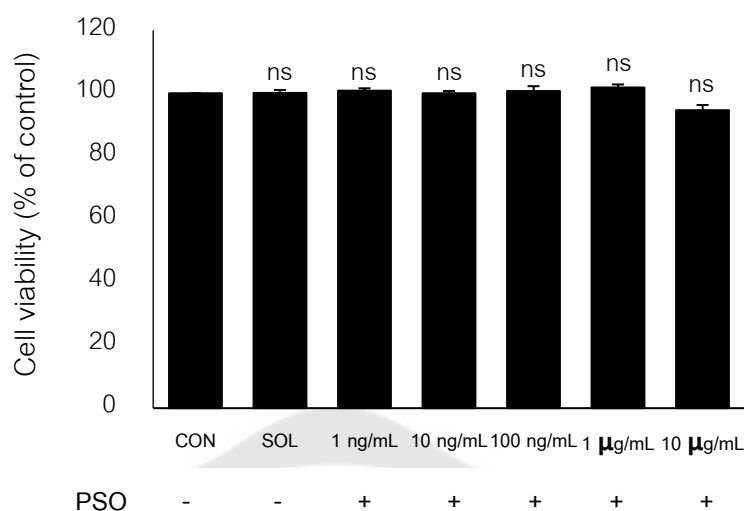
\*\*, \*\*\*; p < 0.01 and 0.001 compared to cells without Aβ<sub>42</sub> exposure

**Figure 20** Effect of beta-amyloid 42 on the viability of human neuroblastoma cell SH-SY5Y

The cytotoxicity of different concentrations of beta-amyloid 42 on human neuroblastoma cells SH-SY5Y. The cells ( $1 \times 10^4$ ) were cultured in 96 well plates and exposed to Aβ<sub>42</sub> (0.15625–2.5 μM) for 24 hours. The % cell viability was measured using the MTT assay.

## 2. Cytotoxicity of pumpkin seed oil on human neuroblastoma SH-SY5Y cells

The MTT assay was used to determine the cytotoxicity of PSO on SH-SY5Y cells. The cells were treated with various concentrations of PSO (0.001 – 10 μg/mL). As shown in Figure 21, PSO with a 0.001-10 μg/mL concentration did not significantly reduce the SH-SY5Y cell viability. The cell viability of SH-SY5Y cells incubated with PSO at 10 μg/mL, 1 μg/mL, 100 ng/mL, 10 ng/mL, and 1 ng/mL were  $94.68 \pm 1.61$ ,  $101.90 \pm 0.92$ ,  $100.70 \pm 1.56$ ,  $100 \pm 0.74$ , and  $100.80 \pm 0.79$  % of control, respectively. Therefore, the present study was selected the highest and lowest doses of PSO (0.001 and 10 μg/mL) to examine the effect on Aβ<sub>42</sub>-induced SH-SY5Y cell death.



The values are expressed as mean  $\pm$  SEM. (N = 4)

ns; not significantly different compared to CON group

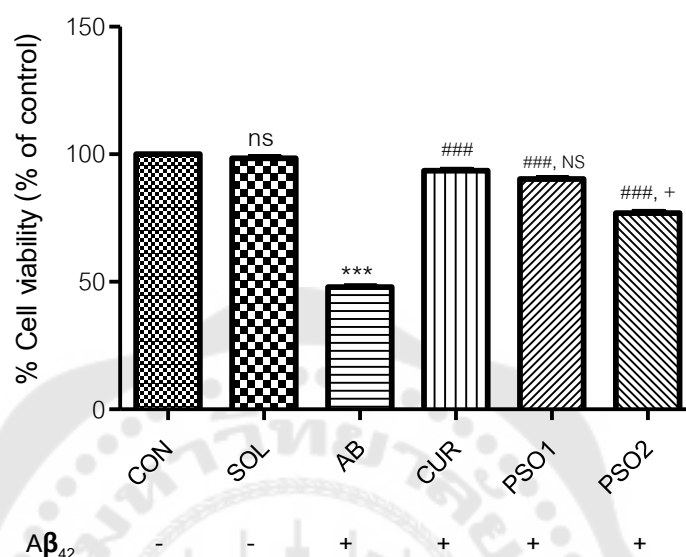
Figure 21 Effect of pumpkin seed oil on the viability of human neuroblastoma cell SH-SY5Y

The cytotoxicity of different concentrations of pumpkin seed oil on human neuroblastoma cells SH-SY5Y. The cells ( $1 \times 10^4$ ) were cultured in 96 well plates and incubated with PSO (0.001 - 10  $\mu\text{g/mL}$ ) for 24 hours. The % cell viability was measured using the MTT assay. CON; normal cell, SOL; normal cell cultured in medium containing 0.5% DMSO, AB; the cells exposed with 1.25  $\mu\text{M}$  of  $\text{A}\beta_{42}$ , PSO1; the cells pretreated with 10  $\mu\text{g/mL}$  of PSO following  $\text{A}\beta_{42}$  exposure, PSO2; the cells pretreated with 0.001  $\mu\text{g/mL}$  of PSO following  $\text{A}\beta_{42}$  exposure

### 3. Effect of pumpkin seed oil on beta-amyloid 42 induced SH-SY5Y cell death

After pretreatment with 0.001 and 10  $\mu\text{g/mL}$  of PSO for 24 hours, the cells were exposed to 1.25  $\mu\text{M}$  of  $\text{A}\beta_{42}$  for another 24 hours. Figure 22 shows 1.25  $\mu\text{M}$  of  $\text{A}\beta_{42}$  (AB group) significantly reduced % cell viability to  $47.95 \pm 0.19\%$  of control as compared to CON group ( $p < 0.001$ ). In contrast, the PSO 0.001 and 10  $\mu\text{g/mL}$  could protect neuronal cell death by increasing % cell viability which was restored to  $6.96 \pm 0.51$  and  $90.27 \pm 0.24\%$  of control, respectively. This result indicates a concentration-dependent cytoprotective effect. In addition, pretreatment with curcumin at 0.001  $\mu\text{g/mL}$  was used as the positive control. The % cell viability of the curcumin pretreated group

(CUR group) was  $93.52 \pm 0.45$  % of control. The % cell viability in PSO pretreated group was not significantly different compared with the positive control.



The values are expressed as mean  $\pm$  SEM. (N = 4)

ns, NS; not significantly different compared to CON and CUR groups, respectively

+,  $p < 0.05$  compared to CUR group

\*\*\*,  $p < 0.001$  compared to CON group

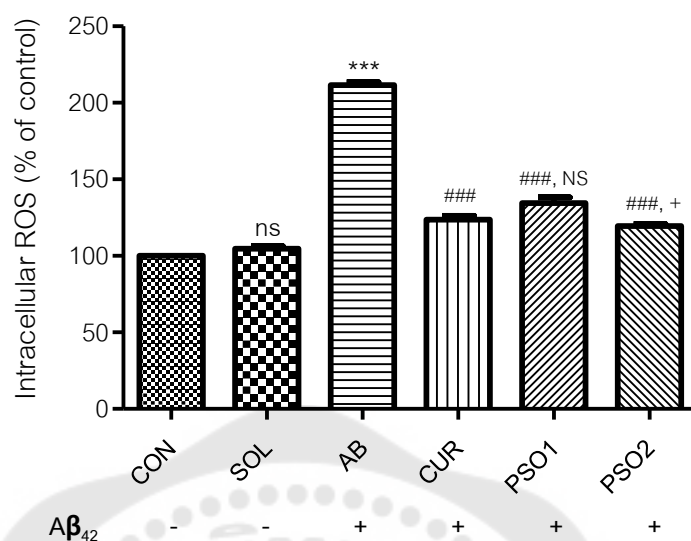
###,  $p < 0.001$  compared to AB group

Figure 22 Effect of pumpkin seed oil on beta-amyloid 42-induced cytotoxicity on human neuroblastoma cell SH-SY5Y

The percentage of cell viability (% cell viability) of human neuroblastoma cells SH-SY5Y after pretreated with PSO at concentrations 10  $\mu\text{g/mL}$  (PSO1) and 0.001  $\mu\text{g/mL}$  (PSO2) using MTT assay. The cells ( $1 \times 10^4$ ) were cultured in 96 well plates, pretreated with PSO (0.001 and 10  $\mu\text{g/mL}$ ) for 24 hours, and following A $\beta_{42}$  exposed for 24 hours. CON; normal cell, SOL; normal cell cultured in medium containing 0.5% DMSO, AB; the cells exposed with 1.25  $\mu\text{M}$  of A $\beta_{42}$ , PSO1; the cells pretreated with 10  $\mu\text{g/mL}$  of PSO following A $\beta_{42}$  exposure, PSO2; the cells pretreated with 0.001  $\mu\text{g/mL}$  of PSO following A $\beta_{42}$  exposure

#### 4. Effect of pumpkin seed oil on beta-amyloid 42 induced intracellular reactive oxygen species production on human neuroblastoma cell SH-SY5Y

Reactive oxygen species (ROS) play a critical role in beta-amyloid-induced neuronal cell death. Therefore, the present study examined the effect of PSO on A $\beta_{42}$ -induced intracellular ROS production. The cells exposed to A $\beta_{42}$  for 24 hours exhibited elevated intracellular ROS levels ( $211.60 \pm 1.89$  % of control) compared to the CON group (Figure 23). In contrast, pretreatment with 0.001 and 10  $\mu\text{g/mL}$  of PSO for 24 hours significantly reduced intracellular ROS compared to AB group ( $p < 0.001$ ). They show the concentration-dependent reduction of A $\beta_{42}$ -induced intracellular ROS levels (from  $211.60 \pm 1.89\%$  to  $134.60 \pm 3.68$  % and  $119.50 \pm 1.25$  % of control, respectively). Furthermore, the positive control (CUR group) significantly reduced the intracellular ROS level to  $123 \pm 2.55\%$  of the control ( $p < 0.001$ ). The results indicated that PSO pre-treated neuronal cell death from intracellular ROS induced by beta-amyloid.



The values are expressed as mean  $\pm$  SEM. (N = 4)

ns; NS; not significantly different compared to CON and CUR groups, respectively

+,  $p < 0.05$  compared to CUR group

\*\*\*,  $p < 0.001$  compared to CON group

###;  $p < 0.001$  compared to AB group

Figure 23 Effect of pumpkin seed oil on beta-amyloid 42 -induced intracellular reactive oxygen species on human neuroblastoma cell SH-SY5Y

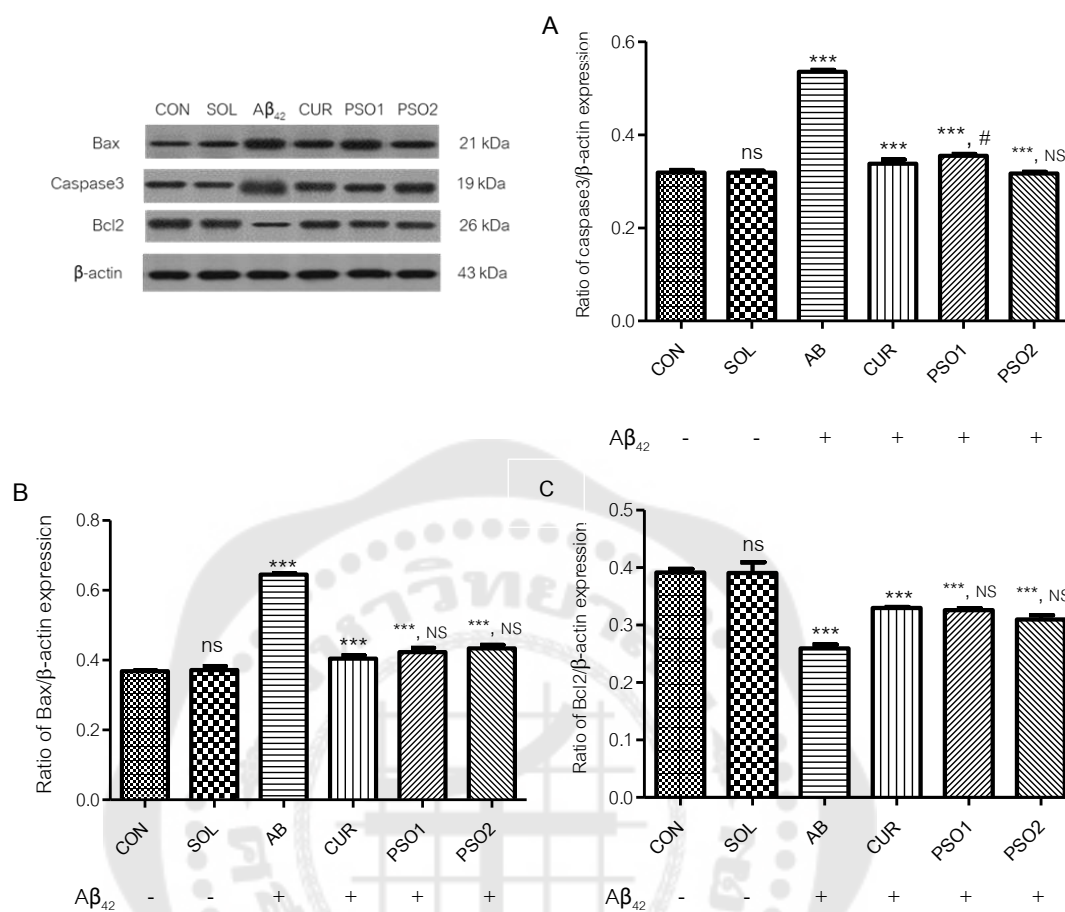
The effect of pumpkin seed oil (PSO) on beta-amyloid 42 ( $A\beta_{42}$ )-induced intracellular reactive oxygen species (ROS) production in human neuroblastoma cell SH-SY5Y were measured using 2', 7'-dichlorofluorescein diacetate ( $H_2DCFDA$ ) probe. The cells ( $1 \times 10^4$ ) cultured in 96 well plates, pretreated with PSO (0.001 and 10  $\mu\text{g/mL}$ ) for 24 hours, and following  $A\beta_{42}$  exposed for 24 hours. CON; normal cell, SOL; normal cell cultured in medium containing 0.5% DMSO, AB; the cells exposed with 1.25  $\mu\text{M}$  of  $A\beta_{42}$ , PSO1; the cells pretreated with 10  $\mu\text{g/mL}$  of PSO following  $A\beta_{42}$  exposure, PSO2; the cells pretreated with 0.001  $\mu\text{g/mL}$  PSO following  $A\beta_{42}$  exposure

##### 5. Effect of pumpkin seed oil on beta-amyloid 42 induced neuronal cell death on human neuroblastoma cell SH-SY5Y

The present study investigated the effects of PSO on the underlying apoptotic pathway by focusing on evaluating the regulation of Bax, Bcl2, and caspase3-induced neuronal cell death. Figure 24 shows the expression of Bax, caspase3, and Bcl2 expression using the western blot analysis. Compared to the CON group, the  $A\beta_{42}$  exposure (AB group) resulting in significantly enhanced neuronal cell death by

increasing the levels of pro-apoptotic protein Bax and caspase3 expression and significantly decreased anti-apoptotic protein Bcl2 expression ( $p < 0.001$ ). In contrast, pretreatment with PSO 0.001 and 10  $\mu\text{g/mL}$  significantly protected neuronal cell death by reducing the expression of Bax and caspase3 levels and increasing Bcl2 expression as compared to the AB group ( $p < 0.001$ ). These results indicated that PSO attenuated downstream of the apoptotic pathway, including Bax and caspase3 activations.





The values are expressed as mean  $\pm$  SEM. (N = 4)

ns and NS; not significantly different compared to CON and CUR group, respectively

+,  $p < 0.05$  compared to CUR group

\*\*\*;  $p < 0.001$  compared to CON group

###;  $p < 0.001$  compared to AB group

Figure 24 Effect of pumpkin seed oil on beta-amyloid 42 regulated anti-apoptotic and apoptotic proteins expression in human neuroblastoma cell SH-SY5Y. (A) The ratio of Bax expression/ $\beta$ -actin, (B) The ratio of caspase3 expression/ $\beta$ -actin, and (C) The ratio of Bcl2 expression/ $\beta$ -actin

The expression of pro-apoptotic proteins, Bax and caspase3 and anti-apoptotic protein, Bcl2 detected using Western blot analysis. The cells ( $2 \times 10^5$ ) cultured in 35 mm plates, pretreated with PSO (0.001 and 10  $\mu$ g/mL) for 24 hours, and following  $A\beta_{42}$  exposed for 24 hours. CON; normal cell, SOL; normal cell cultured in medium containing 0.5% DMSO, AB; the cells exposed with 1.25  $\mu$ M of  $A\beta_{42}$ , PSO1; the cells pretreated with 10  $\mu$ g/mL of PSO following  $A\beta_{42}$  exposure, PSO2; the cells pretreated with 0.001  $\mu$ g/mL of PSO following  $A\beta_{42}$  exposure



### **Part III: The effect of PSO on neuronal cell death and cognitive impairment in high fructose drinking-induced type 2 diabetic rat**

This part reports the effects of PSO on type 2 diabetic-induced neuronal cell death and cognitive impairment through the apoptotic pathway using the type 2 diabetic rat model. Thus, the present study evaluated the metabolic parameters change, cognitive performance, oxidative stress parameters, beta-amyloid 42, and apoptotic parameters.

#### **1. The effect of pumpkin seed oil on metabolic changes in type 2 diabetic rat**

The metabolic parameters that were examined, including body weight (B.W.), fasting blood glucose (FBG), blood cholesterol (CHOL), blood triglyceride (TG), plasma HbA1c, serum insulin, serum free fatty acid (FFA), and HOMA-IR index.

##### **1.1 Body weight, fasting blood glucose, plasma HbA1c, blood cholesterol, and triglyceride**

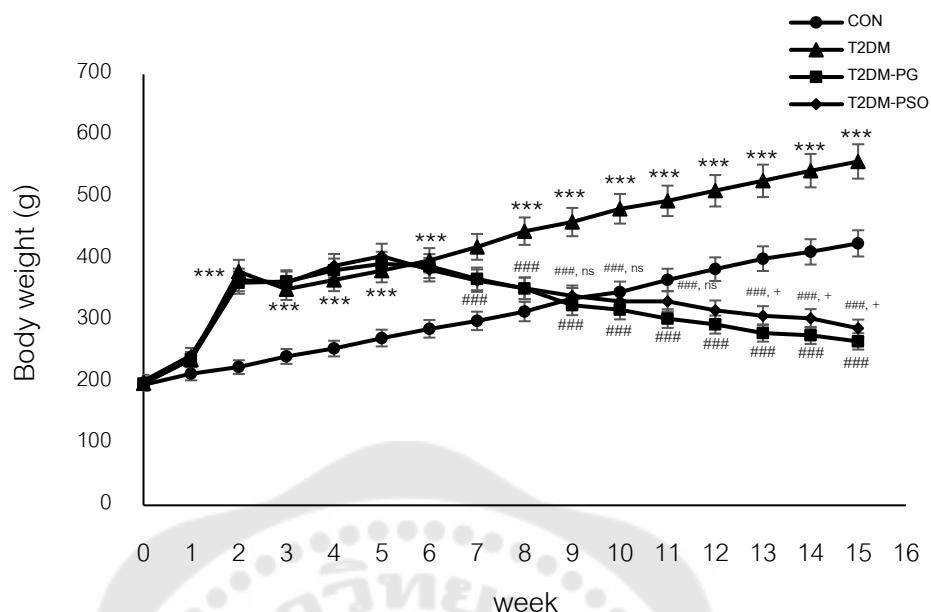
After two weeks of high fructose drinking significantly increased the body weight (B.W.,  $p < 0.001$ ) and maintained until the end of the experiment in comparison to CON rats (Figure 25). It is noted that the B.W. gain in T2DM rats remained significantly high throughout the experimental period (12 weeks). Six weeks after administration of PSO and PG in T2DM-PSO and T2DM-PG, the B.W. showed a significant reduction ( $p < 0.001$ ) compared to T2DM rats. The B.W.'s reduction continued until the experimental period's end (Figure 25).

As shown in Figure 26, the FBG levels in T2DM rats remained significantly high throughout the experimental period. However, two weeks after administration of PSO and PG in fructose drinking rats (T2DM-PSO rats and T2DM-PG rats, respectively), the FBG levels were significantly reduced compared to T2DM rats ( $p < 0.001$ ). The reduction of FBG in T2DM-PSO and T2DM-PG rats was significant until the end of the experiment.

Table 3 demonstrated the FBG, plasma HbA1c, blood CHOL, and blood TG in the last week of the experiment. The FBG, plasma HbA1c, CHOL, and TG levels were significantly elevated in T2DM rats compared to the normal control rats (CON,  $p <$

0.001). Interestingly, administration of PSO and PG in fructose drinking rats for 12 weeks had a strong and significant reduction in FBG, HbA1c, CHOL, and TG levels compared to those monitored from T2DM rats. The percentage change of FBG was 35.15 % and 31.39 % in T2DM-PSO rats and T2DM-PG rats, respectively. Moreover, there was a significant difference between PSO and PG administrated in FBG, HbA1c, and TG levels. However, there was no significant difference ( $p < 0.05$ ) between PSO and PG administrated in blood CHOL levels (Table 4).

As shown in Figure 27, the changes in blood glucose levels from OGTT were used to calculate the area under curve (AUC). As shown in Figure 28, a reduction of AUG by PSO and PG was significantly lower than that of T2DM rats ( $p < 0.001$ ). Therefore, the above results indicated that 12 weeks of PSO administration was able to reduce hyperglycemia, hypercholesterolemia, hypertriglyceridemia and improve abnormal glycosylated hemoglobin in type 2 diabetic states.



The values are expressed as mean  $\pm$  SEM. (N = 8)

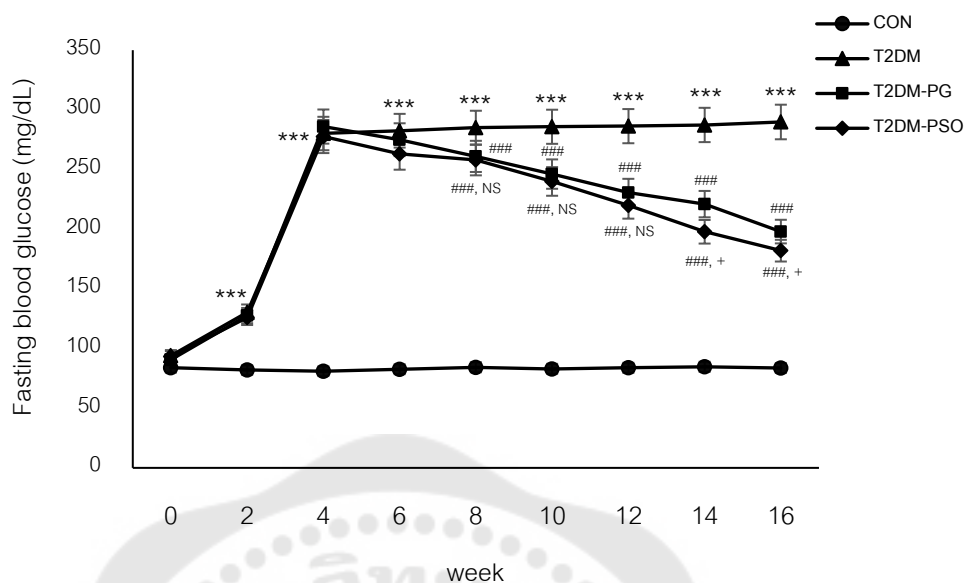
ns; not significantly different compared to T2DM-PG group

+,  $p < 0.005$  compared to T2DM-PG group

\*\*\*, ###;  $p < 0.001$  compared to CON group and T2DM group, respectively

Figure 25 The body weight changes during the experiment

The graph shows the body weight changes between 0-15 weeks of the experimental. The rats in T2DM-PG and T2DM-PSO groups received 10% fructose drinking water for two weeks (week 0 -2) and following streptozotocin (STZ) injection. PSO or PG administration was performed after a week of STZ injection (week 3) for 12 weeks. T2DM, T2DM-PG, and T2DM-PSO rats continuously received 10% fructose drinking water until the end of the experimental or 12 weeks. CON; the normal control rats, T2DM; type 2 diabetic rats, T2DM-PG; type 2 diabetic rats administrated 10 mg/kg B.W. pioglitazone, T2DM-PSO; type 2 diabetic rats administrated 200 mg/kg B.W. pumpkin seed oil



The values are expressed as mean  $\pm$  SEM. (N = 8)

ns; not significantly different compared to T2DM-PG group

+,  $p < 0.05$  compared to T2DM-PG group

\*\*\*, ###;  $p < 0.001$  compared to CON group and T2DM group, respectively

Figure 26 The change in fasting blood glucose level during the experiment

The graph shows the fasting blood glucose (FBG). The rats in T2DM-PG and T2DM-PSO groups received 10% fructose drinking water for two weeks (week 0-2) and following streptozotocin (STZ) injection. PSO or PG administration was performed after a week of STZ injection for 12 weeks (at 2 weeks in the graph is the started PSO or PG administration or 0 weeks from 12 weeks of the experimental). T2DM, T2DM-PG, and T2DM-PSO rats continuously received 10% fructose drinking water until the end of the experimental or 12 weeks. CON; the normal control rats, T2DM; type 2 diabetic rats, T2DM-PG; type 2 diabetic rats administrated 10 mg/kg B.W. pioglitazone, T2DM-PSO; type 2 diabetic rats administrated 200 mg/kg B.W. pumpkin seed oil

Table 5 The fasting blood glucose (FBG), blood cholesterol (CHOL), and blood triglyceride (TG) levels

Group	FBG (mg/dL)	HbA1c (mg/dL)	CHOL (mg/dL)	TG (mg/dL)
CON	98.00 ± 1.41	3.92 ± 0.04	151.60 ± 0.75	124.20 ± 1.80
T2DM	345.40 ± 1.89 <sup>***</sup>	9.58 ± 0.02 <sup>***</sup>	190.60 ± 3.28 <sup>***</sup>	385.00 ± 11.38 <sup>***</sup>
T2DM-PG	235.20 ± 3.83 <sup>###</sup>	5.04 ± 0.11 <sup>###</sup>	162.20 ± 1.28 <sup>###</sup>	244.00 ± 2.45 <sup>###</sup>
T2DM-PSO	216.00 ± 3.35 <sup>###, +</sup>	5.94 ± 0.12 <sup>###, ++</sup>	162.60 ± 1.08 <sup>###, ns</sup>	269.80 ± 8.18 <sup>###, +</sup>

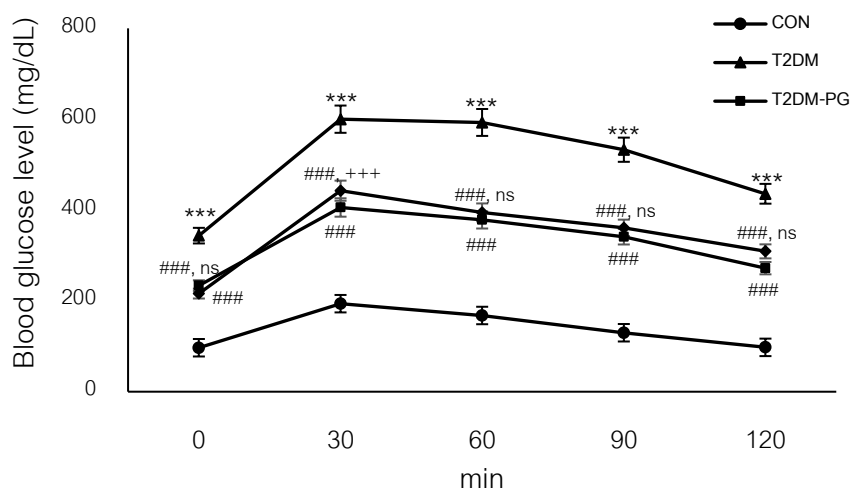
The values are expressed as mean ± SEM. (N = 8)

ns; not significantly compared to T2DM-PG group

+, ++; p < 0.05 and 0.01 compared to T2DM-PG group

\*\*\*, ###; p < 0.001 compared to CON group and T2DM group, respectively

CON; the normal control rats, T2DM; type 2 diabetic rats, T2DM-PG; type 2 diabetic rats administrated 10 mg/kg B.W. pioglitazone, T2DM-PSO; type 2 diabetic rats administrated 200 mg/kg B.W. pumpkin seed oil



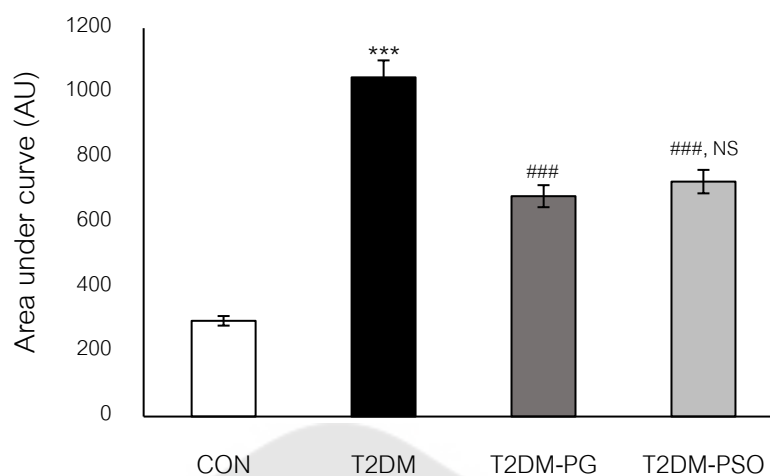
The values are expressed as mean  $\pm$  SEM. (N = 8)

ns; not significantly different compared to the T2DM-PG group

\*\*\*, ###;  $p < 0.001$  compared to CON, T2DM, and T2DM-PG group, respectively

Figure 27 The effect of pumpkin seed oil on glucose tolerance

The graph shows the blood glucose level in the oral glucose tolerance test (OGTT). The rats received a single dose gavage feeding of 50% glucose solution (2 g/kg B.W.). The blood glucose level was measured before glucose administration (0 minutes) and every 30 minutes (30, 60, 90, and 120 minutes up to two hours after glucose administration. CON; the normal control rats, T2DM; type 2 diabetic rats, T2DM-PG; type 2 diabetic rats administrated 10 mg/kg B.W. pioglitazone, T2DM-PSO; type 2 diabetic rats administrated 200 mg/kg B.W. pumpkin seed oil



The values are expressed as mean  $\pm$  SEM. (N = 8)

NS; not significant different compared to T2DM-PG group

\*\*\*, ###;  $p < 0.001$  compared to CON and T2DM group, respectively

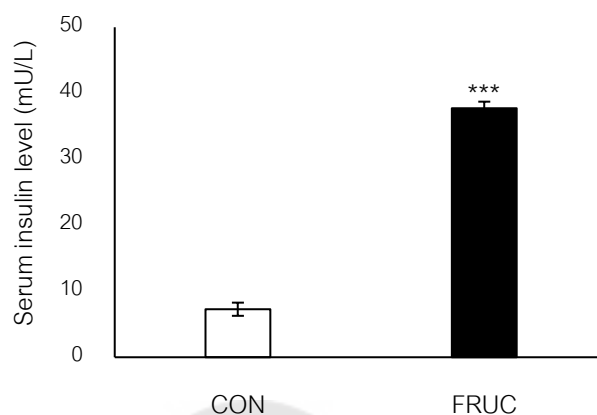
Figure 28 The area under curve (AUC) of OGTT

The graph shows the area under curve (AUC) of OGTT. CON; the normal control rats, T2DM; type 2 diabetic rats, T2DM-PG; type 2 diabetic rats administrated 10 mg/kg B.W. pioglitazone, T2DM-PSO; type 2 diabetic rats administrated 200 mg/kg B.W. pumpkin seed oil

### 1.2 Serum insulin, calculated homeostatic model assessment for insulin resistance, and serum free fatty acid levels

After two weeks of 10% fructose drinking feeding (Figure 29), the rats were received 10% fructose drinking (FRUC rats) showed significantly increased serum insulin level compared with normal drinking water rats (CON rats) ( $p < 0.001$ ). Therefore, 10% fructose intake leads to hyperinsulinemia, which is the characteristic of T2DM.

At 12 weeks of the experimental, the fasting serum insulin level of T2DM rats was significantly higher than that of the normal control rats ( $p < 0.001$ ), as shown in Figure 30. The calculated HOMA-IR (Figure 31), which indicated a degree of insulin resistance and level of serum FFA were significantly higher in T2DM rats compared to the CON rats ( $p < 0.001$ ) (Figure 32). The PSO and PG administration to type 2 diabetic rats significantly reduced serum insulin, HOMA-IR index, and serum FFA compared to T2DM rats ( $p < 0.001$ ).

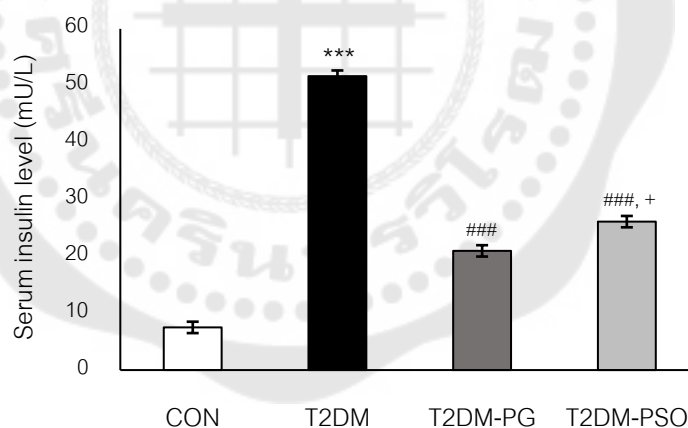


The values are expressed as mean  $\pm$  SEM. (N = 8)

\*\*\* p < 0.001 compared to CON group

Figure 29 The serum insulin level after two weeks of 10% w/v fructose drinking water

The graph shows the serum insulin level after two weeks of 10% drinking water feeding. FRUC; rats received 10% fructose drinking, CON; normal control rats



The values are expressed as mean  $\pm$  SEM. (N = 8)

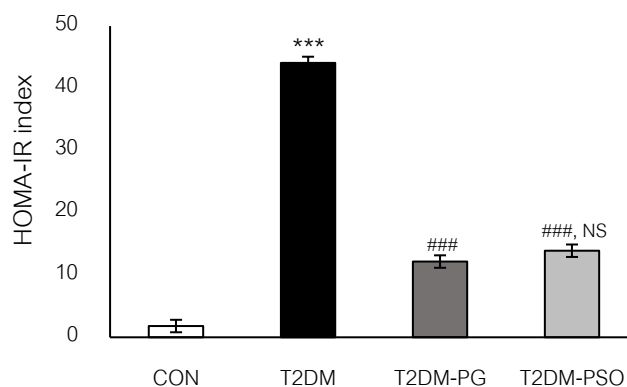
\*\*\*, ###; p < 0.001 compared to CON group and T2DM group, respectively

+, p < 0.05 compared to T2DM-PG group

Figure 30 The fasting serum insulin level

The graph shows the serum insulin level after 12 weeks of PSO or PG administration. CON; the normal control rats, T2DM; type 2 diabetic rats, T2DM-PG; type 2 diabetic rats administrated 10 mg/kg B.W. pioglitazone, T2DM-PSO; type 2 diabetic rats administrated 200 mg/kg B.W. pumpkin seed oil





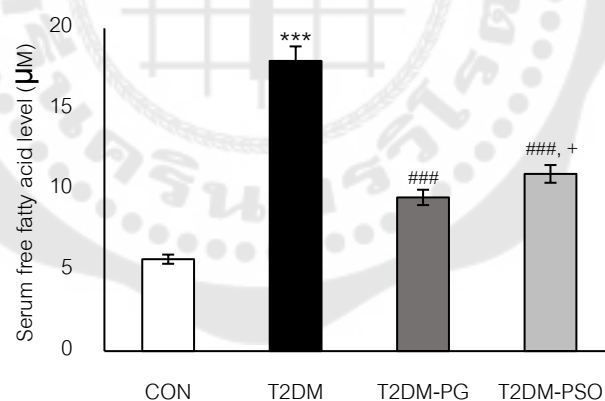
The values are expressed as mean ± SEM. (N = 8)

NS; not significantly different compared to the T2DM-PG group

\*\*\*, ###;  $p < 0.001$  compared to CON group and T2DM group, respectively

Figure 31 The homeostatic model assessment for insulin resistance (HOMA-IR) index

The graph shows the HOMA-IR index after 12 weeks of PSO or PG administration. CON; the normal control rats, T2DM; type 2 diabetic rats, T2DM-PG; type 2 diabetic rats administrated 10 mg/kg B.W. pioglitazone, T2DM-PSO; type 2 diabetic rats administrated 200 mg/kg B.W. pumpkin seed oil



The values are expressed as mean ± SEM. (N = 8)

+  $p < 0.05$  compared to the T2DM-PG group

\*\*\*, ###;  $p < 0.001$  compared to CON group and T2DM group, respectively

Figure 32 The serum free fatty acid level

The graph shows the serum free fatty acid (FFA) level after 12 weeks of PSO or PG administration. CON; the normal control rats, T2DM; type 2 diabetic rats, T2DM-PG; type 2 diabetic rats administrated 10 mg/kg B.W. pioglitazone, T2DM-PSO; type 2 diabetic rats administrated 200 mg/kg B.W. pumpkin seed oil

Table 6 The serum insulin, serum free fatty acid, and HOMA-IR index

Group	Serum insulin (mU/L)	Serum FFA ( $\mu$ M)	HOMA-IR
CON	7.50 $\pm$ 0.23	5.69 $\pm$ 0.01	1.81 $\pm$ 0.04
T2DM	51.68 $\pm$ 1.58 <sup>***</sup>	17.98 $\pm$ 0.53 <sup>***</sup>	44.08 $\pm$ 1.40 <sup>***</sup>
T2DM-PG	20.96 $\pm$ 0.29 <sup>###</sup>	9.52 $\pm$ 0.28 <sup>###</sup>	12.17 $\pm$ 0.26 <sup>###</sup>
T2DM-PSO	26.10 $\pm$ 0.73 <sup>###, +</sup>	10.98 $\pm$ 0.31 <sup>###, +</sup>	13.19 $\pm$ 0.39 <sup>###, NS</sup>

The values are expressed as mean  $\pm$  SEM. (N = 8)

NS; not significantly compared to T2DM-PG group

+, p < 0.05 compared to T2DM-PG group

\*\*\*, ### p < 0.001 compared to CON group and T2DM group, respectively

CON; the normal control rats, T2DM; type 2 diabetic rats, T2DM-PG; type 2 diabetic rats administrated 10 mg/kg B.W.

pioglitazone, T2DM-PSO; type 2 diabetic rats administrated 200 mg/kg B.W. pumpkin seed oil

## 2. Effect of pumpkin seed oil on cognitive performance in type 2 diabetic rat

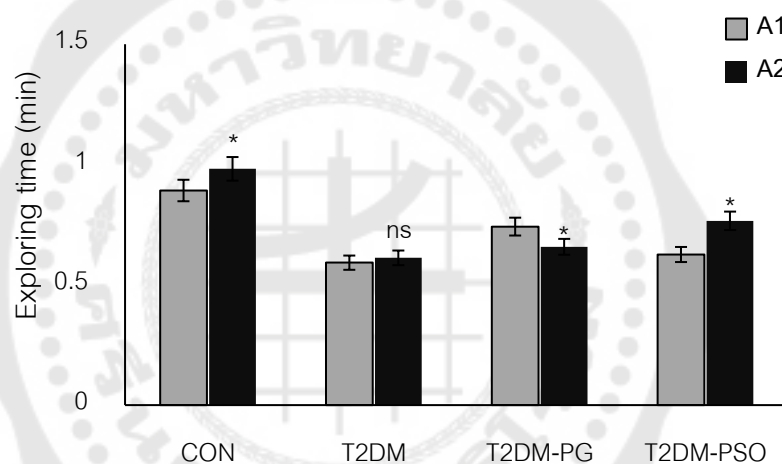
### 2.1 Non-spatial learning and memory assessment

Novel object recognition (NOR) test was used for non-spatial learning and memory assessment. This test normally assesses an animal's behavior when it's exposed to a novel and a familiar object. The exploring time in each object was used to calculate the percentage of the recognition index (%recognition index; %RI). The % RI defines as the ability of the rats to remember the object. Normally, the rats have more exploration time in the novel object than in the old object.

Figure 33 shows the exploring time between the identical objects (A1 and A2) during the familiarization phase of all groups. The normal control rats, T2DM-PG rats, and T2DM-PSO rats spent significantly more exploring time in object A2 than in object A1 (p < 0.05). In contrast, the exploring time in object A2 is no longer than in object A1 in T2DM rats.

As shown in Figure 34, the normal control rats spent more time exploring the novel object (B) than the familiar object (A), both 2 hours (short-term memory) and

24 hours (long-term memory) after the familiarization phase, as shown in Figure 34A and 34B, respectively. In contrast to normal control rats, the T2DM rats spent significantly less time exploring the novel object (% RI) both 2 and 24 hours after the familiarization phase ( $p < 0.001$ ). This observation indicated that T2DM rats had a cognitive deficit in short- and long-term learning and memory impairment. Administration with PSO and PG in type 2 diabetic rats significantly improved both short- and long-term learning and memory function compared to T2DM rats ( $p < 0.001$ ). Moreover, there was no significant difference between the efficiency of PSO and PG on the % RI (Figure 35).



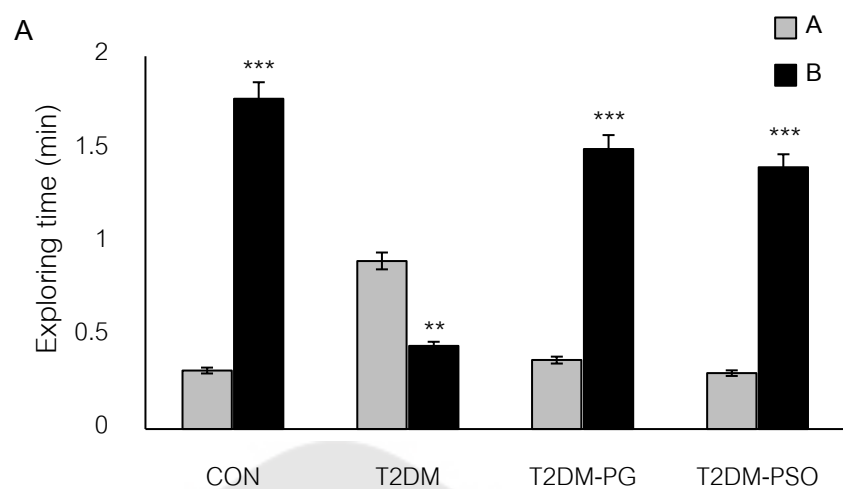
The values are expressed as mean  $\pm$  SEM. (N = 8)

ns; not significantly different compared to object A1

\*;  $p < 0.05$  compared to object A1

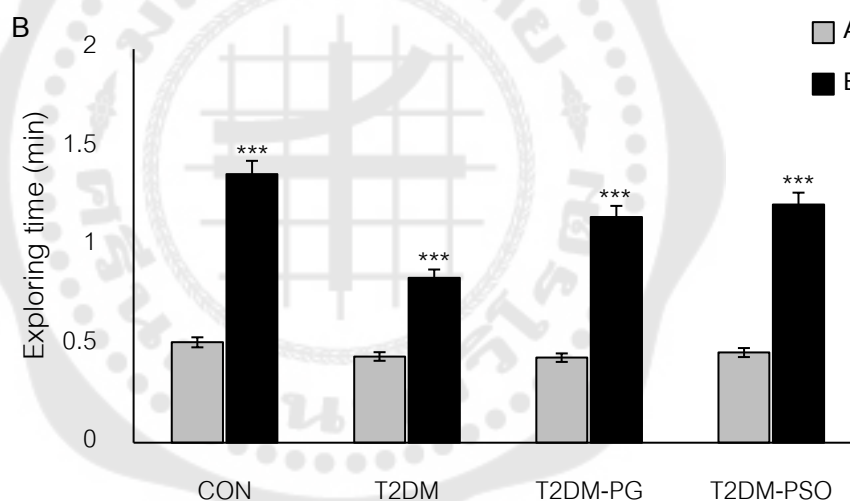
Figure 33 The exploring time between identical objects in the familiarization phase

The graph shows the exploring time between identical objects (A1 and A2) in the familiarization phase. CON; the normal control rats, T2DM; type 2 diabetic rats, T2DM-PG; type 2 diabetic rats administrated 10 mg/kg B.W. pioglitazone, T2DM-PSO; type 2 diabetic rats administrated 200 mg/kg B.W. pumpkin seed oil



The values are expressed as mean  $\pm$  SEM. (N = 8)

\*\*, \*\*\*;  $p < 0.01$  and  $0.001$  compared to object A

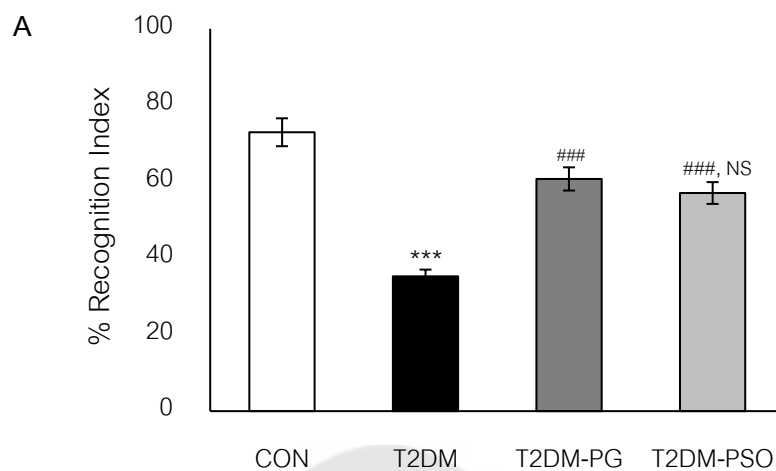


The values are expressed as mean  $\pm$  SEM. (N = 8)

\*\*\*;  $p < 0.001$  compared to object A

Figure 34 The exploring time in the test phase

The graph shows the exploring time in the test phase, including (A) short term memory or after 2 hours and (B) long term memory after 24 hours of the familiarization phase of normal control rats. CON; the normal control rats, T2DM; type 2 diabetic rats, T2DM-PG; type 2 diabetic rats administrated 10 mg/kg B.W. pioglitazone, T2DM-PSO; type 2 diabetic rats administrated 200 mg/kg B.W. pumpkin seed oil

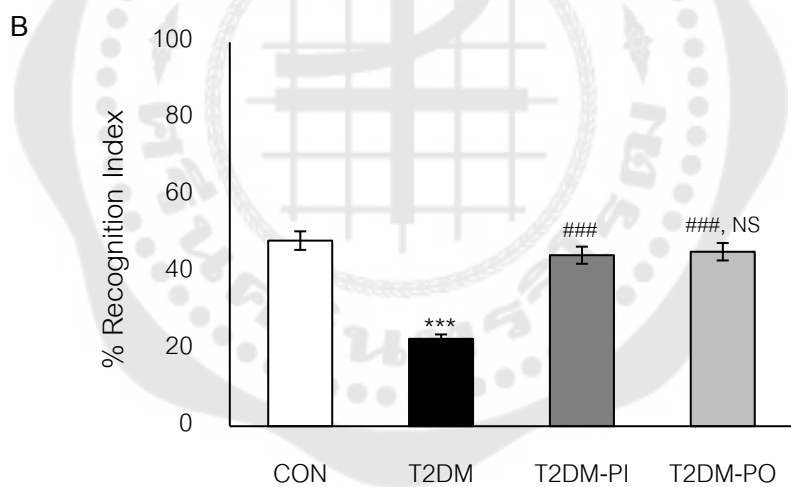


The values are expressed as mean  $\pm$  SEM. (N = 8)

NS; not significant different compared to T2DM-PG group

\*\*\*;  $p < 0.001$  compared to CON group

###;  $p < 0.001$  compared to T2DM group



The values are expressed as mean  $\pm$  SEM. (N = 8)

NS; not significant different compared to T2DM-PI group

\*\*\*;  $p < 0.001$  compared to CON group

###;  $p < 0.001$  compared to T2DM group

Figure 35 The percentage of Recognition index (% RI) in the test phase

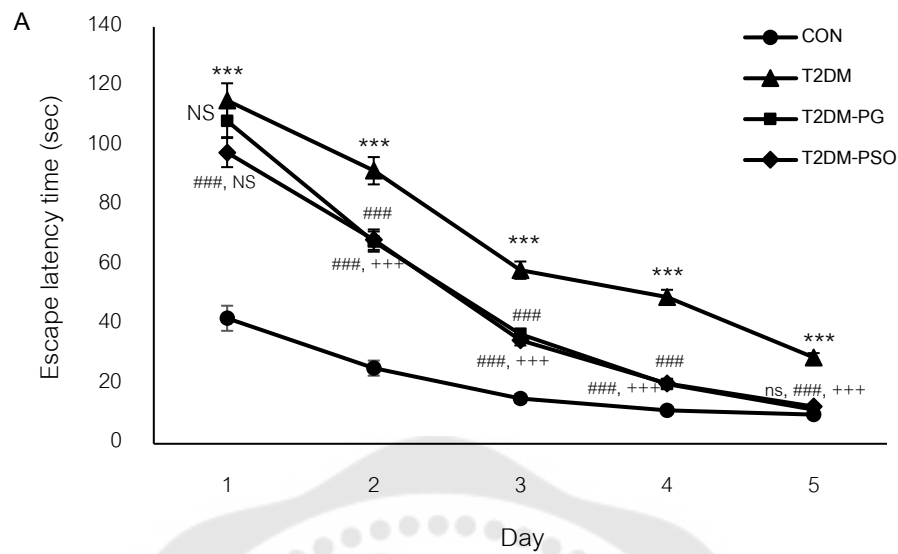
The graph shows the % Recognition index (RI) in the test phase, including (A) short term memory or after 2 hours and (B) long term memory after 24 hours of the familiarization phase of normal control rats. CON; the normal control rats, T2DM; type 2 diabetic rats, T2DM-PG; type 2 diabetic rats administrated 10 mg/kg B.W. pioglitazone, T2DM-PSO; type 2 diabetic rats administrated 200 mg/kg B.W. pumpkin seed oil

## 2.2 Spatial learning and memory assessment

Morris's water maze (MWM) test assessed spatial learning and memory function. Two indices were used to determine learning and memory ability which was 1) the escape latency time (the time that rats used for finding the hidden platform) and 2) the time spent in the target quadrant (the time that rats spent in the quadrant that used to place the hidden platform).

As shown in Figure 36A, the T2DM rats needed more time to find the hidden platform throughout the five days of the test. Therefore, the escape latency time was significantly increased in T2DM rats compared to the normal control rats ( $p < 0.001$ ). However, PSO and PG administration in type 2 diabetic rats caused a decrease in escape latency time compared to the T2DM rats ( $p < 0.001$ ).

After five days, the platform was removed, and time spent in the target quadrant was significantly reduced compared to the normal control rats ( $p < 0.001$ ). Moreover, PSO and PG administration in type 2 diabetic rats were significantly prolonged compared to T2DM rats ( $p < 0.001$ ). However, there was no significant difference in time spent in the target quadrant between T2DM-PSO rats and T2DM-PG rats (Figure 36B).

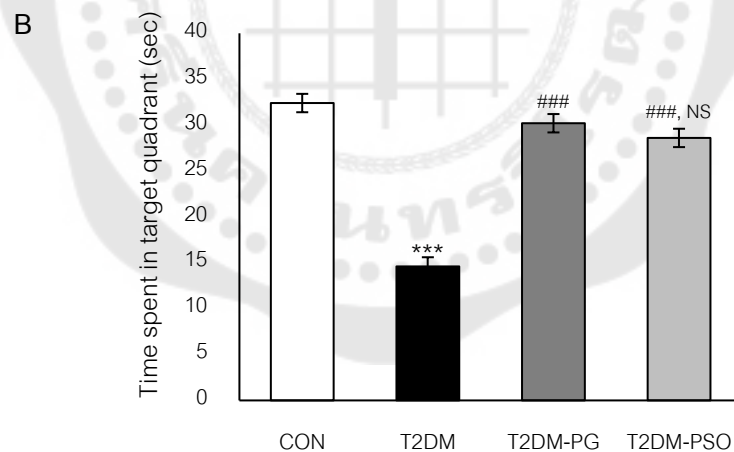


The values are expressed as mean  $\pm$  SEM. (N = 8)

NS, ns; not significantly different compared to T2DM and T2DM-PG groups, respectively

\*\*\*, ###;  $p < 0.001$  compared to CON group and T2DM group, respectively

+++;  $p < 0.001$  compared to T2DM-PG group



The values are expressed as mean  $\pm$  SEM. (N = 8)

NS; not significantly different compared to T2DM-PG group

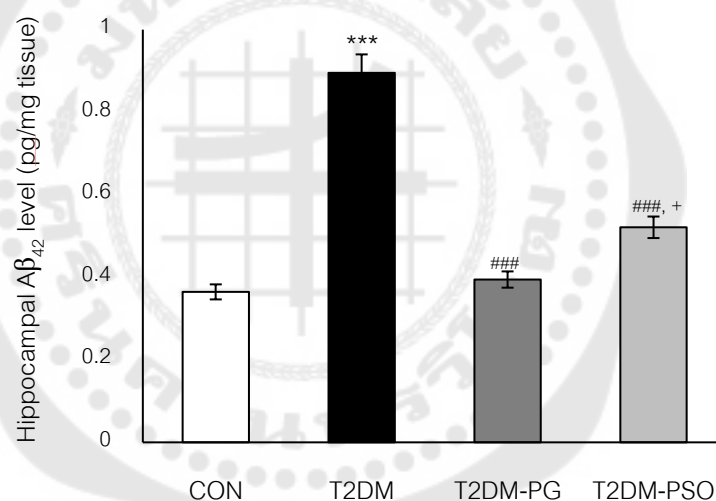
\*\*\*, ###  $p < 0.001$  compared to CON group and T2DM group, respectively

Figure 36 The escape latency time and time spent in the target quadrant

The graph shows the escape latency time (A) and time spent in the target quadrant (B) from the MWM test. CON; the normal control rats, T2DM; type 2 diabetic rats, T2DM-PG; type 2 diabetic rats administrated 10 mg/kg B.W. pioglitazone, T2DM-PSO; type 2 diabetic rats administrated 200 mg/kg B.W. pumpkin seed oil

### 3. Effect of pumpkin seed oil on hippocampal beta-amyloid 42 ( $A\beta_{42}$ ) and beta-secretase (BACE1) expression

Beta-amyloid is an important characteristic of cognitive impairment in Alzheimer's disease (AD)<sup>(10)</sup>. As shown in Figure 37, the hippocampal  $A\beta_{42}$  level in T2DM rats was significantly higher than in the normal control rats ( $p < 0.001$ ). In addition, the PSO and PG administration in type 2 diabetic rats exhibited a significant reduction of the hippocampal  $A\beta_{42}$  compared to T2DM rats ( $p < 0.001$  and  $p < 0.001$ , respectively). Moreover, the present study demonstrated that the effect of PSO on BACE1 plays an important role in the generation of  $A\beta_{42}$ . As shown in Figure 38, the hippocampus BACE1 expression was exhibited in the same manner as the result of  $A\beta_{42}$  levels.



The values are expressed as mean  $\pm$  SEM. (N=8)

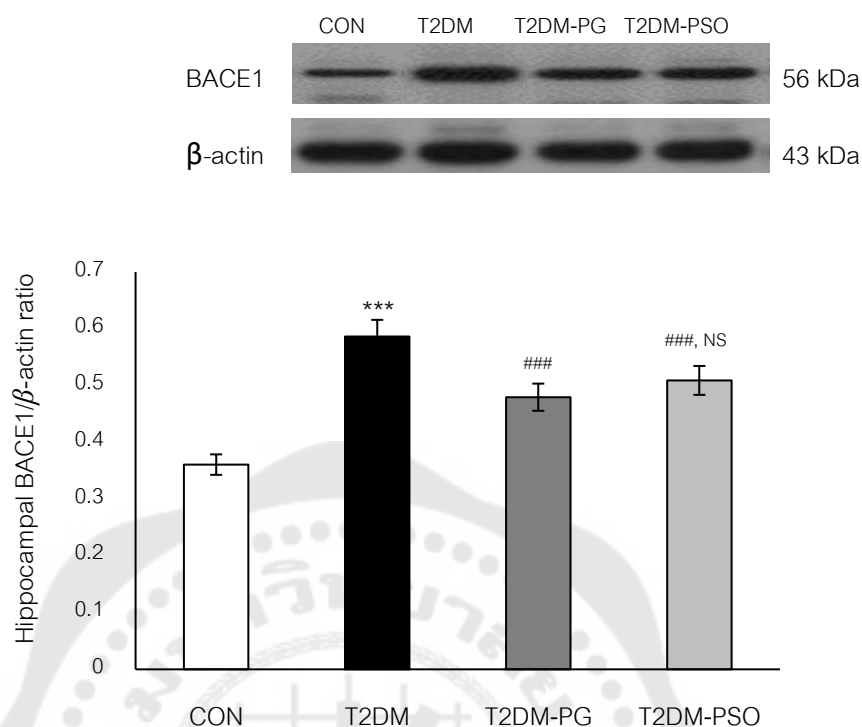
\*\*\*, ###;  $p < 0.001$  compared to CON group and T2DM group, respectively

+;  $p < 0.05$  compared to the T2DM-PG group

Figure 37 The hippocampal beta-amyloid 42 levels of normal control rats

The graph shows the hippocampal beta-amyloid 42 level after 12 weeks of PSO or PG administration. CON; the normal control rats, T2DM; type 2 diabetic rats, T2DM-PG; type 2 diabetic rats administrated 10 mg/kg B.W. pioglitazone, T2DM-PSO; type 2 diabetic rats administrated 200 mg/kg B.W. pumpkin seed oil





The values are expressed as mean ± SEM. (N = 8)

NS;  $p < 0.001$  compared to the T2DM-PG group

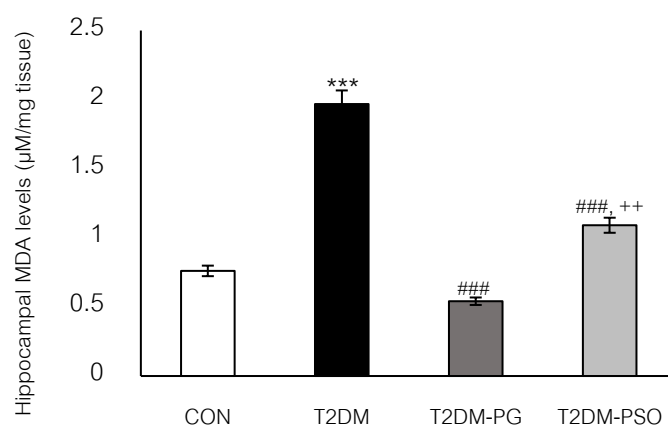
\*\*\*, ###;  $p < 0.001$  compared to CON group and T2DM group, respectively

Figure 38 The hippocampal BACE1 expression

The graph shows the hippocampal BACE1 expression after 12 weeks of PSO or PG administration. CON; the normal control rats, T2DM; type 2 diabetic rats, T2DM-PG; type 2 diabetic rats administrated 10 mg/kg B.W. pioglitazone, T2DM-PSO; type 2 diabetic rats administrated 200 mg/kg B.W. pumpkin seed oil

#### 4. Effect of pumpkin seed oil on oxidative stress and antioxidant in type 2 diabetic rat

As shown in Figure 39, high fructose drinking and low dose STZ induced type 2 diabetes resulted in a significant elevation of lipid peroxidation by-product; malondialdehyde (MDA) ( $p < 0.001$ ), antioxidant (SOD) activity, and nrf2 ( $p < 0.001$  and  $0.001$ , respectively) as compared to those of the normal control rats. However, PSO and PG administration in type 2 diabetic rats significantly decreased the MDA level in the hippocampus ( $p < 0.001$ ). Additionally, PSO and PG administration significantly increased SOD activity and nrf2 expression (Figure 40 and 41, respectively) compared to those of T2DM rats.



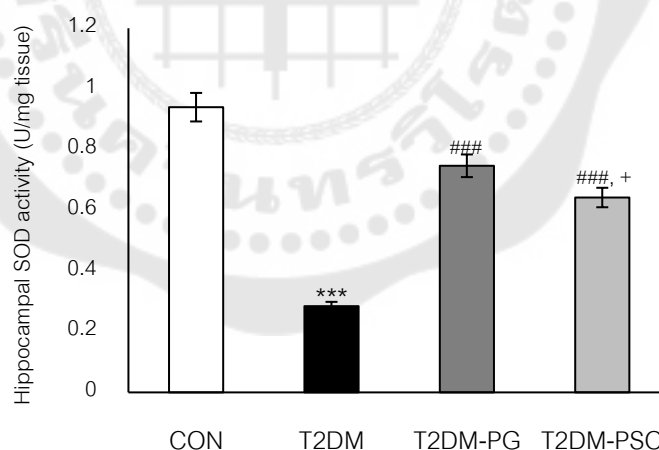
The values are expressed as mean  $\pm$  SEM. (N = 8)

\*\*\*, ###;  $p < 0.001$  compared to CON and T2DM group, respectively

++;  $p < 0.01$  compared to the T2DM-PG group

Figure 39 The hippocampal malondialdehyde (MDA) level

The graph shows the hippocampal malondialdehyde (MDA) level after 12 weeks of PSO or PG administration. CON; the normal control rats, T2DM; type 2 diabetic rats, T2DM-PG; type 2 diabetic rats administrated 10 mg/kg B.W. pioglitazone, T2DM-PSO; type 2 diabetic rats administrated 200 mg/kg B.W. pumpkin seed oil



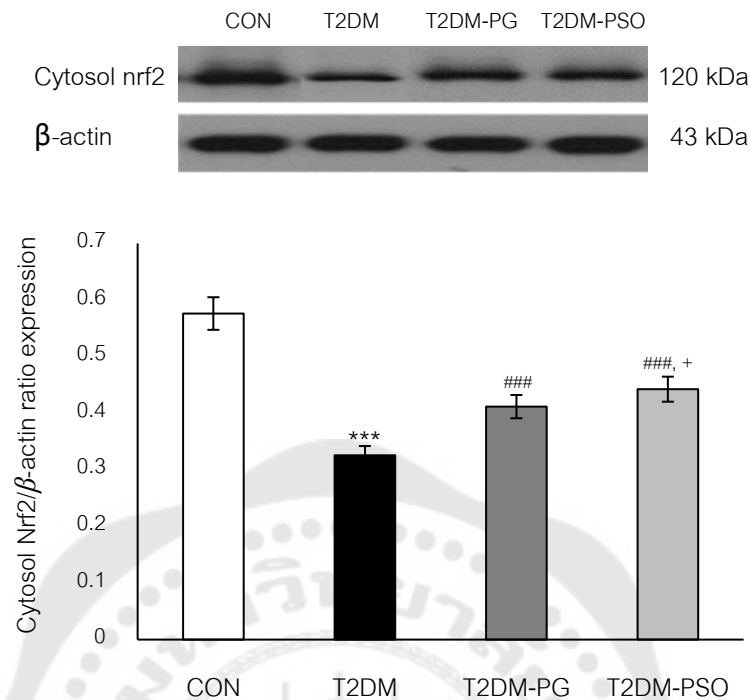
The values are expressed as mean  $\pm$  SEM. (N = 8)

++;  $p < 0.05$  compared to the T2DM-PG group

\*\*\*, ###;  $p < 0.001$  compared to CON group and T2DM group, respectively

Figure 40 The hippocampal superoxide dismutase (SOD) activity

The graph shows the hippocampal superoxide dismutase (SOD) activity after 12 weeks of PSO or PG administration. CON; the normal control rats, T2DM; type 2 diabetic rats, T2DM-PG; type 2 diabetic rats administrated 10 mg/kg B.W. pioglitazone, T2DM-PSO; type 2 diabetic rats administrated 200 mg/kg B.W. pumpkin seed oil



The values are expressed as mean ± SEM. (N = 8)

+,  $p < 0.05$  compared to the T2DM-PG group

\*\*\*, ###,  $p < 0.001$  compared to CON group and T2DM group, respectively

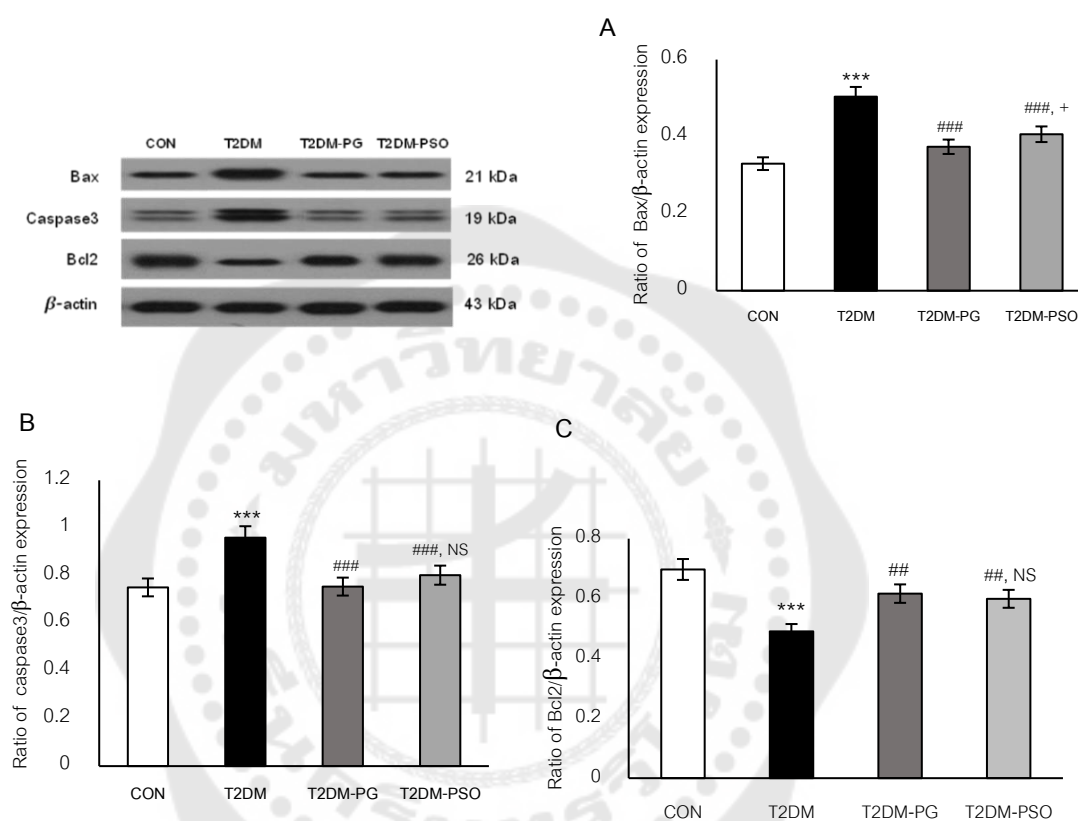
Figure 41 The hippocampal nrf2 expression

The graph shows the hippocampal nrf2 (cytosol) expression after 12 weeks of PSO or PG administration. CON; the normal control rats, T2DM; type 2 diabetic rats, T2DM-PG; type 2 diabetic rats administrated 10 mg/kg B.W. pioglitazone, T2DM-PSO; type 2 diabetic rats administrated 200 mg/kg B.W. pumpkin seed oil

## 5. Effect of pumpkin seed oil on Bcl2, Bax, and caspase3 protein expression in type 2 diabetic rat

As shown in Figure 42C, the western blot results showed that the expression of Bcl2 in T2DM rats was significantly lower than the normal control rats ( $p < 0.001$ ). However, PSO and PG administration in type 2 diabetic rats significantly increased the expression of Bcl2 compared to those of the normal control rats ( $p < 0.001$  and  $0.001$ , respectively). Compared to the normal control rats, the expression of Bax and caspase3 were significantly increased in T2DM rats ( $p < 0.001$ ). Moreover, Bax and caspase3 expression were significantly decreased in type 2 diabetic rats administrated with PSO

and PG compared to those of T2DM rats (Figure 42A and 42B,  $p < 0.001$  and  $0.001$ , respectively).



The values are expressed as mean  $\pm$  SEM. (N = 8)

NS; not significantly different compared to the T2DM-PG group

+,  $p < 0.05$  compared to the T2DM-PG group

\*\*\*;  $p < 0.001$  compared to the CON group

##, ###;  $p < 0.01$  and  $0.001$  compared to the T2DM group

Figure 42 The hippocampal apoptotic and anti-apoptotic proteins expression

The graph shows the hippocampal anti-apoptotic and apoptotic proteins expression after 12 weeks of PSO or PG administration, including A; Hippocampal Bax expression, B; Hippocampal caspase3 expression, and C; Hippocampal Bcl2 expression. CON; the normal control rats, T2DM; type 2 diabetic rats, T2DM-PG; type 2 diabetic rats administrated 10 mg/kg B.W. pioglitazone, T2DM-PSO; type 2 diabetic rats administrated 200 mg/kg B.W. pumpkin seed oil

## CHAPTER V

### DISCUSSION

Type 2 diabetes has been shown to be an important risk factor for cognitive impairment. Numerous studies, both in AD patients and animal models, have shown that cognitive impairment results from a disorder of insulin signaling correlated with the extracellular accumulation of A $\beta$  plaques in the brain<sup>(177-181)</sup>. Moreover, the underlying mechanisms between type 2 diabetes and A $\beta$  accumulation focuses on oxidative stress<sup>(13, 108, 182)</sup>. However, the clinical drug treatment for protection or improvement of cognitive deficit in type 2 diabetes is limited. Due to the involvement of oxidative stress in diabetes-induced cognitive impairment, previous research has focused on the potential effects of natural antioxidant compounds. Therefore, the present study attempted to provide experimental evidence to examine the neuroprotective effect of pumpkin seed oil (PSO) on A $\beta_{42}$ -induced cell toxicity in human neuroblastoma; SH-SY5Y cells in *in vitro* model. In addition, to investigate the molecular mechanisms of PSO on type 2 diabetes-induced cognitive impairment, the high fructose drinking combined with a low dose of streptozotocin-induced type 2 diabetic rat model was used as *in vivo* study.

The important findings of the present study are: 1) PSO protected A $\beta_{42}$ -induced neuronal apoptosis in human neuroblastoma; SH-SY5Y cells through reduced oxidative stress and, 2) PSO ameliorated cognitive impairment, reduced hippocampal A $\beta_{42}$  accumulation, protected against oxidative stress, and alleviated neuronal apoptosis in high fructose drinking combined with a low dose of STZ-induced type 2 diabetic rats.

**The neuroprotective effects of pumpkin seed oil on beta-amyloid 42-induced neuronal apoptosis in human neuroblastoma; SH-SY5Y cell**

The present *in vitro* study demonstrated for the first time that PSO, the natural oil derived from the pumpkin seed extract has a neuroprotective effect against A $\beta_{42}$ -induced neuronal apoptosis. A few numbers of evidence have indicated that A $\beta_{42}$  directly induced neuronal cell death/apoptosis through oxidative stress<sup>(16, 158, 183)</sup>. In the present study, human neuroblastoma; SH-SY5Y cells were used to study the toxicity

caused by A $\beta$  stimulation on neuronal cells. The human neuroblastoma; SH-SY5Y cells have been used extensively to investigate and assess the changes in neurotransmitter release and secretion, neuronal cell death/apoptosis<sup>(184-186)</sup>, as well as to study drug and natural substances against neurodegenerative disease models such as AD<sup>(187-190)</sup>.

A $\beta$  is an important hallmark of AD pathogenesis which can trigger neuronal apoptosis<sup>(16)</sup>. Numerous studies have been reported that A $\beta$  toxic to neurons through several mechanisms, including reactive oxygen species (ROS) production, mitochondrial dysfunction, and cell death/ apoptosis<sup>(29, 191)</sup>. There are several amyloid peptides, among which, A $\beta_{42}$  has been reported as the most neurotoxic one<sup>(10)</sup>. In the present study, the MTT assay was used to examine the cytotoxicity of A $\beta_{42}$  on human neuroblastoma; SH-SY5Y cells. The results demonstrated that exposure of SH-SY5Y cells to A $\beta_{42}$  could decrease cell viability in a concentration-dependent manner. Moreover, pretreatment of PSO and curcumin significantly increased cell viability. According to these results, we suggested that PSO and curcumin can inhibit neurotoxicity from A $\beta_{42}$ . Curcumin has been used as a positive control since several studies revealed that curcumin could inhibit cytotoxicity induced by A $\beta$  through its antioxidant<sup>(192-194)</sup>. To examine the mechanism of the neuroprotective effect of PSO, the intracellular ROS as well as apoptotic parameters, including the expression of apoptotic proteins (Bax and caspase3) and anti-apoptotic protein (Bcl2) were determined. The present results demonstrated that A $\beta_{42}$ -induced the production of intracellular ROS as well as neuronal apoptotic cell death. These results were consistent with the previous studies indicating that A $\beta_{42}$  caused neuronal cell death<sup>(29, 31, 158)</sup>.

Pretreatment with PSO significantly decreased intracellular ROS, apoptotic protein Bax, caspase3 expression, and significantly increased anti-apoptotic protein Bcl2 expression. ROS are involved in the apoptotic mechanism that induces the pathogenesis of neurodegenerative disease<sup>(16, 19, 195)</sup>. Our results from HPLC analysis found that PSO contains six fatty acids, including oleic acid, linoleic acid, alpha-linoleic acid, palmitic acid, stearic acid, and arachidic acid, as shown in Table 3. A study by Tang *et al.* (2014) reported that linoleic acid and arachidic acid could protect against

cell death by inhibiting MPP<sup>+</sup>- induced toxicity in PC12 cells<sup>(196)</sup>. In addition, Yaguchi *et al.* (2010) demonstrated the protective effect of linoleic acid on sodium-nitroprusside-induced neuronal cell death through oxidative stress<sup>(197)</sup>. Consistent with this study, we suggested that the protective effect of PSO against A $\beta$ <sub>42</sub>-induced neuronal cell death/apoptosis might be partly due to its antioxidant property.

#### **Pumpkin seed oil administration attenuates the metabolic disorders in fructose drinking water combined with low dose STZ injection**

As proposed in the objective of the present study, we aimed to examine the effects and potential mechanisms of PSO on neuronal cell death and cognitive impairment in type 2 diabetic rats.

Numerous mechanisms have been proposed for the occurrence of neurodegeneration and impaired cognition in type 2 diabetes, including hyperglycemia, insulin resistance, neuroinflammation, oxidative stress, and neuronal apoptosis<sup>(77, 198, 199)</sup>. In the present study, 10% w/v fructose drinking water followed by a single low dose STZ intravenous injection was used as a type 2 diabetic rat model. Consistent with previous studies, our results demonstrated that this type 2 diabetic rat model exhibited metabolic disorders, including body weight gain, hyperglycemia, hyperinsulinemia, dyslipidemia, and increased serum free fatty acid (FFA), and HOMA-IR index, which indicated the development of insulin resistance. Fructose is a monosaccharide, the primary natural sugar found in various fruits, vegetables, and honey which is absorbed and metabolized by the liver<sup>(200)</sup>. Notably, large amounts and long-term fructose feeding caused rapid stimulation of lipogenesis and triglyceride accumulation in the liver, which leads to decreased insulin sensitivity and glucose intolerance<sup>(147, 201, 202)</sup>.

To examine the effects of PSO on metabolic disorders in type 2 diabetic rats, PSO and positive control drug; pioglitazone (PG) were administered for 12 weeks in T2DM-PSO and T2DM-PG rats, respectively. From the present results, administration of PSO demonstrated the attenuation of metabolic disorders, including body weight, FBG, HbA1c, FFA, serum insulin, and calculated HOMA-IR index. The results agreed with several studies where the diabetic rats treated with PSO significantly reduced blood glucose, glycated hemoglobin, and insulin levels<sup>(39, 203-205)</sup>. According to the change in



metabolic parameters, it is suggested that PSO shows the potential to reduce obesity, hyperglycemia, and hyperinsulinemia, as well as improve insulin sensitivity. PSO contains several active compounds such as tocopherol, fatty acids, and flavonoids<sup>(40, 206)</sup>. Our study found that the active ingredients of PSO are linoleic acid, oleic acid, and palmitic acid, which are unsaturated fatty acids. Eyjolfson *et al.* (2004) studied the effect of linoleic acid on obese diabetic rats. They suggested that linoleic acid has an anti-diabetic property by reducing FBG and improving insulin sensitivity<sup>(41)</sup>. In addition, Feng *et al.* (2006) reported that linoleic acid is the major fatty acid in PSO that activates pancreatic  $\beta$ -cell function<sup>(42)</sup>. According to the previous studies and the present results, we suggested that PSO has the potential to attenuate metabolic disorders in type 2 diabetes model induced by high fructose drinking combined with a low dose STZ injection in part by improving pancreatic  $\beta$ -cell function.

#### **Antioxidant and anti-apoptotic properties of pumpkin seed oil on type 2 diabetes-induced cognitive impairment**

Several studies have reported that type 2 diabetes (T2DM) is the major risk factor for cognitive impairment and Alzheimer's disease (AD)<sup>(4, 75)</sup>. T2DM is characterized by hyperglycemia, hyperinsulinemia, and insulin resistance<sup>(59)</sup>. It is well established that AD is a crucial neurodegenerative disorder characterized by progressive dementia and loss of cognitive ability<sup>(207)</sup>. Accumulating evidence revealed that diabetic patients, especially T2DM have a two-fold increased incidence of AD<sup>(208)</sup>.

In the present study, we demonstrated that type 2 diabetic rats with hyperglycemia, hyperinsulinemia, and insulin resistance showed a reduction in learning and memory abilities which were assessed by Novel object recognition (NOR) and Morris's water maze (MWM) tests. NOR and MWM are the non-spatial and spatial learning and memory assessment tasks. Spatial learning and memory define the storage and retrieval of information in the brain needed to plan a route to the desired location and remember where an object is located, or an event occurred. In contrast, non-spatial learning and memory is the behavior process associated with the memory of the object's identity and location<sup>(209)</sup>. The impairment of this cognition in non-spatial and spatial learning and memory was considered to be the dysfunction of the hippocampus and



cortex brain areas<sup>(210)</sup>. In the NOR test, T2DM rats demonstrated a decrease in the exploration of a new object. In contrast, the administration of PSO and PG in T2DM-PSO and T2DM-PG resulted in a higher exploring time of a novel object than a familiar one. In addition, T2DM rats exhibited a significantly reduced recognition index compared with normal control rats. This reduction was reversed in T2DM-PSO and T2DM-PG rats. These results indicated that PSO and PG improved T2DM-induced cognitive impairment. This test is based on the spontaneous tendency of rats to spend more exploring time on a novel object than on an old object. Therefore, the rats with better memory spent more time exploring new object than the old one. Similarly, in the MWM test, T2DM rats exhibited significantly higher escape latency time on days 1, 2, 3, 4, and 5 than the normal control rats. Our finding is in accordance with the previous studies, which demonstrated spatial learning and memory deficit in diabetic rats<sup>(25, 132)</sup>. However, administration with PSO in T2DM-PSO rats significantly reduced escape latency time, this effect was also exhibited in the PG administration. In the probe trial test on day 6 when the platform was removed, T2DM rats exhibited significantly reduced time spent in the platform area compared with the normal control rats. In contrast, administration of PSO and PG in T2DM-PSO and T2DM-PG rats significantly increased the time spent in the target quadrant. The longer escape latency is defined as rats' poor ability to learn. In contrast, more time was used in the target quadrant, meaning the rats remembered the platform location. According to the behavioral results, we suggested that both PSO and PG have the potential to improve cognitive impairment in type 2 diabetic rats. Furthermore, chronic hyperglycemia and insulin resistance are considered major causes of diabetic complications, which trigger structural and functional brain abnormalities, including A $\beta$  deposition, neuronal loss, and apoptosis<sup>(11, 211, 212)</sup>. It is known that the hippocampus and cortex are two key brain regions involved in learning and memory formation<sup>(213, 214)</sup>. Especially, the hippocampus is one of the most sensitive brain regions to metabolic abnormalities, including diabetes<sup>(215)</sup>. According to the present results, impaired learning and memory was found in T2DM. Consistent with the previous studies, the present results also demonstrated the rising of A $\beta$ <sub>42</sub> and BACE1 expression in the

hippocampal T2DM rats<sup>(216-218)</sup>. A $\beta$  protein is the major biomarker for AD. A $\beta_{42}$  is generated from amyloid-beta precursor protein cleaving enzyme 1 (BACE1) and subsequently cleaved by  $\gamma$ -secretase<sup>(219)</sup>. Wang *et al.* (2019) demonstrated that the level of hippocampal A $\beta_{42}$  was significantly higher in diabetic rats than the normal control rats<sup>(220)</sup>. Moreover, several studies suggested that type 2 diabetes with hyperglycemia and insulin resistance induced A $\beta$  protein accumulation, leading to synaptic plasticity abnormality, neuronal cell death, and apoptosis<sup>(221, 222)</sup>. According to these abnormalities, the impairment of cognitive function is developed. Interestingly, in the present study, administration of PSO and PG significantly reduced the accumulation of A $\beta_{42}$  and the expression of BACE1. Taken together, we suggested that administration of PSO demonstrated the potential to improve cognitive impairment in T2DM through the anti-diabetic property.

To further examine the more potential mechanisms of PSO to improve cognitive impairment in type 2 diabetes. We further investigated the role of PSO on neuronal oxidative stress and apoptosis. Oxidative stress plays an important role in the pathogenesis of the neurodegenerative disease, including cognitive impairment, dementia, and AD<sup>(19, 26, 91)</sup>. Hyperglycemia, hyperinsulinemia, and free fatty acids can cause increased generation of reactive oxygen species (ROS) through the accumulation of advanced glycation end products (AGEs)<sup>(223, 224)</sup> and decreased antioxidant system<sup>(225)</sup>. It is well known that AGEs produce superoxide and hydrogen peroxide, leading to increased lipid peroxidation and neuronal cell damage<sup>(226)</sup>. This imbalance between ROS and the antioxidant system causes oxidative stress, which is observed in AD and T2DM<sup>(227)</sup>. It is well known that oxidative stress and A $\beta$  are linked to each other, in other words, oxidative stress induces the accumulation of A $\beta$ <sup>(16)</sup>, and A $\beta$  induces oxidative stress both *in vivo* and *in vitro* studies. We found significantly increased intracellular ROS in A $\beta$ -induced human neuroblastoma, SH-SY5Y cells, compared with SH-SY5Y cells without A $\beta$  exposure. Moreover, in the present *in vivo* type 2 diabetic rats, we found significantly increase in malondialdehyde (MDA), hippocampal lipid peroxidation product, while superoxide dismutase (SOD) and cytosol nuclear factor

erythroid 2-related factor 2 (nrf2) were significantly decreased compared with the normal control rats. To exemplify, Nrf2 is a transcription factor that regulates the cellular defense against toxic and oxidative stress insults through the expression of genes involved in oxidative stress response. Nrf2 is activated in response to oxidative stress and induces the target gene expression by binding to the antioxidant response element (ARE)<sup>(228)</sup>. Consistent with Wang *et al.* (2020), they reported that type 2 diabetic mice exhibited cognitive deficit, which was assessed by the MWM test. In addition, they found that hippocampal nrf2 oxidative stress indicators were reduced<sup>(199)</sup>. Taken together from other previous studies and our present results indicated that the type 2 diabetic state exhibited hippocampal oxidative stress. Recently, several studies have shown the potential of antioxidant in ROS inhibition<sup>(25, 199)</sup> and A $\beta$  production<sup>(188, 194)</sup>. As shown in our study, we demonstrated that administration of PSO and PG in T2DM-PSO and T2DM-PG significantly reduced oxidative stress by reducing lipid peroxidation and increasing antioxidant SOD and nrf2. The antioxidant effects of PSO were in accordance with the previous report<sup>(37, 38, 229)</sup>.

An increase in ROS level can cause lipid peroxidation, and DNA damage thereby inducing neuronal cell death or apoptosis, leading to cognitive impairment<sup>(17, 18, 91)</sup>. Moreover, AD and diabetes especially type 2 diabetes, share risk factors such as insulin resistance, oxidative stress, A $\beta$  accumulation, neuroinflammation, glycogen synthesis kinase 3 (GSK3), and neuronal apoptosis<sup>(6, 230-234)</sup>. It is well recognized that apoptosis is associated with the development of neurodegenerative diseases, including diabetes-induced cognitive impairment and AD<sup>(234)</sup>.

Apoptosis is an important mechanism for hyperglycemia and insulin resistance-induced neuronal cell death<sup>(33)</sup>. Enzyme cysteine protease (caspase) and proteins in the Bcl2 family are related to the apoptosis mechanism<sup>(33, 34)</sup>. Bcl2 family is composed of Bcl2 and Bax proteins which are functionally opposed. Bcl2 is the apoptosis inhibitory protein, whereas Bax acts to promote apoptosis<sup>(35)</sup>. The reduction in Bcl2 and increase in Bax activates the increase in caspase3, the most important key regulator in promoting apoptosis.

To explore the neuroprotective mechanisms of PSO in type 2 diabetes-induced cognitive impairment, we investigated the expression of Bax, caspase3, and Bcl2. Our results demonstrated that hippocampal anti-apoptotic protein Bcl2 was significantly decreased, whereas proteins-induced apoptosis, Bax and caspase3, as well as the ratio of Bax/Bcl2 were significantly increased in T2DM rats. However, administration of PSO and PG reversed the alteration of Bcl2, Bax, and caspase3 protein expression. Recent studies have demonstrated that ROS/oxidative stress is the major driving factor of neuronal apoptosis in diabetic conditions<sup>(95, 132, 235, 236)</sup>. Moreover, other studies and our *in vitro* results demonstrated that exposure of human neuroblastoma; SH-SY5Y cells to A $\beta$  peptide induced neuronal cell apoptosis<sup>(30, 31, 185, 193)</sup>. Taken together, our *in vitro* and *in vivo* results indicated PSO has a potent neuroprotective effect which improved T2DM-induced cognitive impairment through anti-diabetic, increased insulin sensitivity, anti-apoptotic, and antioxidant properties.

## CONCLUSION

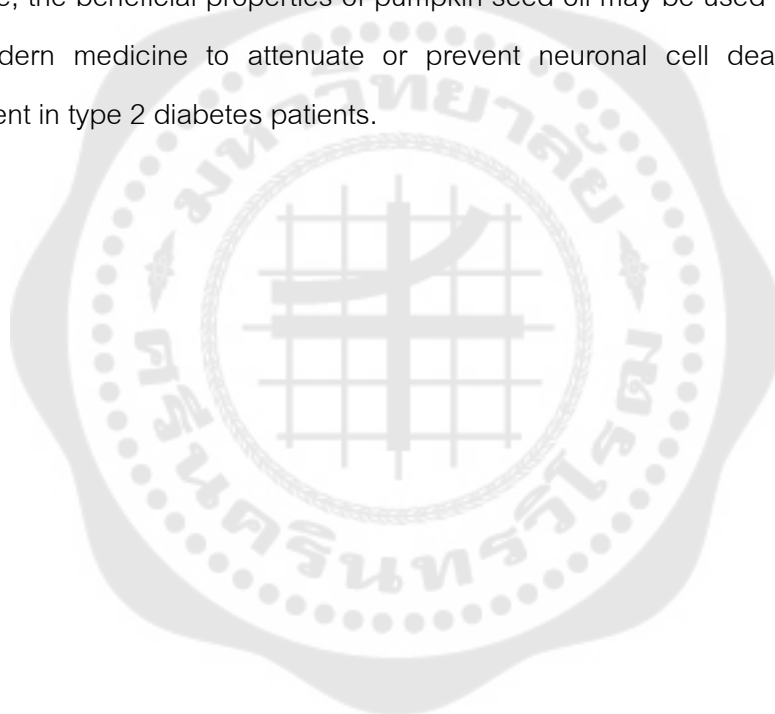
The present study revealed that pumpkin seed oil has a neuroprotective effect by protecting neuronal cell death through reduced beta-amyloid ( $A\beta$ ) accumulation and oxidative stress, both in human neuroblastoma; SH-SY5Y cells and type 2 diabetic rat model. Furthermore, the present study demonstrated that high fructose drinking water combined with a single low dose STZ injection is an acceptable model to induce type 2 diabetes mellitus in rats. Type 2 diabetic rats showed insulin resistance, hyperglycemia, and dyslipidemia for the entire experiment.

*In vitro* study demonstrated that human neuroblastoma SH-SY5Y cells pretreated with pumpkin seed oil could be protected against  $A\beta_{42}$ -induced neuronal cell death by reducing intracellular reactive oxygen species (ROS) production, apoptotic proteins (Bax and caspase3), and increasing anti-apoptotic protein (Bcl2). In addition, it is well known that type 2 diabetes induces cognitive impairment through  $A\beta$  accumulation, oxidative stress, and neuronal cell death. Therefore, we investigated the possible mechanism of pumpkin seed oil on type 2 diabetic-induced cognitive impairment through  $A\beta$  accumulation, oxidative stress, and neuronal apoptosis. The results revealed that oxidative stress and neuronal apoptosis in the type 2 diabetic rat hippocampal tissues had a low level of nrf2 transcription factor and superoxide dismutase (SOD), while lipid peroxidation (malondialdehyde; MDA) level was higher than the normal control rats. At the same time, the present study discovered that type 2 diabetic hippocampal tissues had a higher expression of  $A\beta_{42}$  and  $\beta$ -secretase (BACE1) enzyme. Furthermore, the oxidative stress and  $A\beta_{42}$  accumulation activated high expression of apoptotic proteins (Bax and caspase3) and suppressed the anti-apoptotic protein (Bcl2) expression. Therefore, we suggested there is a cause of cognitive impairment in type 2 diabetes.

Interestingly, pumpkin seed oil administration can enhance cognitive performance in non-spatial and spatial learning and memory. Moreover, the pumpkin seed oil is also able to reverse hyperglycemia and insulin resistance in type 2 diabetic

rats. The enhancement of cognitive function is related to metabolic disorders and insulin resistance improvement. The present study demonstrated that pumpkin seed oil consists of linoleic acid and oleic acid contents, the major fatty acid composition found in pumpkin seed oil. Therefore, we suggested that linoleic and oleic acids in pumpkin seed oil could improve cognitive function in type 2 diabetes through anti-diabetic, anti-hyperlipidemia, and antioxidant properties.

Following our results, the pumpkin seed oil can potentially improve insulin resistance, anti-diabetic, anti-hyperlipidemia, anti-oxidation, and neuroprotection prevention. Therefore, the beneficial properties of pumpkin seed oil may be used as a co-treatment with modern medicine to attenuate or prevent neuronal cell death and cognitive impairment in type 2 diabetes patients.





## A. Table of materials and reagents

No.	Materials and reagents	Sources
1	Antibiotic-antimycotic	Invitrogen, USA
2	Anti- $\beta$ -actin antibody	Millipore, MO, USA
3	Anti-Bax antibody	Abcam, USA
4	Anti-Bcl-2 antibody	Abcam, USA
5	Anti-BACE1 antibody	Abcam, USA
6	Anti-caspase3 antibody	Abcam, USA
7	Anti-nrf2 antibody	Abcam, USA
8	Anti-rabbit IgG HRP-linked antibody	Bio-Rad, CA, USA
9	Beta-amyloid 42	Millipore, MO, USA
10	Cholesterol strip	Roche, Germany
11	Curcumin	Millipore, MO, USA
12	Dimethyl sulfoxide	Invitrogen, USA
13	Dulbecco's Modified Eagle's-Medium	Gibco, USA
14	Enhance chemiluminescence	Pierce, USA
15	F12 medium	Gibco, USA
16	Fetal bovine serum	Invitrogen, USA
17	Fluorescent CM-H <sub>2</sub> DCFDA dye	Invitrogen, USA
18	Fructose powder	Charoentavorn, Thailand
19	Human neuroblastoma cell line SH-SY5Y	ATTC, USA
20	Pioglitazone	Millipore, MO, USA
22	Polyvinylidene difluoride membrane	Millipore, MO, USA
22	Protease inhibitor cocktails	Millipore, MO, USA
23	Radioimmunoprecipitation assay buffer	Millipore, MO, USA
24	Rat A $\beta$ <sub>42</sub> ELISA assay kit	Invitrogen, USA
25	Rat free fatty acid ELISA assay kit	Cayman Chemical, USA
26	Rat insulin ELISA assay kit	Millipore, MO, US



## A. (Continued)

No.	Materials and reagents	Sources
27	Sodium pyruvate	Invitrogen, USA
28	Streptozotocin	Millipore, MO, USA
29	Superoxide dismutase assay kit	Cayman Chemical, USA
30	Thiobarbituric acid reactive substances assay kit	Cayman Chemical, USA
31	Triglyceride strip	Roche, Germany
32	Trypan blue	Invitrogen, USA
33	X-ray film	Kodak, US
34	3-(4,5-dimethylthiazol-2-yl)-2,5-diphenyltetrazolium bromide (MTT) dye	Invitrogen, USA

## B. Table of saturated and unsaturated fatty acids in PSO extracted

Saturated fatty acids (g/100 g)		Unsaturated fatty acid (g/100 g)	
Palmitic acid (C16:0)	19.30	Cis-9-oleic acid (C18:1n:9c)	28.10
Stearic acid (C18:0)	8.02	Linoleic acid (C18:2n6c)	39.11
Arachidic acid (C20:0)	0.37	Alpha-linoleic acid (C18:3n3c)	0.27

C. Table of the fasting blood glucose (FBG), blood cholesterol (CHOL), and blood triglyceride (TG) levels

Group	FBG (mg/dL)	HbA1c (mg/dL)	CHOL (mg/dL)	TG (mg/dL)
CON	98.00 ± 1.41	3.92 ± 0.04	151.60 ± 0.75	124.20 ± 1.80
T2DM	345.40 ± 1.89 <sup>***</sup>	9.58 ± 0.02 <sup>***</sup>	190.60 ± 3.28 <sup>***</sup>	385.00 ± 11.38 <sup>***</sup>
T2DM-PG	235.20 ± 3.83 <sup>###</sup>	5.04 ± 0.11 <sup>###</sup>	162.20 ± 1.28 <sup>###</sup>	244.00 ± 2.45 <sup>###</sup>
T2DM-PSO	216.00 ± 3.35 <sup>###, +</sup>	5.94 ± 0.12 <sup>###, ++</sup>	162.60 ± 1.08 <sup>###, ns</sup>	269.80 ± 8.18 <sup>###, +</sup>

The values are expressed as mean ± SEM. (N = 8)

ns; not significantly compared to T2DM-PG group

+, ++; p < 0.05 and 0.01 compared to T2DM-PG group

\*\*\*, ###; p < 0.001 compared to CON group and T2DM group, respectively

CON; the normal control rats, T2DM; type 2 diabetic rats, T2DM-PG; type 2 diabetic rats administrated 10 mg/kg B.W. pioglitazone, T2DM-PSO; type 2 diabetic rats administrated 200 mg/kg B.W. pumpkin seed oil



## REFERENCES

1. Artasensi A, Pedretti A, Vistoli G, Fumagalli L. Type 2 Diabetes Mellitus: A Review of Multi-Target Drugs. *Molecules*. 2020;25(8):1987.
2. Biessels GJ, Strachan MW, Visseren FL, Kappelle LJ, Whitmer RA. Dementia and cognitive decline in type 2 diabetes and prediabetic stages: towards targeted interventions. *Lancet Diabetes Endocrinol*. 2014;2(3):246-55.
3. Brownlee M. The pathobiology of diabetic complications: a unifying mechanism. *Diabetes*. 2005;54(6):1615-25.
4. Jayaraman A, Pike CJ. Alzheimer's disease and type 2 diabetes: multiple mechanisms contribute to interactions. *Curr Diab Rep*. 2014;14(4):476.
5. Park SA. A Common Pathogenic Mechanism Linking Type-2 Diabetes and Alzheimer's Disease: Evidence from Animal Models. *J Clin Neurol*. 2011;7(1):10-8.
6. Arnold SE, Arvanitakis Z, Macauley-Rambach SL, Koenig AM, Wang HY, Ahima RS, et al. Brain insulin resistance in type 2 diabetes and Alzheimer disease: concepts and conundrums. *Nat Rev Neurol*. 2018;14(3):168-81.
7. Chatterjee S, Mudher A. Alzheimer's Disease and Type 2 Diabetes: A Critical Assessment of the Shared Pathological Traits. *Frontiers in Neuroscience*. 2018;12.
8. Butterfield DA, Di Domenico F, Barone E. Elevated risk of type 2 diabetes for development of Alzheimer disease: A key role for oxidative stress in brain. *Biochimica et Biophysica Acta (BBA) - Molecular Basis of Disease*. 2014;1842(9):1693-706.
9. David JA, Rifkin WJ, Rabbani PS, Ceradini DJ. The Nrf2/Keap1/ARE Pathway and Oxidative Stress as a Therapeutic Target in Type II Diabetes Mellitus. *J Diabetes Res*. 2017;2017:4826724.
10. Murphy MP, LeVine H, 3rd. Alzheimer's disease and the amyloid-beta peptide. *J Alzheimers Dis*. 2010;19(1):311-23.
11. Mullins RJ, Diehl TC, Chia CW, Kapogiannis D. Insulin Resistance as a Link between Amyloid-Beta and Tau Pathologies in Alzheimer's Disease. *Front Aging Neurosci*. 2017;9:118.

12. Sharma G, Parihar A, Talaiya T, Dubey K, Porwal B, Parihar MS. Cognitive impairments in type 2 diabetes, risk factors and preventive strategies. *Journal of Basic and Clinical Physiology and Pharmacology*. 2020;31(2).
13. Umegaki H. Type 2 diabetes as a risk factor for cognitive impairment: current insights. *Clin Interv Aging*. 2014;9:1011-9.
14. Rajmohan R, Reddy PH. Amyloid-Beta and Phosphorylated Tau Accumulations Cause Abnormalities at Synapses of Alzheimer's disease Neurons. *Journal of Alzheimer's disease : JAD*. 2017;57(4):975-99.
15. Rad SK, Arya A, Karimian H, Madhavan P, Rizwan F, Koshy S, et al. Mechanism involved in insulin resistance via accumulation of  $\beta$ -amyloid and neurofibrillary tangles: link between type 2 diabetes and Alzheimer's disease. *Drug Des Devel Ther*. 2018;12:3999-4021.
16. Tamagno E, Parola M, Guglielmotto M, Santoro G, Bardini P, Marra L, et al. Multiple signaling events in amyloid beta-induced, oxidative stress-dependent neuronal apoptosis. *Free Radic Biol Med*. 2003;35(1):45-58.
17. Salim S. Oxidative Stress and the Central Nervous System. *J Pharmacol Exp Ther*. 2017;360(1):201-5.
18. Uttara B, Singh AV, Zamboni P, Mahajan RT. Oxidative stress and neurodegenerative diseases: a review of upstream and downstream antioxidant therapeutic options. *Curr Neuropharmacol*. 2009;7(1):65-74.
19. Sayre LM, Perry G, Smith MA. Oxidative Stress and Neurotoxicity. *Chemical Research in Toxicology*. 2008;21(1):172-88.
20. Holmström KM, Baird L, Zhang Y, Hargreaves I, Chalasani A, Land JM, et al. Nrf2 impacts cellular bioenergetics by controlling substrate availability for mitochondrial respiration. *Biol Open*. 2013;2(8):761-70.
21. Lee JM, Shih AY, Murphy TH, Johnson JA. NF-E2-related factor-2 mediates neuroprotection against mitochondrial complex I inhibitors and increased concentrations of intracellular calcium in primary cortical neurons. *J Biol Chem*. 2003;278(39):37948-56.
22. Vargas MR, Johnson JA. The Nrf2-ARE cytoprotective pathway in astrocytes.

Expert Rev Mol Med. 2009;11:e17.

23. Manczak M, Anekonda TS, Henson E, Park BS, Quinn J, Reddy PH. Mitochondria are a direct site of A beta accumulation in Alzheimer's disease neurons: implications for free radical generation and oxidative damage in disease progression. *Hum Mol Genet.* 2006;15(9):1437-49.
24. Uruno A, Matsumaru D, Ryoike R, Saito R, Kadoguchi S, Saigusa D, et al. Nrf2 Suppresses Oxidative Stress and Inflammation in App Knock-In Alzheimer's Disease Model Mice. *Mol Cell Biol.* 2020;40(6).
25. Gao M, Kang Y, Zhang L, Li H, Qu C, Luan X, et al. Troxerutin attenuates cognitive decline in the hippocampus of male diabetic rats by inhibiting NADPH oxidase and activating the Nrf2/ARE signaling pathway. *Int J Mol Med.* 2020;46(3):1239-48.
26. Tarafdar A, Pula G. The Role of NADPH Oxidases and Oxidative Stress in Neurodegenerative Disorders. *Int J Mol Sci.* 2018;19(12).
27. Fricker M, Tolkovsky AM, Borutaite V, Coleman M, Brown GC. Neuronal Cell Death. *Physiol Rev.* 2018;98(2):813-80.
28. D'Amelio M, Cavallucci V, Cecconi F. Neuronal caspase-3 signaling: not only cell death. *Cell Death & Differentiation.* 2010;17(7):1104-14.
29. Muthaiyah B, Essa MM, Chauhan V, Chauhan A. Protective effects of walnut extract against amyloid beta peptide-induced cell death and oxidative stress in PC12 cells. *Neurochem Res.* 2011;36(11):2096-103.
30. Wang H, Xu Y, Yan J, Zhao X, Sun X, Zhang Y, et al. Acteoside protects human neuroblastoma SH-SY5Y cells against beta-amyloid-induced cell injury. *Brain Res.* 2009;1283:139-47.
31. Zhang L, Yu H, Zhao X, Lin X, Tan C, Cao G, et al. Neuroprotective effects of salidroside against beta-amyloid-induced oxidative stress in SH-SY5Y human neuroblastoma cells. *Neurochem Int.* 2010;57(5):547-55.
32. Soleymaninejad M, Joursaraei SG, Feizi F, Jafari Anarkooli I. The Effects of Lycopene and Insulin on Histological Changes and the Expression Level of Bcl-2 Family Genes in the Hippocampus of Streptozotocin-Induced Diabetic Rats. *J Diabetes Res.*

2017;2017:4650939.

33. Elmore S. Apoptosis: a review of programmed cell death. *Toxicol Pathol.* 2007;35(4):495-516.

34. Topuridze ML, Kipiani VA, Pavliashvili NS, Kipiani NV, Petriashvili TG. [Molecular mechanisms of apoptosis]. *Georgian Med News.* 2007(150):38-45.

35. Czabotar PE, Lessene G, Strasser A, Adams JM. Control of apoptosis by the BCL-2 protein family: implications for physiology and therapy. *Nature Reviews Molecular Cell Biology.* 2014;15(1):49-63.

36. Yadav M, Jain S, Tomar R, Prasad GB, Yadav H. Medicinal and biological potential of pumpkin: an updated review. *Nutr Res Rev.* 2010;23(2):184-90.

37. Abou Seif HS. Ameliorative effect of pumpkin oil (*Cucurbita pepo* L.) against alcohol-induced hepatotoxicity and oxidative stress in albino rats. *Beni-Suef University Journal of Basic and Applied Sciences.* 2014;3(3):178-85.

38. Eraslan G, Kanbur M, Aslan Ö, Karabacak M. The antioxidant effects of pumpkin seed oil on subacute aflatoxin poisoning in mice. *Environmental Toxicology.* 2013;28(12):681-8.

39. MAJID AK, AHMED Z, KHAN R. Effect of pumpkin seed oil on cholesterol fractions and systolic/diastolic blood pressure. *Food Science and Technology.* 2020;40:769-77.

40. Montesano D, Blasi F, Simonetti MS, Santini A, Cossignani L. Chemical and Nutritional Characterization of Seed Oil from *Cucurbita maxima* L. (var. Berrettina) Pumpkin. *Foods.* 2018;7(3):30.

41. Eyjolfson V, Spriet LL, Dyck DJ. Conjugated linoleic acid improves insulin sensitivity in young, sedentary humans. *Med Sci Sports Exerc.* 2004;36(5):814-20.

42. Feng DD, Luo Z, Roh SG, Hernandez M, Tawadros N, Keating DJ, et al. Reduction in voltage-gated K<sup>+</sup> currents in primary cultured rat pancreatic beta-cells by linoleic acids. *Endocrinology.* 2006;147(2):674-82.

43. Sen S, Chakraborty R. Treatment and Diagnosis of Diabetes Mellitus and Its Complication: Advanced Approaches. *Mini Rev Med Chem.* 2015;15(14):1132-3.

44. <Definition, diagnosis and classification of diabetes mellitus and.pdf>.

45. Walker CG, Zariwala MG, Holness MJ, Sugden MC. Diet, obesity and diabetes: a current update. *Clin Sci (Lond)*. 2007;112(2):93-111.
46. Schlienger JL. [Type 2 diabetes complications]. *Presse Med*. 2013;42(5):839-48.
47. Guthrie RA, Guthrie DW. Pathophysiology of diabetes mellitus. *Crit Care Nurs Q*. 2004;27(2):113-25.
48. Pandey A, Chawla S, Guchhait P. Type-2 diabetes: Current understanding and future perspectives. *IUBMB Life*. 2015;67(7):506-13.
49. Jung U, Choi M-S. Obesity and Its Metabolic Complications: The Role of Adipokines and the Relationship between Obesity, Inflammation, Insulin Resistance, Dyslipidemia and Nonalcoholic Fatty Liver Disease. *International journal of molecular sciences*. 2014;15:6184-223.
50. Liu H, Yang H, Wang D, Liu Y, Liu X, Li Y, et al. Insulin regulates P-glycoprotein in rat brain microvessel endothelial cells via an insulin receptor-mediated PKC/NF-kappaB pathway but not a PI3K/Akt pathway. *Eur J Pharmacol*. 2009;602(2-3):277-82.
51. Hopkins DF, Williams G. Insulin receptors are widely distributed in human brain and bind human and porcine insulin with equal affinity. *Diabet Med*. 1997;14(12):1044-50.
52. Schulingkamp RJ, Pagano TC, Hung D, Raffa RB. Insulin receptors and insulin action in the brain: review and clinical implications. *Neurosci Biobehav Rev*. 2000;24(8):855-72.
53. Blázquez E, Velázquez E, Hurtado-Carneiro V, Ruiz-Albusac J. Insulin in the Brain: Its Pathophysiological Implications for States Related with Central Insulin Resistance, Type 2 Diabetes and Alzheimer's Disease. *Frontiers in endocrinology*. 2014;5:161.
54. Plum L, Schubert M, Brüning JC. The role of insulin receptor signaling in the brain. *Trends Endocrinol Metab*. 2005;16(2):59-65.
55. Derakhshan F, Toth C. Insulin and the brain. *Curr Diabetes Rev*. 2013;9(2):102-16.
56. Hallschmid M, Schultes B. Central nervous insulin resistance: a promising target in the treatment of metabolic and cognitive disorders? *Diabetologia*. 2009;52(11):2264-9.
57. Bedse G, Di Domenico F, Serviddio G, Cassano T. Aberrant insulin signaling in Alzheimer's disease: current knowledge. *Frontiers in Neuroscience*. 2015;9.



58. Lebovitz HE. Insulin resistance: definition and consequences. *Exp Clin Endocrinol Diabetes*. 2001;109 Suppl 2:S135-48.
59. Taylor R. Insulin resistance and type 2 diabetes. *Diabetes*. 2012;61(4):778-9.
60. Zheng Y, Ley SH, Hu FB. Global aetiology and epidemiology of type 2 diabetes mellitus and its complications. *Nat Rev Endocrinol*. 2018;14(2):88-98.
61. Kahn BB. Adipose Tissue, Inter-Organ Communication, and the Path to Type 2 Diabetes: The 2016 Banting Medal for Scientific Achievement Lecture. *Diabetes*. 2019;68(1):3-14.
62. Leong YQ, Ng KY, Chye SM, Ling APK, Koh RY. Mechanisms of action of amyloid-beta and its precursor protein in neuronal cell death. *Metabolic Brain Disease*. 2020;35(1):11-30.
63. Dimitriadis G, Mitrou P, Lambadiari V, Maratou E, Raptis SA. Insulin effects in muscle and adipose tissue. *Diabetes Res Clin Pract*. 2011;93 Suppl 1:S52-9.
64. Yazıcı D, Sezer H. Insulin Resistance, Obesity and Lipotoxicity. *Adv Exp Med Biol*. 2017;960:277-304.
65. Barazzoni R, Gortan Cappellari G, Ragni M, Nisoli E. Insulin resistance in obesity: an overview of fundamental alterations. *Eat Weight Disord*. 2018;23(2):149-57.
66. Guilherme A, Virbasius JV, Puri V, Czech MP. Adipocyte dysfunctions linking obesity to insulin resistance and type 2 diabetes. *Nat Rev Mol Cell Biol*. 2008;9(5):367-77.
67. Yadav A, Kataria MA, Saini V, Yadav A. Role of leptin and adiponectin in insulin resistance. *Clin Chim Acta*. 2013;417:80-4.
68. Sripetchwandee J, Chattipakorn N, Chattipakorn SC. Links Between Obesity-Induced Brain Insulin Resistance, Brain Mitochondrial Dysfunction, and Dementia. *Front Endocrinol (Lausanne)*. 2018;9:496.
69. Shoelson SE, Lee J, Goldfine AB. Inflammation and insulin resistance. *J Clin Invest*. 2006;116(7):1793-801.
70. Boden G. Fatty acid—induced inflammation and insulin resistance in skeletal muscle and liver. *Current Diabetes Reports*. 2006;6(3):177-81.
71. Rhea EM, Banks WA. Role of the Blood-Brain Barrier in Central Nervous System

Insulin Resistance. *Front Neurosci.* 2019;13:521.

72. Liu Y, Liu F, Grundke-Iqbal I, Iqbal K, Gong CX. Deficient brain insulin signalling pathway in Alzheimer's disease and diabetes. *J Pathol.* 2011;225(1):54-62.

73. D'Oria R, Laviola L, Giorgino F, Unfer V, Bettocchi S, Scioscia M. PKB/Akt and MAPK/ERK phosphorylation is highly induced by inositols: Novel potential insights in endothelial dysfunction in preeclampsia. *Pregnancy Hypertension: An International Journal of Women's Cardiovascular Health.* 2017;10.

74. Tumminia A, Vinciguerra F, Parisi M, Frittitta L. Type 2 Diabetes Mellitus and Alzheimer's Disease: Role of Insulin Signalling and Therapeutic Implications. *International Journal of Molecular Sciences.* 2018;19:3306.

75. Tumminia A, Vinciguerra F, Parisi M, Frittitta L. Type 2 Diabetes Mellitus and Alzheimer's Disease: Role of Insulin Signalling and Therapeutic Implications. *Int J Mol Sci.* 2018;19(11).

76. Kandimalla R, Thirumala V, Reddy PH. Is Alzheimer's disease a Type 3 Diabetes? A critical appraisal. *Biochimica et Biophysica Acta (BBA) - Molecular Basis of Disease.* 2017;1863(5):1078-89.

77. Kothari V, Luo Y, Tornabene T, O'Neill AM, Greene MW, Geetha T, et al. High fat diet induces brain insulin resistance and cognitive impairment in mice. *Biochim Biophys Acta Mol Basis Dis.* 2017;1863(2):499-508.

78. Frisardi V, Solfrizzi V, Seripa D, Capurso C, Santamato A, Sancarolo D, et al. Metabolic-cognitive syndrome: a cross-talk between metabolic syndrome and Alzheimer's disease. *Ageing Res Rev.* 2010;9(4):399-417.

79. Pratchayasakul W, Kerdphoo S, Petsophonakul P, Pongchaidecha A, Chattipakorn N, Chattipakorn SC. Effects of high-fat diet on insulin receptor function in rat hippocampus and the level of neuronal corticosterone. *Life Sci.* 2011;88(13-14):619-27.

80. Tong M, de la Monte SM. Mechanisms of ceramide-mediated neurodegeneration. *J Alzheimers Dis.* 2009;16(4):705-14.

81. Sartorius T, Peter A, Schulz N, Drescher A, Bergheim I, Machann J, et al. Cinnamon extract improves insulin sensitivity in the brain and lowers liver fat in mouse

models of obesity. *PLoS One*. 2014;9(3):e92358.

82. Bedse G, Di Domenico F, Serviddio G, Cassano T. Aberrant insulin signaling in Alzheimer's disease: current knowledge. *Front Neurosci*. 2015;9:204.

83. Zlokovic BV. Neurovascular pathways to neurodegeneration in Alzheimer's disease and other disorders. *Nat Rev Neurosci*. 2011;12(12):723-38.

84. Kahn AM, Husid A, Allen JC, Seidel CL, Song T. Insulin acutely inhibits cultured vascular smooth muscle cell contraction by a nitric oxide synthase-dependent pathway. *Hypertension*. 1997;30(4):928-33.

85. Bhamra MS, Ashton NJ. Finding a pathological diagnosis for Alzheimer's disease: are inflammatory molecules the answer? *Electrophoresis*. 2012;33(24):3598-607.

86. Sokolova A, Hill MD, Rahimi F, Warden LA, Halliday GM, Shepherd CE. Monocyte chemoattractant protein-1 plays a dominant role in the chronic inflammation observed in Alzheimer's disease. *Brain Pathol*. 2009;19(3):392-8.

87. Nakamura M, Watanabe N. Ubiquitin-like protein MNSF $\beta$ /endophilin II complex regulates Dectin-1-mediated phagocytosis and inflammatory responses in macrophages. *Biochem Biophys Res Commun*. 2010;401(2):257-61.

88. Ma QL, Yang F, Rosario ER, Ubeda OJ, Beech W, Gant DJ, et al. Beta-amyloid oligomers induce phosphorylation of tau and inactivation of insulin receptor substrate via c-Jun N-terminal kinase signaling: suppression by omega-3 fatty acids and curcumin. *J Neurosci*. 2009;29(28):9078-89.

89. Akash MS, Rehman K, Chen S. Role of inflammatory mechanisms in pathogenesis of type 2 diabetes mellitus. *J Cell Biochem*. 2013;114(3):525-31.

90. Erickson MA, Hansen K, Banks WA. Inflammation-induced dysfunction of the low-density lipoprotein receptor-related protein-1 at the blood-brain barrier: protection by the antioxidant N-acetylcysteine. *Brain Behav Immun*. 2012;26(7):1085-94.

91. Tönnies E, Trushina E. Oxidative Stress, Synaptic Dysfunction, and Alzheimer's Disease. *J Alzheimers Dis*. 2017;57(4):1105-21.

92. Balbaa M, Abdulmalek SA, Khalil S. Oxidative stress and expression of insulin signaling proteins in the brain of diabetic rats: Role of *Nigella sativa* oil and antidiabetic

drugs. PLoS One. 2017;12(5):e0172429.

93. Steen E, Terry BM, Rivera EJ, Cannon JL, Neely TR, Tavares R, et al. Impaired insulin and insulin-like growth factor expression and signaling mechanisms in Alzheimer's disease--is this type 3 diabetes? J Alzheimers Dis. 2005;7(1):63-80.

94. Muriach M, Flores-Bellver M, Romero FJ, Barcia JM. Diabetes and the Brain: Oxidative Stress, Inflammation, and Autophagy. Oxidative Medicine and Cellular Longevity. 2014;2014:102158.

95. Ahmad W, Ijaz B, Shabbiri K, Ahmed F, Rehman S. Oxidative toxicity in diabetes and Alzheimer's disease: mechanisms behind ROS/ RNS generation. J Biomed Sci. 2017;24(1):76.

96. Sies H. Oxidative stress: a concept in redox biology and medicine. Redox Biol. 2015;4:180-3.

97. Jung UJ, Choi MS. Obesity and its metabolic complications: the role of adipokines and the relationship between obesity, inflammation, insulin resistance, dyslipidemia and nonalcoholic fatty liver disease. Int J Mol Sci. 2014;15(4):6184-223.

98. Yaribeygi H, Sathyapalan T, Atkin SL, Sahebkar A. Molecular Mechanisms Linking Oxidative Stress and Diabetes Mellitus. Oxid Med Cell Longev. 2020;2020:8609213.

99. Ganjifrockwala FA, Joseph JT, George G. Decreased total antioxidant levels and increased oxidative stress in South African type 2 diabetes mellitus patients. Journal of Endocrinology, Metabolism and Diabetes of South Africa. 2017;22(2):21-5.

100. Vomund S, Schäfer A, Parnham MJ, Brüne B, von Knethen A. Nrf2, the Master Regulator of Anti-Oxidative Responses. Int J Mol Sci. 2017;18(12).

101. Ma Q. Role of nrf2 in oxidative stress and toxicity. Annu Rev Pharmacol Toxicol. 2013;53:401-26.

102. Kensler TW, Wakabayashi N, Biswal S. Cell survival responses to environmental stresses via the Keap1-Nrf2-ARE pathway. Annu Rev Pharmacol Toxicol. 2007;47:89-116.

103. David J, Rifkin W, Rabbani P, Ceradini D. The Nrf2/Keap1/ARE Pathway and Oxidative Stress as a Therapeutic Target in Type II Diabetes Mellitus. Journal of Diabetes Research. 2017;2017:1-15.

104. Itoh K, Chiba T, Takahashi S, Ishii T, Igarashi K, Katoh Y, et al. An Nrf2/small Maf heterodimer mediates the induction of phase II detoxifying enzyme genes through antioxidant response elements. *Biochem Biophys Res Commun*. 1997;236(2):313-22.
105. McMahon M, Itoh K, Yamamoto M, Hayes JD. Keap1-dependent proteasomal degradation of transcription factor Nrf2 contributes to the negative regulation of antioxidant response element-driven gene expression. *J Biol Chem*. 2003;278(24):21592-600.
106. Uruno A, Furusawa Y, Yagishita Y, Fukutomi T, Muramatsu H, Negishi T, et al. The Keap1-Nrf2 system prevents onset of diabetes mellitus. *Mol Cell Biol*. 2013;33(15):2996-3010.
107. Kahn SE, Hull RL, Utzschneider KM. Mechanisms linking obesity to insulin resistance and type 2 diabetes. *Nature*. 2006;444(7121):840-6.
108. Maciejczyk M, Żebrowska E, Chabowski A. Insulin Resistance and Oxidative Stress in the Brain: What's New? *Int J Mol Sci*. 2019;20(4).
109. Lin MT, Beal MF. Mitochondrial dysfunction and oxidative stress in neurodegenerative diseases. *Nature*. 2006;443(7113):787-95.
110. Gerbitz KD, Gempel K, Brdiczka D. Mitochondria and diabetes. Genetic, biochemical, and clinical implications of the cellular energy circuit. *Diabetes*. 1996;45(2):113-26.
111. Cheng H, Gang X, Liu Y, Wang G, Zhao X, Wang G. Mitochondrial dysfunction plays a key role in the development of neurodegenerative diseases in diabetes. *Am J Physiol Endocrinol Metab*. 2020;318(5):E750-e64.
112. de la Monte SM. Brain insulin resistance and deficiency as therapeutic targets in Alzheimer's disease. *Curr Alzheimer Res*. 2012;9(1):35-66.
113. Shieh J, Huang P-T, Lin Y-F. Alzheimer's Disease and Diabetes: Insulin Signaling as the Bridge Linking Two Pathologies. *Molecular Neurobiology*. 2020;57.
114. Shieh JC-C, Huang P-T, Lin Y-F. Alzheimer's Disease and Diabetes: Insulin Signaling as the Bridge Linking Two Pathologies. *Molecular Neurobiology*. 2020;57(4):1966-77.
115. Ittner LM, Ke YD, Delerue F, Bi M, Gladbach A, van Eersel J, et al. Dendritic

function of tau mediates amyloid-beta toxicity in Alzheimer's disease mouse models. *Cell*. 2010;142(3):387-97.

116. Hong M, Lee VM. Insulin and insulin-like growth factor-1 regulate tau phosphorylation in cultured human neurons. *The Journal of biological chemistry*. 1997;272(31):19547-53.

117. Freude S, Plum L, Schnitker J, Leeser U, Udelhoven M, Krone W, et al. Peripheral hyperinsulinemia promotes tau phosphorylation in vivo. *Diabetes*. 2005;54(12):3343-8.

118. Sims-Robinson C, Kim B, Rosko A, Feldman EL. How does diabetes accelerate Alzheimer disease pathology? *Nat Rev Neurol*. 2010;6(10):551-9.

119. Schubert M, Gautam D, Surjo D, Ueki K, Baudler S, Schubert D, et al. Role for neuronal insulin resistance in neurodegenerative diseases. *Proc Natl Acad Sci U S A*. 2004;101(9):3100-5.

120. Green DR. Apoptotic pathways: paper wraps stone blunts scissors. *Cell*. 2000;102(1):1-4.

121. Micheau O, Tschopp J. Induction of TNF receptor I-mediated apoptosis via two sequential signaling complexes. *Cell*. 2003;114(2):181-90.

122. Scaffidi C, Schmitz I, Krammer PH, Peter ME. The role of c-FLIP in modulation of CD95-induced apoptosis. *J Biol Chem*. 1999;274(3):1541-8.

123. Youle RJ, Strasser A. The BCL-2 protein family: opposing activities that mediate cell death. *Nat Rev Mol Cell Biol*. 2008;9(1):47-59.

124. Fukui K, Onodera K, Shinkai T, Suzuki S, Urano S. Impairment of learning and memory in rats caused by oxidative stress and aging, and changes in antioxidative defense systems. *Ann N Y Acad Sci*. 2001;928:168-75.

125. Sa-Nguanmoo P, Tanajak P, Kerdphoo S, Satjaritanun P, Wang X, Liang G, et al. FGF21 improves cognition by restored synaptic plasticity, dendritic spine density, brain mitochondrial function and cell apoptosis in obese-insulin resistant male rats. *Horm Behav*. 2016;85:86-95.

126. Koliaki C, Roden M. Alterations of Mitochondrial Function and Insulin Sensitivity in Human Obesity and Diabetes Mellitus. *Annu Rev Nutr*. 2016;36:337-67.



127. Pamidi N, Satheesha Nayak BN. Effect of streptozotocin induced diabetes on rat hippocampus. *Bratisl Lek Listy*. 2012;113(10):583-8.
128. Foghi K, Ahmadpour S. Diabetes mellitus type 1 and neuronal degeneration in ventral and dorsal hippocampus. *Iranian Journal of Pathology*. 2013;9:33-7.
129. Sima AA, Kamiya H, Li ZG. Insulin, C-peptide, hyperglycemia, and central nervous system complications in diabetes. *Eur J Pharmacol*. 2004;490(1-3):187-97.
130. Li ZG, Zhang W, Grunberger G, Sima AA. Hippocampal neuronal apoptosis in type 1 diabetes. *Brain Res*. 2002;946(2):221-31.
131. Yonguc GN, Dodurga Y, Adiguzel E, Gundogdu G, Kucukatay V, Ozbal S, et al. Grape seed extract has superior beneficial effects than vitamin E on oxidative stress and apoptosis in the hippocampus of streptozotocin induced diabetic rats. *Gene*. 2015;555(2):119-26.
132. Chen Y, Li L, Li Z, Huang X, Zhang L, Chen W. [Effects of naokang erhao decoction on cognitive ability and hippocampal apoptosis-related proteins in diabetic rats]. *Zhongguo Zhong Yao Za Zhi*. 2011;36(11):1519-23.
133. Schinas P, Karavalakis G, Davaris C, Anastopoulos G, Karonis D, Zannikos F, et al. Pumpkin (*Cucurbita pepo* L.) seed oil as an alternative feedstock for the production of biodiesel in Greece. *Biomass and Bioenergy*. 2009;33(1):44-9.
134. Badr SEA, Shaaban M, Elkholy YM, Helal MH, Hamza AS, Masoud MS, et al. Chemical composition and biological activity of ripe pumpkin fruits (*Cucurbita pepo* L.) cultivated in Egyptian habitats. *Natural Product Research*. 2011;25(16):1524-39.
135. El-Boghdady NA. Protective effect of ellagic acid and pumpkin seed oil against methotrexate-induced small intestine damage in rats. *Indian J Biochem Biophys*. 2011;48(6):380-7.
136. Bharti SK, Kumar A, Sharma NK, Prakash O, Jaiswal SK, Krishnan S, et al. Tocopherol from seeds of *Cucurbita pepo* against diabetes: validation by in vivo experiments supported by computational docking. *J Formos Med Assoc*. 2013;112(11):676-90.
137. King AJ. The use of animal models in diabetes research. *Br J Pharmacol*.

2012;166(3):877-94.

138. Lin S, Thomas TC, Storlien LH, Huang XF. Development of high fat diet-induced obesity and leptin resistance in C57Bl/6J mice. *International Journal of Obesity*. 2000;24(5):639-46.

139. Dong F, Zhang X, Yang X, Esberg LB, Yang H, Zhang Z, et al. Impaired cardiac contractile function in ventricular myocytes from leptin-deficient ob/ob obese mice. *J Endocrinol*. 2006;188(1):25-36.

140. Flanagan AM, Brown JL, Santiago CA, Aad PY, Spicer LJ, Spicer MT. High-fat diets promote insulin resistance through cytokine gene expression in growing female rats. *J Nutr Biochem*. 2008;19(8):505-13.

141. Fraulob JC, Ogg-Diamantino R, Fernandes-Santos C, Aguila MB, Mandarim-de-Lacerda CA. A Mouse Model of Metabolic Syndrome: Insulin Resistance, Fatty Liver and Non-Alcoholic Fatty Pancreas Disease (NAFPD) in C57BL/6 Mice Fed a High Fat Diet. *J Clin Biochem Nutr*. 2010;46(3):212-23.

142. Storlien LH, Kraegen EW, Jenkins AB, Chisholm DJ. Effects of sucrose vs starch diets on in vivo insulin action, thermogenesis, and obesity in rats. *Am J Clin Nutr*. 1988;47(3):420-7.

143. Oliart Ros RM, Torres-Márquez ME, Badillo A, Angulo Guerrero O. Dietary fatty acids effects on sucrose-induced cardiovascular syndrome in rats. *J Nutr Biochem*. 2001;12(4):207-12.

144. Santuré M, Pitre M, Marette A, Deshaies Y, Lemieux C, Larivière R, et al. Induction of insulin resistance by high-sucrose feeding does not raise mean arterial blood pressure but impairs haemodynamic responses to insulin in rats. *Br J Pharmacol*. 2002;137(2):185-96.

145. Pagliassotti MJ, Prach PA. Quantity of sucrose alters the tissue pattern and time course of insulin resistance in young rats. *Am J Physiol*. 1995;269(3 Pt 2):R641-6.

146. Perona JS, Vögler O, Sánchez-Domínguez JM, Montero E, Escribá PV, Ruiz-Gutierrez V. Consumption of virgin olive oil influences membrane lipid composition and regulates intracellular signaling in elderly adults with type 2 diabetes mellitus. *J Gerontol A*



Biol Sci Med Sci. 2007;62(3):256-63.

147. Teff KL, Elliott SS, Tschöp M, Kieffer TJ, Rader D, Heiman M, et al. Dietary fructose reduces circulating insulin and leptin, attenuates postprandial suppression of ghrelin, and increases triglycerides in women. *J Clin Endocrinol Metab.* 2004;89(6):2963-72.

148. Roglans N, Vilà L, Farré M, Alegret M, Sánchez RM, Vázquez-Carrera M, et al. Impairment of hepatic Stat-3 activation and reduction of PPAR $\alpha$  activity in fructose-fed rats. *Hepatology.* 2007;45(3):778-88.

149. Lê KA, Faeh D, Stettler R, Ith M, Kreis R, Vermathen P, et al. A 4-wk high-fructose diet alters lipid metabolism without affecting insulin sensitivity or ectopic lipids in healthy humans. *Am J Clin Nutr.* 2006;84(6):1374-9.

150. Reed MJ, Meszaros K, Entes LJ, Claypool MD, Pinkett JG, Gadbois TM, et al. A new rat model of type 2 diabetes: the fat-fed, streptozotocin-treated rat. *Metabolism.* 2000;49(11):1390-4.

151. Zhang M, Lv XY, Li J, Xu ZG, Chen L. The characterization of high-fat diet and multiple low-dose streptozotocin induced type 2 diabetes rat model. *Exp Diabetes Res.* 2008;2008:704045.

152. Wang Y, Campbell T, Perry B, Beaurepaire C, Qin L. Hypoglycemic and insulin-sensitizing effects of berberine in high-fat diet- and streptozotocin-induced diabetic rats. *Metabolism.* 2011;60(2):298-305.

153. Szkudelski T. The mechanism of alloxan and streptozotocin action in B cells of the rat pancreas. *Physiol Res.* 2001;50(6):537-46.

154. Srinivasan K, Viswanad B, Asrat L, Kaul CL, Ramarao P. Combination of high-fat diet-fed and low-dose streptozotocin-treated rat: a model for type 2 diabetes and pharmacological screening. *Pharmacol Res.* 2005;52(4):313-20.

155. Sahin K, Onderci M, Tuzcu M, Ustundag B, Cikim G, Ozercan IH, et al. Effect of chromium on carbohydrate and lipid metabolism in a rat model of type 2 diabetes mellitus: the fat-fed, streptozotocin-treated rat. *Metabolism.* 2007;56(9):1233-40.

156. Wilson RD, Islam MS. Fructose-fed streptozotocin-injected rat: an alternative model for type 2 diabetes. *Pharmacol Rep.* 2012;64(1):129-39.

157. Kovalevich J, Langford D. Considerations for the use of SH-SY5Y neuroblastoma cells in neurobiology. *Methods Mol Biol.* 2013;1078:9-21.
158. Wang H, Ma J, Tan Y, Wang Z, Sheng C, Chen S, et al. Amyloid-beta1-42 induces reactive oxygen species-mediated autophagic cell death in U87 and SH-SY5Y cells. *J Alzheimers Dis.* 2010;21(2):597-610.
159. Liu J, Huang C, Wang J, Huang L, Chen S. COX-2/C-MET/KRAS status-based prognostic nomogram for colorectal cancer: A multicenter cohort study. *Neural Regeneration Research.* 2020;15(2):293-301.
160. Yki-Järvinen H. Thiazolidinediones. *N Engl J Med.* 2004;351(11):1106-18.
161. Sourij H, Wascher T. Pioglitazone in the management of Type 2 diabetes and beyond. *Therapy.* 2007;4:517-33.
162. Fujiwara T, Yoshioka S, Yoshioka T, Ushiyama I, Horikoshi H. Characterization of new oral antidiabetic agent CS-045. Studies in KK and ob/ob mice and Zucker fatty rats. *Diabetes.* 1988;37(11):1549-58.
163. Olefsky JM. Treatment of insulin resistance with peroxisome proliferator-activated receptor gamma agonists. *J Clin Invest.* 2000;106(4):467-72.
164. Nicholson G, Hall GM. Diabetes mellitus: new drugs for a new epidemic. *Br J Anaesth.* 2011;107(1):65-73.
165. Saltiel AR, Olefsky JM. Thiazolidinediones in the treatment of insulin resistance and type II diabetes. *Diabetes.* 1996;45(12):1661-9.
166. Miyazaki Y, Matsuda M, DeFronzo RA. Dose-response effect of pioglitazone on insulin sensitivity and insulin secretion in type 2 diabetes. *Diabetes Care.* 2002;25(3):517-23.
167. Kaku K. Efficacy and safety of therapy with metformin plus pioglitazone in the treatment of patients with type 2 diabetes: a double-blind, placebo-controlled, clinical trial. *Curr Med Res Opin.* 2009;25(5):1111-9.
168. Zeender E, Maedler K, Bosco D, Berney T, Donath MY, Halban PA. Pioglitazone and sodium salicylate protect human beta-cells against apoptosis and impaired function induced by glucose and interleukin-1beta. *J Clin Endocrinol Metab.* 2004;89(10):5059-66.

169. Marx N, Wöhrle J, Nusser T, Walcher D, Rinker A, Hombach V, et al. Pioglitazone reduces neointima volume after coronary stent implantation: a randomized, placebo-controlled, double-blind trial in nondiabetic patients. *Circulation*. 2005;112(18):2792-8.
170. Flemmer M, Scott J. Mechanism of action of thiazolidinediones. *Curr Opin Investig Drugs*. 2001;2(11):1564-7.
171. Pavo I, Jermendy G, Varkonyi TT, Kerenyi Z, Gyimesi A, Shoustov S, et al. Effect of pioglitazone compared with metformin on glycemic control and indicators of insulin sensitivity in recently diagnosed patients with type 2 diabetes. *J Clin Endocrinol Metab*. 2003;88(4):1637-45.
172. Yanagawa T, Araki A, Sasamoto K, Shirabe S, Yamanouchi T. Effect of antidiabetic medications on microalbuminuria in patients with type 2 diabetes. *Metabolism*. 2004;53(3):353-7.
173. Srbinoska M, Hrabovski N, Rafajlovska V, Sinadinović-Fišer S. Characterization of the seed and seed extracts of the pumpkins *Cucurbita maxima* D. and *Cucurbita pepo* L. from Macedonia. *Macedonian Journal of Chemistry and Chemical Engineering*. 2012;31.
174. Guo H, Ling W, Wang Q, Liu C, Hu Y, Xia M, et al. Effect of anthocyanin-rich extract from black rice (*Oryza sativa* L. indica) on hyperlipidemia and insulin resistance in fructose-fed rats. *Plant Foods Hum Nutr*. 2007;62(1):1-6.
175. Vorhees CV, Williams MT. Morris water maze: procedures for assessing spatial and related forms of learning and memory. *Nature Protocols*. 2006;1(2):848-58.
176. Rahim NS, Lim SM, Mani V, Abdul Majeed AB, Ramasamy K. Enhanced memory in Wistar rats by virgin coconut oil is associated with increased antioxidative, cholinergic activities and reduced oxidative stress. *Pharmaceutical Biology*. 2017;55(1):825-32.
177. Takeda S, Sato N, Uchio-Yamada K, Sawada K, Kunieda T, Takeuchi D, et al. Diabetes-accelerated memory dysfunction via cerebrovascular inflammation and A $\beta$  deposition in an Alzheimer mouse model with diabetes. *Proceedings of the National Academy of Sciences*. 2010;107(15):7036-41.
178. Guo Z, Chen Y, Mao Y-F, Zheng T, Jiang Y, Yan Y, et al. Long-term treatment with intranasal insulin ameliorates cognitive impairment, tau hyperphosphorylation, and

microglial activation in a streptozotocin-induced Alzheimer's rat model. *Scientific Reports*. 2017;7(1):45971.

179. Wakabayashi T, Yamaguchi K, Matsui K, Sano T, Kubota T, Hashimoto T, et al. Differential effects of diet- and genetically-induced brain insulin resistance on amyloid pathology in a mouse model of Alzheimer's disease. *Molecular Neurodegeneration*. 2019;14(1):15.

180. Talbot K, Wang H-Y, Kazi H, Han L-Y, Bakshi KP, Stucky A, et al. Demonstrated brain insulin resistance in Alzheimer's disease patients is associated with IGF-1 resistance, IRS-1 dysregulation, and cognitive decline. *The Journal of clinical investigation*. 2012;122(4):1316-38.

181. Calvo-Ochoa E, Arias C. Cellular and metabolic alterations in the hippocampus caused by insulin signalling dysfunction and its association with cognitive impairment during aging and Alzheimer's disease: studies in animal models. *Diabetes/metabolism research and reviews*. 2015;31(1):1-13.

182. Muriach M, Flores-Bellver M, Romero FJ, Barcia JM. Diabetes and the brain: oxidative stress, inflammation, and autophagy. *Oxid Med Cell Longev*. 2014;2014:102158.

183. Morishima Y, Gotoh Y, Zieg J, Barrett T, Takano H, Flavell R, et al. Beta-amyloid induces neuronal apoptosis via a mechanism that involves the c-Jun N-terminal kinase pathway and the induction of Fas ligand. *J Neurosci*. 2001;21(19):7551-60.

184. Strother L, Miles GB, Holiday AR, Cheng Y, Doherty GH. Long-term culture of SH-SY5Y neuroblastoma cells in the absence of neurotrophins: A novel model of neuronal ageing. *Journal of Neuroscience Methods*. 2021;362:109301.

185. Feng J, Song G, Shen Q, Chen X, Wang Q, Guo S, et al. Protect Effects of Seafood-Derived Plasmalogens Against Amyloid-Beta (1–42) Induced Toxicity via Modulating the Transcripts Related to Endocytosis, Autophagy, Apoptosis, Neurotransmitter Release and Synaptic Transmission in SH-SY5Y Cells. *Frontiers in aging neuroscience*. 2021;13.

186. Bell M, Zempel H. SH-SY5Y-derived neurons: a human neuronal model system for investigating TAU sorting and neuronal subtype-specific TAU vulnerability. *Rev Neurosci*.

2022;33(1):1-15.

187. Kalagatur NK, Abd\_Allah EF, Poda S, Kadirvelu K, Hashem A, Mudili V, et al. Quercetin mitigates the deoxynivalenol mycotoxin induced apoptosis in SH-SY5Y cells by modulating the oxidative stress mediators. *Saudi Journal of Biological Sciences*. 2021;28(1):465-77.

188. Sato A, Tagai N, Ogino Y, Uozumi H, Kawakami S, Yamamoto T, et al. Passion fruit seed extract protects beta-amyloid-induced neuronal cell death in a differentiated human neuroblastoma SH-SY5Y cell model. *Food Science & Nutrition*. 2022.

189. Agholme L, Lindström T, Kågedal K, Marcusson J, Hallbeck M. An in vitro model for neuroscience: differentiation of SH-SY5Y cells into cells with morphological and biochemical characteristics of mature neurons. *J Alzheimers Dis*. 2010;20(4):1069-82.

190. Garcia G, Pinto S, Cunha M, Fernandes A, Koistinaho J, Brites D. Neuronal Dynamics and miRNA Signaling Differ between SH-SY5Y APPSwe and PSEN1 Mutant iPSC-Derived AD Models upon Modulation with miR-124 Mimic and Inhibitor. *Cells*. 2021;10(9):2424.

191. Eckert A, Keil U, Marques CA, Bonert A, Frey C, Schüssel K, et al. Mitochondrial dysfunction, apoptotic cell death, and Alzheimer's disease. *Biochem Pharmacol*. 2003;66(8):1627-34.

192. Chen M, Du Z-Y, Zheng X, Li D-L, Zhou R-P, Zhang K. Use of curcumin in diagnosis, prevention, and treatment of Alzheimer's disease. *Neural Regeneration Research*. 2018;13(4).

193. Zheng K-m, Zhang J, Zhang C-l, Zhang Y-w, Chen X-c. Curcumin inhibits appoptosin-induced apoptosis via upregulating heme oxygenase-1 expression in SH-SY5Y cells. *Acta Pharmacologica Sinica*. 2015;36(5):544-52.

194. Thapa A, Jett SD, Chi EY. Curcumin Attenuates Amyloid- $\beta$  Aggregate Toxicity and Modulates Amyloid- $\beta$  Aggregation Pathway. *ACS Chemical Neuroscience*. 2016;7(1):56-68.

195. Yorek MA. The role of oxidative stress in diabetic vascular and neural disease. *Free Radic Res*. 2003;37(5):471-80.

196. Tang KS. Protective effect of arachidonic acid and linoleic acid on 1-methyl-4-phenylpyridinium-induced toxicity in PC12 cells. *Lipids in Health and Disease*. 2014;13(1):197.
197. Yaguchi T, Fujikawa H, Nishizaki T. Linoleic acid derivative DCP-LA protects neurons from oxidative stress-induced apoptosis by inhibiting caspase-3/-9 activation. *Neurochem Res*. 2010;35(5):712-7.
198. Cassano V, Leo A, Tallarico M, Nesci V, Cimellaro A, Fiorentino TV, et al. Metabolic and Cognitive Effects of Ranolazine in Type 2 Diabetes Mellitus: Data from an in vivo Model. *Nutrients*. 2020;12(2):382.
199. Wang X, Fang H, Xu G, Yang Y, Xu R, Liu Q, et al. Resveratrol Prevents Cognitive Impairment in Type 2 Diabetic Mice by Upregulating Nrf2 Expression and Transcriptional Level. *Diabetes Metab Syndr Obes*. 2020;13:1061-75.
200. Feinman RD, Fine EJ. Fructose in perspective. *Nutrition & Metabolism*. 2013;10(1):45.
201. Basciano H, Federico L, Adeli K. Fructose, insulin resistance, and metabolic dyslipidemia. *Nutr Metab (Lond)*. 2005;2(1):5.
202. Bray GA, Nielsen SJ, Popkin BM. Consumption of high-fructose corn syrup in beverages may play a role in the epidemic of obesity. *Am J Clin Nutr*. 2004;79(4):537-43.
203. abd-elnoor ev. Hypoglycemic and Hypolipidemic Effects of Pumpkin Seeds Powder and Oil on Alloxan-induced Diabetic in Rats. *Egyptian Journal of Food Science*. 2019;47(2):255-69.
204. Adams G, Jiwani S, Wang S, Mohammed A, Kök M, Gray D, et al. The Hypoglycemic Effect of Pumpkin Seeds, Trigonelline (TRG), Nicotinic Acid (NA), and D-Chiro-inositol (DCI) in Controlling Glycemic Levels in Diabetes Mellitus. *Critical reviews in food science and nutrition*. 2014;54:1322-9.
205. Sharma A, Sharma A, Chand T, Khardiya M. Antidiabetic and Antihyperlipidemic Activity of Cucurbita maxima Duchense (Pumpkin) Seeds on Streptozotocin Induced Diabetic Rats. *Journal of Pharmacognosy and Phytochemistry*. 2013;1:108-16.
206. Stevenson DG, Eller FJ, Wang L, Jane JL, Wang T, Inglett GE. Oil and tocopherol



content and composition of pumpkin seed oil in 12 cultivars. *J Agric Food Chem.* 2007;55(10):4005-13.

207. de la Monte SM, Wands JR. Alzheimer's Disease is Type 3 Diabetes—Evidence Reviewed. *Journal of Diabetes Science and Technology.* 2008;2(6):1101-13.

208. Yuan X-Y, Wang X-G. Mild cognitive impairment in type 2 diabetes mellitus and related risk factors: a review. *Reviews in the Neurosciences.* 2017;28(7):715-23.

209. Cohen SJ, Munchow AH, Rios LM, Zhang G, Asgeirsdóttir HN, Stackman RW, Jr. The rodent hippocampus is essential for nonspatial object memory. *Curr Biol.* 2013;23(17):1685-90.

210. Kumaran D, Hassabis D, Spiers HJ, Vann SD, Vargha-Khadem F, Maguire EA. Impaired spatial and non-spatial configural learning in patients with hippocampal pathology. *Neuropsychologia.* 2007;45(12):2699-711.

211. de la Monte SM. Contributions of brain insulin resistance and deficiency in amyloid-related neurodegeneration in Alzheimer's disease. *Drugs.* 2012;72(1):49-66.

212. Stanciu GD, Bild V, Ababei DC, Rusu RN, Cobzaru A, Paduraru L, et al. Link Between Diabetes and Alzheimer's Disease due to the Shared Amyloid Aggregation and Deposition Involving both Neurodegenerative Changes and Neurovascular Damages. *J Clin Med.* 2020;9(6):1713.

213. Anand KS, Dhikav V. Hippocampus in health and disease: An overview. *Ann Indian Acad Neurol.* 2012;15(4):239-46.

214. Preston AR, Eichenbaum H. Interplay of hippocampus and prefrontal cortex in memory. *Curr Biol.* 2013;23(17):R764-R73.

215. Saeed V-N, Masood V-N, Mehri S, Samira E. The Impact of Diabetes on Hippocampus. 2021.

216. Lupaescu A-V, Iavorschi M, Covasa M. The Use of Bioactive Compounds in Hyperglycemia- and Amyloid Fibrils-Induced Toxicity in Type 2 Diabetes and Alzheimer's Disease. *Pharmaceutics.* 2022;14(2):235.

217. Do J, Kim N, Jeon S, Gee M, Ju Y-J, Kim J-H, et al. Trans-Cinnamaldehyde Alleviates Amyloid-Beta Pathogenesis via the SIRT1-PGC1 $\alpha$ -PPAR $\gamma$  Pathway in 5XFAD

Transgenic Mice. *International Journal of Molecular Sciences*. 2020;21:4492.

218. Bonds JA, Shetti A, Bheri A, Chen Z, Disouky A, Tai L, et al. Depletion of Caveolin-1 in Type 2 Diabetes Model Induces Alzheimer's Disease Pathology Precursors. *The Journal of Neuroscience*. 2019;39(43):8576-83.

219. Nguyen KV. The human  $\beta$ -amyloid precursor protein: biomolecular and epigenetic aspects. *Biomol Concepts*. 2015;6(1):11-32.

220. Wang K, Chen Q, Wu N, Li Y, Zhang R, Wang J, et al. Berberine Ameliorates Spatial Learning Memory Impairment and Modulates Cholinergic Anti-Inflammatory Pathway in Diabetic Rats. *Frontiers in Pharmacology*. 2019;10.

221. Xu W, Liu J, Ma D, Yuan G, Lu Y, Yang Y. Capsaicin reduces Alzheimer-associated tau changes in the hippocampus of type 2 diabetes rats. *PLoS One*. 2017;12(2):e0172477.

222. Abdel-Moneim A, Yousef AI, Abd El-Twab SM, Abdel Reheim ES, Ashour MB. Gallic acid and p-coumaric acid attenuate type 2 diabetes-induced neurodegeneration in rats. *Metab Brain Dis*. 2017;32(4):1279-86.

223. Nowotny K, Jung T, Höhn A, Weber D, Grune T. Advanced glycation end products and oxidative stress in type 2 diabetes mellitus. *Biomolecules*. 2015;5(1):194-222.

224. Volpe CMO, Villar-Delfino PH, dos Anjos PMF, Nogueira-Machado JA. Cellular death, reactive oxygen species (ROS) and diabetic complications. *Cell Death & Disease*. 2018;9(2):119.

225. Park S, Park S-Y. Can antioxidants be effective therapeutics for type 2 diabetes? *Yeungnam Univ J Med*. 2021;38(2):83-94.

226. Hanaa Ali Hassan Mostafa Abd E-A. Lipid Peroxidation End-Products as a Key of Oxidative Stress: Effect of Antioxidant on Their Production and Transfer of Free Radicals. 2012.

227. Tangvarasittichai S. Oxidative stress, insulin resistance, dyslipidemia and type 2 diabetes mellitus. *World J Diabetes*. 2015;6(3):456-80.

228. He F, Ru X, Wen T. NRF2, a Transcription Factor for Stress Response and Beyond. *International journal of molecular sciences*. 2020;21(13):4777.

229. Makni M, Fetoui H, Gargouri NK, Garoui el M, Zeghal N. Antidiabetic effect of flax



and pumpkin seed mixture powder: effect on hyperlipidemia and antioxidant status in alloxan diabetic rats. *J Diabetes Complications*. 2011;25(5):339-45.

230. Reddy VP, Zhu X, Perry G, Smith MA. Oxidative stress in diabetes and Alzheimer's disease. *Journal of Alzheimer's disease : JAD*. 2009;16(4):763-74.

231. Wong CHY, Wanrooy BJ, Bruce DG. Chapter 10 - Neuroinflammation, Type 2 Diabetes, and Dementia. In: Srikanth V, Arvanitakis Z, editors. *Type 2 Diabetes and Dementia*: Academic Press; 2018. p. 195-209.

232. Gao C, Hölscher C, Liu Y, Li L. GSK3: a key target for the development of novel treatments for type 2 diabetes mellitus and Alzheimer disease. *Rev Neurosci*. 2011;23(1):1-11.

233. Teresa P-L, Andrew Michael S-V, Alma Patricia B-L, José L-M, Miguel Angel O-T, Ignacio V-F, et al. *Diabetes Mellitus and Amyloid Beta Protein Pathology in Dementia*. 2019.

234. Sadeghi A, Hami J, Razavi S, Esfandiary E, Hejazi Z. The Effect of Diabetes Mellitus on Apoptosis in Hippocampus: Cellular and Molecular Aspects. *Int J Prev Med*. 2016;7:57.

235. Wang G, Fang H, Zhen Y, Xu G, Tian J, Zhang Y, et al. Sulforaphane Prevents Neuronal Apoptosis and Memory Impairment in Diabetic Rats. *Cell Physiol Biochem*. 2016;39(3):901-7.

236. Xu Y, Liu S, Zhu L, Dai L, Qian W, Zhang J, et al. Green tea protects against hippocampal neuronal apoptosis in diabetic encephalopathy by inhibiting JNK/MLCK signaling. *Mol Med Rep*. 2021;24(2):575.



## VITA

NAME Chonticha Areebambud

DATE OF BIRTH 23 March 1985

PLACE OF BIRTH Yala

HOME ADDRESS 2634 Intramansion 2 Soi Raminthra 15 Anusawari Bangken  
Bangkok 10220

PUBLICATION Wongchaiya C, Areebambud C, Benjatham N,  
Jariyapongskul A. Effect of pomelo crude extract (Thong  
Dee cultivar) on insulin resistance and cognitive impairment  
in type 2 diabetic rats. Journal of Medicine and Health  
Science. 2020.

Jariyapongskul A, Areebambud C, Hideyuki N.  
Microhemodynamic indices to evaluate the effectiveness of  
herbal medicine in diabetes: A comparison between alpha-  
mangostin and curcumin in the retina of type 2 diabetic rats.  
Clinical Hemorheology and Microcirculation. 2018.

Jariyapongskul A, Areebambud C, Suksamrarn S,  
Mekseepralard C. Alpha-Mangostin Attenuation of  
Hyperglycemia-Induced Ocular Hypoperfusion and Blood  
Retinal Barrier Leakage in the Early Stage of Type 2  
Diabetes Rats. BioMed Research International. 2015.

Mekseepralard C, Areebambud C, Suksamrarn S,  
Jariyapongskul A. Effects of Long-Term Alpha-mangostin  
Supplementation on Hyperglycemia and Insulin Resistance

in Type 2 Diabetic Rats Induced by High Fat Diet and Low Dose Streptozotocin. Journal of Medicine and Health Science. 2015

**AWARD RECEIVED**

Distinguished Thesis Award Project, Graduate School of Srinakharinwirot University. 2015. The antioxidant and anti-Inflammatory effects of alpha- mangostinon retinal vascular dysfunction in type 2 diabetic rats.

